universität wien

MASTERARBEIT / MASTER'S THESIS

Titel der Masterarbeit / Title of the Master's Thesis

"The application of $n(^{87}Sr)/n(^{86}Sr)$ isotope analysis to study human migration in the late Bronze Age in Stillfried/March, Austria"

verfasst von / submitted by

Anna-Maria Kriechbaum, BSc BA MSc

angestrebter akademischer Grad / in partial fulfilment of the requirements for the degree of

Master of Arts (MA)

Wien, 2022 / Vienna 2022

Studienkennzahl lt. Studienblatt / degree programme code as it appears on the student record sheet:	UA 066801
Studienrichtung lt. Studienblatt / degree programme as it appears on the student record sheet:	Urgeschichte und Historische Archäologie
Betreut von / Supervisor:	ao. Univ.-Prof. Dr. Gerhard Trnka

Danksagung

Ein großer Dank geht an Univ.Prof. Dipl.-Ing. Dr.techn. Thomas Prohaska, der es mir als „Nicht-Chemikerin“ ermöglicht hat, eine interdisziplinäre Masterarbeit in seinem Team an der Universität für Bodenkultur zu verfassen. Weiters möchte ich mich bei ihm für die Betreuung sowie die Möglichkeit meine Arbeit auf der „European Winter Conference on Plasma Spectrochemistry“ als Poster zu präsentieren, danken.

Anika Retzmann, PhD möchte ich für die tolle Betreuung, die vielen Erklärungen und fachlichen Inputs danken. Es war ganz bestimmt nicht immer einfach einer Archäologin und Anthropologin Chemie zu erklären.

Weiters möchte ich Tine Opper und Melanie Diesner für ihre Unterstützung im Labor Dank sagen. Mein Dank gilt auch an alle damaligen Mitglieder des VIRIS Teams für die Aufnahme in die Gemeinschaft.

Dank gilt auch Monika Griebl im Rahmen deren FWF Projekt (P28005–‘Resource management, power and cult in Stillfried?’) die Untersuchungen meiner Masterarbeit stattgefunden haben.

Ao. Univ.-Prof. Dr. Gerhard Trnka möchte ich für die archäologische Betreuung an der Universität Wien danken.

Bei meinen Eltern möchte ich mich bedanken, dass sie mir ermöglicht haben ein zweites Masterstudium zu absolvieren.

Ein großer Dank gilt auch meinem Freund, Felix Köstelbauer, der mir mit den Tücken von ArcGIS geholfen hat, mir Mut zugesprochen hat meine Arbeit noch fertigzustellen und zuguterletzt, der sich an seinen arbeitsfreien Tagen vermehrt um unsere Tochter gekümmert hat um mir die Zeit für diese Arbeit freizuschaufeln. Danke!

In diesem Sinne möchte ich diese Masterarbeit meinem Freund Felix und meiner Tochter Emilia widmen.

TABLE OF CONTENTS

Kommentar der Autorin/Comment of the author:

Ein Teil der Ergebnisse dieser Masterarbeit wurden bereit in „Retzmann, A*, Kriechbaum, A-M*, Griebl, M, Wiltschke-Schotta, K, Teschler-Nicola, M, Irrgeher, J, Prohaska, T (2020) Sr Isotope Analysis of Human Remains from Settlement Pits at Stillfried/March – Reassessing Diagenetic Changes, Archaeologia Austriaca.” publiziert. Sie stammen von dieser Arbeit und wurden von der Autorin verfasst.

(*gleicher Beitrag)

Text modules of this work were included in the publication „Retzmann, A*, Kriechbaum, A-M*, Griebl, M, Wiltschke-Schotta, K, Teschler-Nicola, M, Irrgeher, J, Prohaska, T (2020) Sr Isotope Analysis of Human Remains from Settlement Pits at Stillfried/March – Reassessing Diagenetic Changes, Archaeologia Austriaca.”. They all come from this master's thesis and were written by its author.

(* equal contribution)

1 Introduction

Stillfried/March is an intensive investigated archaeological finding spot in Austria. The Late Bronze Age takes an exceptional position in the settlement history of Stillfried. However, the settlement history already started during the Palaeolithic (Felgenhauer, 1978a, p. 96, Felgenhauer, 1980a, p. 177f, Felgenhauer, 1980b, p. 7 ff, Felgenhauer, 1985, p. 7). At the latest, during the younger Urnfield Period, the settlement in Stillfried was a place of supraregional importance. Until now, only a small part of the settlement has been archaeologically investigated. Nevertheless, a large number of findings and archaeological records are known. Records like human and animal skeletal depositions in former storage pits stand out. Especially the human skeletal depositions of pit V1141, better known as 'The seven of the pit' (ger. 'Die Sieben aus der Grube') are well-known among archaeologists (Griebl&Hellerschmid, 2011, p. 39, Griebl&Hellerschmid, 2013, p. 327, Griebl&Hellerschmid, 2015, p. 184, Teschler-Nicola, Irrgeher&Prohaska, 2016, p. 159 ff, Griebl, Biederer, Jachs et al., 2017, p. 198).

The deposition of those human skeletons shows strong discrepancies in contrast to the custom mode of funerary at that time. Furthermore the health state of the skeletons also differs between the pits (Griebl&Hellerschmid, 2013, p. 329, 333, 335ff, 341). Even though there are no signs in the material findings, the question arises, whether those individuals were foreigners and therefore treated differently due to a different provenance.

During the last decades, strontium (Sr) isotope ratio analysis in human and animal remains applying either thermal ionization mass spectrometry (TIMS) or (multi-collector) inductively coupled plasma mass spectrometry ((MC) ICP-MS) are increasingly used in archaeology and anthropology to answer questions about provenance and migration. The incorporated $n(^{87}Sr)/n(^{86}Sr)$ isotope-amount ratio of a tooth enamel preserves information about the place of residence of an individual during its childhood years ('archive of the childhood') (Grupe, 1998, p. 337, Prohaska, Latkoczy, Schultheis et al., 2002, p. 890) while the tooth dentine and bone tissue preserve the $n(^{87}Sr)/n(^{86}Sr)$ isotope-amount ratio of its last years prior to death (Price, Knipper, Grupe et al., 2013, p. 14).

The aim of this master thesis was to investigate the provenance of selected individuals found in the pits V1133, V0841 and V1141 using $n(^{87}Sr)/n(^{86}Sr)$ isotope-amount ratio analysis.

1.1 Stillfried/March – Archaeological Overview

The first archaeological findings in Stillfried date back to the Palaeolithic. Those include the production place of chipped stones within the area of the later to come Urnfield Culture settlement and several camp sites in the Stillfried area (Felgenhauer, 1978a, p. 96, Weiser, 1978, p. 5ff, Felgenhauer, 1980a, p. 177f, Felgenhauer, 1980b, p. 7ff, Antl-Weiser, 1985, p. 19ff, Felgenhauer, 1985, p. 7).

Several findings of the Neolithic as well as the Early and Middle Bronze Age are also known for the area of Stillfried (Felgenhauer, 1985, p. 7). Concerning the Neolithic, in the area of the hill fort settlement only stray finds were found. Settlement areas of that period were found at Rochusberg and Haspelberg (Frank, 1990, p. 9).

Findings of the Early and Middle Bronze Age could for example be located at the brick manufacture in Stillfried (Trnka, 1978, p. 15 ff). Furthermore, an early Bronze Age settlement of the Únětice culture can be located near the Rochuskapelle (Museum-Stillfried, 2017a) . Several burials of the Early Bronze Age werde found at the Rochusberg and at the Kirchhügel (Museum-Stillfried, 2017a).

The Middle Bronze Age marks the beginning of the settlement at the Kirchhügel (Museum-Stillfried, 2017a).

During the years of 1969-1989 an about 23 hectar large Bronze Age settlement was partly excavated by Felgenhauer (1985, p. 7, Hellerschmid, 2006, p. 9, p. 16). Concerning the Urnfield Period, the earlier stages of BZ-D and Ha A are primarily represented in the northern area of the settlement. The hill site settlement and its rampart were first discovered in 1874 and published by Matthäus Much in 1875 (Felgenhauer, 1996, p. 9, Hellerschmid, 2021, p. 71).

Typologically, some of the findings were eponymous and those terms are still used today. Oswald Menghin defined the term '*Stillfrieder Gruppe*' for a certain group of ceramics found in Stillfried (Hellerschmid, 2021, p. 71). Furthermore the term '*Stillfrieder Tasse'*, a certain type of cups, made of bronze sheet was defined after it was found at the burial site *'In der Gans'* in Stillfried (Strohschneider, 1974, p. 61ff, Eibner, 1985, p. 35f, Felgenhauer, 1996, p. 9).

Felgenhauer's excavations (1969-1989) were the first long-term systematic excavations of the Urnfield Culture settlement in Stillfried. Their main focus was on the *'Hügelfeld'*.

Pit houses containing, for example, multiple weight looms, dating in the time of the Hallstatt Culture demonstrate a continuing existence of the settlement (Eibner, 1974, p. 76ff, Felgenhauer, 1978a, p. 96, Felgenhauer, 1980a, Langenecker, 1988, p. 121, Hellerschmid, 2006, p. 318f). It's core area seems to have been the area around the 'Wagneracker' (Griebl&Hellerschmid, 2013, p. 329). The settlement of that time was probably not having a rampart (settlement phase IV – V). The end of the continuous settlement dates to the beginning of Ha D1 which can be assigned to settlement phase V (Hellerschmid, 2006, p. 18).
During the late La Tène Period, a weaver's house was built on the western hill fort itself (Felgenhauer, 1980a, p. 177f, Felgenhauer, 1985, p. 11, Urban, 1985, p. 49, p. 52, Langenecker, 1988, p. 122). Otherwise, there are only a few findings of that period (Hellerschmid, 2006, p. 18).

Even though, Stillfried is located north of the Danube, findings indicate a Roman base in Stillfried (Felgenhauer, 1978a, p. 96, p. 98, p. 100, Felgenhauer, 1985, p. 11), probably during the 2nd and 4th century AD (Felgenhauer, 1996, p. 17). Most of the roman findings within the area of the Urnfield settlement could be located at the '*Römerhügel'* (Frank, 1990, p. 10). Furthermore, Germanic Peoples also settled in Stillfried (Felgenhauer, 1973, p. 52, Felgenhauer, 1980a, p. 178, Felgenhauer, 1985, p. 11f). However, for the first two centuries AD the number of Germanic findings is small (Hellerschmid, 2006, p. 18).
Concerning the Early Middle Ages, a few Slavic findings and graves are known near the Urnfield Period's settlement (Felgenhauer-Schmiedt, 1985, p. 55, Museum-Stillfried, 2017b).
The archaeological record of the High and Late Middle Ages show many findings of that time period. A medieval settlement at the former location of the Urnfield Period settlement came to surface during Felgenhauer's excavations (Felgenhauer, 1978a, p. 96, p. 98, p. 100, p. 103, Felgenhauer, 1978b, p. 58 ff, Felgenhauer, 1980a, p. 178, 181f, Felgenhauer, 1985, p. 12). Multiple basements of the Modern Age were found during the excavations in 1974 (Felgenhauer, 1978a, p. 99)
Trenches of World War II conclude the archaeological record on the hill site (Barg, 1988, p. 103, Felgenhauer, 1996, p. 19).

Near the Urnfield Culture settlement, two Urnfield Culture burial grounds, *'Alter Mühlgraben'* and '*In der Gans'* can be located. The latter was discovered in 1879 and partly excavated by Matthäus Much. During the 1970's Felgenhauer continued the excavations (Felgenhauer, 1978a, p. 96ff, Hellerschmid, 2006, p. 318).
After Felgenhauer's excavations ended in 1989, Eibner continued them in irregular intervals (Hellerschmid, 2015, p. 205).

1.1.1 The Late Urnfield Settlement in Stillfried/March

1.1.1.1 Topography and Geology

Stillfried/March is located in the south-eastern part of the Weinviertel in Lower Austria near the Austrian/Slovakian border. The settlement of the Urnfield Period is mostly located in the cadastral municipality of Stillfried/March. A small part of the settlement is part of the cadastral municipality of Grub/March, which is located north of Stillfried.
The settlement of the Late Urnfield Period is located on an elevation near the Amber Road. The elevation of the settlement's position is extending from west to east in the direction to the March river. In the east, the elevation is steeply sloping, northern and southern parts are each a vale which is nowadays in a dry state. In the western part, the elevation turns into a broadening plain (Hellerschmid, 2015, p. 205).

Stillfried is located in the northern Vienna Basin (Rögl&Summesberger, 1978, p. 76, Rögl&Summesberger, 1988, p. 148). Tertiary Sediments (for example clay, clay marl, sand, gravel), quaternary loess deposits and holocene flood plain sediments of the March distinguish the geology of the region (Hellerschmid, 2006, p. 11) (see Fig. 1). A seismic refraction survey detected a height of the loess deposits of 30-40 m at the site of the Urnfield settlement (Felgenhauer, 1980b, p. 9). The loess stratigraphy of Stillfried and the soil formation complexes *Stillfried A and B* serve as a reference for the climatology and pedology of the Pleistocene (Fink, 1954, p. 85ff, Antl, 1985, p. 15, Hellerschmid, 2006, p. 16, Sprafke, 2016, p. 154ff, Riegler&Peticzka, 2004, p. 41ff).
As for the soil, chernozem on loess are predominant in the hill site (see Fig. 1 and 2). This kind of soil can be determined as high-quality soil for farming (Kohler-Schneider, 2001, p. 16, p. 163, Hellerschmid, 2006, p. 11). Of all the agricultural lands in this area, over 50 % are on chernozem on loess. The characteristics of this type of soil is their high content of

lime and alkaline soil reactions. Furthermore, they have a high reservoir potential and a moderate water permeability (Kohler-Schneider, 2001, p. 16).

At the hill site toe, to some extent chernozem on colluvial soil can be found as result of erosion. Moist black soil is also a high-quality soil for farming. However, this type of soil develops mainly through dewatering of agricultural used floodplains. In Stillfried, those can be found at anthropogenic dewatered stream sites. The risk of flooding in times of heavy rains are a disadvantage of this type of soil. About 5% of the soil in the area of Stillfried is moist black soil. Flood plain soils of the March often show a gley horizon up to the surface. Before the anthropogenic dewatering activities, the only agricultural use of the March lowlands was probably the retrieval of litter and animal feed (Kohler-Schneider, 2001, p. 16f).

In her study about the food of the Bronze age settlement in Stillfried/March, Kohler-Schneider (2001, p. 16f) wasn't able to retrieve detailed soil or geological maps of the Slovakian area near Stillfried. She assumed, that the lowlands on the slovakian side of the March, at least those in a diameter of 5 km surrounding Stillfried, show similar soil types than they do at the Austrian side of the March. According to the map of Fordinál, Maglay, Elečko et al. (2012), her assumption is true.

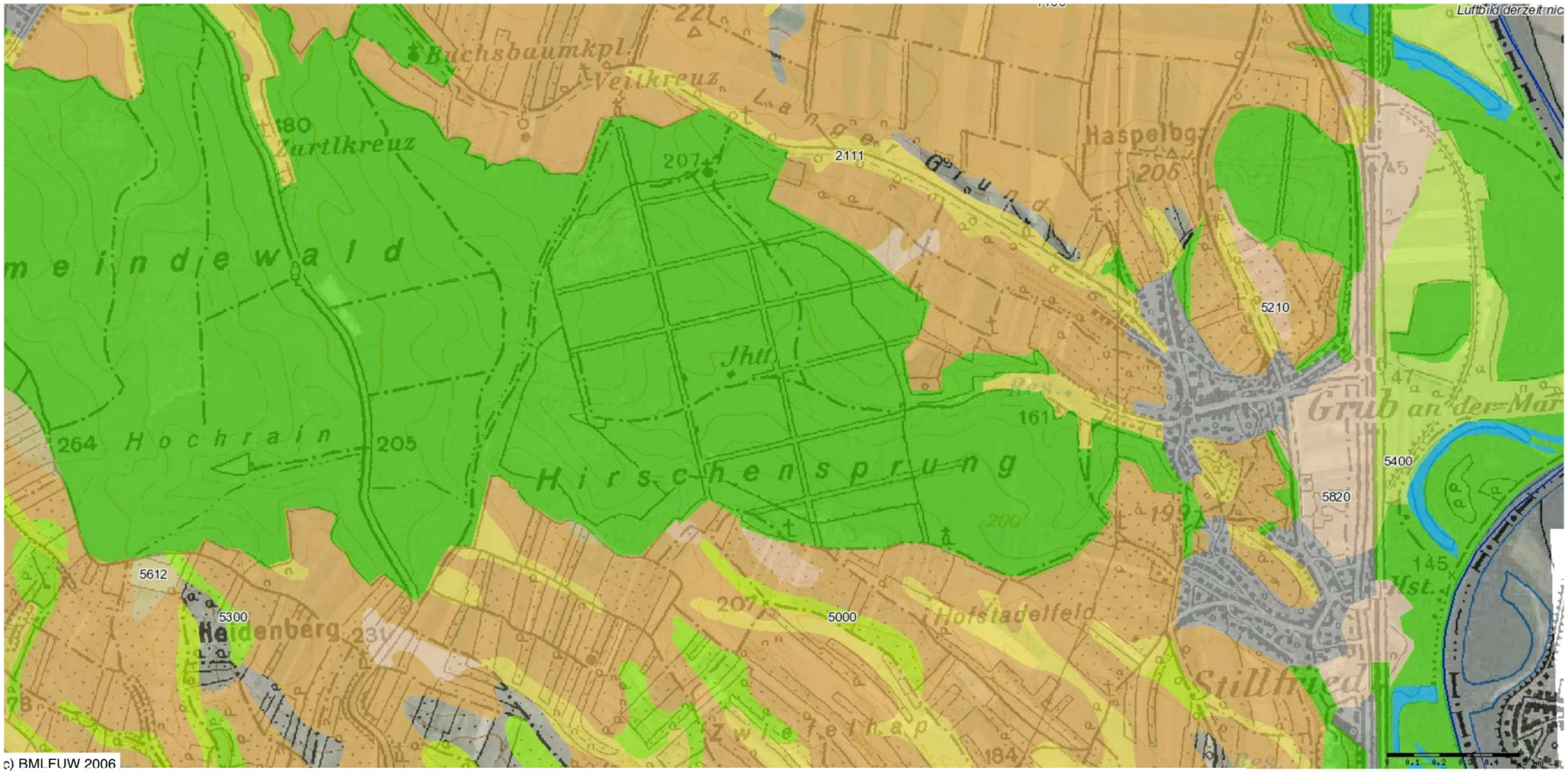

Figure 1 Geological Map of Stillfried/March (source: Digitale Bodenkarte von Österreich, 1km-Raster, Bundesforschungs- und Ausbildungszentrum für Wald, Naturgefahren und Landschaft (BFW)) Note: only the areas free of forests were mapped (forests in green)

Figure 2 Soil Map of Stillfried/March (source: Digitale Bodenkarte von Österreich, 1km-Raster, Bundesforschungs- und Ausbildungszentrum für Wald, Naturgefahren und Landschaft (BFW)), Note: only the areas free of forests were mapped (forests in green)Figure 3 Geological Map of Stillfried/March (source: Digitale Bodenkarte von Österreich, 1km-Raster, Bundesforschungs- und Ausbildungszentrum für Wald, Naturgefahren und Landschaft (BFW)) Note: only the areas free of forests were mapped (forests in green)

Figure 4 Soil Map of Stillfried/March (source: Digitale Bodenkarte von Österreich, 1km-Raster, Bundesforschungs- und Ausbildungszentrum für Wald, Naturgefahren und Landschaft (BFW)), Note: only the areas free of forests were mapped (forests in green)

Figure 5 Soil Map of Stillfried/March (source: Digitale Bodenkarte von Österreich, 1km-Raster, Bundesforschungs- und Ausbildungszentrum für Wald, Naturgefahren und Landschaft (BFW)), Note: only the areas free of forests were

1.1.1.2 Vegetation

Kohler-Schneider (2001, p. 50ff) examined plant remains that were found during the flotation of soil samples from the excavations within the settlement area. The following chapter describes the uncultivated plants she could identify. Her findings give an indication of how the vegetation in Stillfried looked like during the time of the Urnfield Period.

Kohler-Schneider (2001, p. 160) found remains of *Stellaria alsine (*bog stitchwort*), Sambucus nigra* (black elder) and *Physalis* (bladder cherry) within the settlement of Stillfried. Hence, it is assumed that they possibly grew in the floodplain forests of the March river lowlands and they were probably collected (Kohler-Schneider, 2001, p. 160).
Charcoal of willow *(Salix sp.)* definitely originates of the floodplain forests near the March river. The field elm *(Ulmus minor)*, which was used for the purposeful charring of the fortification, is also a typical tree growing in floodplain forests. In this case it most likely originates from floodplain forests of the March (Kohler-Schneider, 2001, p. 160f).
Grey alders *(Alnus incana)*, which were found to be part of the fortification, are untypical for the March area. As of today, they only exist near Marchegg in the area of the March river. However, since grey alders were used for the fortification, they probably must have grown somewhere near Stillfried (Kohler-Schneider, 2001, p. 191).

Apple, pear, cherry and sour cherry trees were most certain located in the hill country side of Stillfried since remains of those could be found during the excavations (Kohler-Schneider, 2001, p. 161).

Charcoal of ash tree (probably *Fraxinus excelsior),* elm tree *(Ulmus minor)*, linden tree *(Tilia cordata* and probably also *Tilia platyphyllos)* and oak tree *(Quercus petraea, Quercus cerris* or *Quercus robur)* distinguish the typical forest trees of the late Bronze Age. Spores of those trees were also found in the settlement of Stillfried. (Kohler-Schneider, 2001, p. 161).

Plants that grow on grassland and dry grassland were also found within the settlement. Those indicate some kind of subsistence concerning that type of vegetation. Some pits contained great numbers of such plants. This could indicate, that they were used as hay (Kohler-Schneider, 2001, p. 28f, p. 52, p. 88, p. 161).

1.1.1.3 Climate

As for the palaeoclimatic reconstruction, the Urnfield Period can be assigned to the younger Subboreal which was warmer than the previous Atlantic. The end of the Bronze Age correlated with a cooling phase which stayed on for the following Iron Age (Kohler-Schneider, 2001, p. 22f). This cooling phase can also be related to a more rain-laden period (Popovtschak, Heiss&Drescher-Schneider, 2021, p. 41). The climate change at the end of the Bronze Age most definitely had an influence on the subsistence and in general on the life of the people at that time (Hellerschmid, 2004, Hellerschmid, 2006, p. 13, Popovtschak, Heiss&Drescher-Schneider, 2021, p. 41). In the opinion of Kohler-Schneider (2001, p. 24), the climate at the end of the Bronze Age did not differ much from today's climate in eastern Austria.

The water meadows of the March were a swampy area, with many sand dunes and rubble accumulations at that time (Hellerschmid, 2006, p. 13). Furthermore, some parts were forested steppe. Most areas were probably oak forests or oak-hornbeam forests (Kohler-Schneider, 2001, p. 24f).

1.1.1.4 The settlement

The first settlement phase dates to Ha A2/B1. During this phase, the western rampart only consisted of a palisade. During the main phase of the settlement, a hill fort and a ditch were built. The main phase of the Urnfield Period's settlement dates to about 900-750 BC (Griebl&Hellerschmid, 2015, p. 179). Two construction phases of the western rampart can be detected. The first one correlates to settlement phase II-III/1 (Ha B2/early B3). After its destruction by fire, a second one was built during settlement phase III/2 (Ha B3) which marks the beginning of the last settlement phase (Hellerschmid, Kern&Lochner, 2010, p. 286). Many findings which can be assigned to the metalworking category of this time period were found (Hellerschmid, 2006, p. 318). At the end of the Urnfield Period, the hill fort was completely destroyed by fire (Ha B3/C1a) (Hellerschmid, Kern&Lochner, 2010, p. 286, Hellerschmid, 2015, p. 206).

The settlement of that time is often described as a central place with the primary importance in material production and trade (Felgenhauer, 1985, p. 11f). Findings of amber beads and amber fragments could be seen as an indication for that (Eibner, 1985, p. 35).

Since there are many archaeological findings indicating ritual actions, such as a concentration of human and animal skeletal depositions as well as findings like masses of barley glumes probably mixed with salt which could be similar to the roman *mola salsa* (Felgenhauer, 1985, p. 10), Stillfried can be described as a ritual centre as well (Griebl&Hellerschmid, 2015, p. 196 f, Hellerschmid, 2015, p. 206). The cultic actions of the settlement were investigated by Griebl&Hellerschmid (2011, p. 39f) and Griebl, Biederer, Jachs et al. (2017, p. 197, 201).

The so called '*Kirchhügel*' is the highest part of the settlement. It was most likely connected to the upper-class of Stillfried and might have served them as a place of residence or/and a place for ceremonial gatherings (Hellerschmid, 2015, p. 206).

As the result of multiple cappings of the surface, the type of housing within the settlement is mostly unclear. Starting in Ha B3 (settlement phase III/1), the first pit houses occurred (e.g. Object V601). This form of housing continued until the late La Tène Period (Hellerschmid, 2006, p. 318).

As for the domestic animals, cattle seem to have played an important role. Furthermore, horses, pigs, sheep, goats, chicken and dogs form the main spectrum of the animal findings in the archaeological record (Hellerschmid, 2006, p. 14). Based on the number of findings of wild animals in Stillfried, it is assumed, that red deer were an often-hunted animal in Stillfried. Furthermore, animals such as beaver, fox, wolf and brown bear were hunted too (Hellerschmid, 2006, p. 15).
The record of pike and carp, pond turtles, mussels, ducks and geese prove that the water resources were hunted as well (Hellerschmid, 2006, p. 15).

1.1.1.5 Nutrition in the Urnfield Culture settlement of Stillfried/March

The nutrition in Stillfried was versatile. It included grains, fruits, leguminous plants and vine, which is described in the following.

1.1.1.5.1 Grains

During the Urnfield Period, spelt (*Triticum spelta L.)* was one of the most cultivated type of grains in Stillfried. It mostly occurs combined with barley emmer *(Triticum dicoccum (Schrank) Schübl.)* and broomcorn millet *(Panicum miliaceum)* (Kohler-Schneider, 2001, p. 51, p. 106). As of today, spelt is a typical winter grain. Due to that fact, Kohler-Schneider (2001, p. 110) holds the assumption, that it was the same during the time of the Urnfield Period.

Next to spelt, broomcorn millet *(Panicum miliaceum L.)* was one of the most cultivated grains. In general, the appearance of broomcorn millet is rising during the late Bronze Age. It is a typical summer grain due to its requirement for a certain temperature. In addition to panicum, foxtail millet *(Setaria italica L.)* was also grown in Stillfried though in a smaller number (Kohler-Schneider, 2001, p. 106, p. 131, p. 133). Since broomcorn millet is a summer grain, Kohler-Schneider (2001, p. 110) argues, that a crop rotation of broomcorn millet and spelt was possible during the Urnfield Period.

Einkorn wheat *(Triticum monococcum L.)* was also one of the most important grown grains in Stillfried. This is atypical for that time period, since einkorn loses its importance during the late Bronze Age. A similar high frequency of einkorn at that time in eastern Austria could only be found in Gars/Thunau (Kohler-Schneider, 2001, p. 112, p. 115).

Barley emmer *(Triticum dicoccum (Schrank) Schübl.)* was also a commonly used grain, even though it was not cultivated as intensive as einkorn or spelt (Kohler-Schneider, 2001, p. 115f).

The good suitability for baking is the reason why the flour of bread wheat and durum wheat *(Triticum aestivum L. s. I., Triticum durum Desf., Triticum turgidum L.)* was used for bread (Kohler-Schneider, 2001, p. 52, p. 127f). Charred leftovers of bread-like objects prove that it was part of the nutrition at that time. Chemical analysis show ingredients like hulled barley *(Hordeum vulgare)* and a wheat species *(Tritium sp.)* (Heiss, Antolín, Berihuete Azorín et al., 2019, p. 14ff). Concerning soil quality, water supply and climate, contemporary sorts of

these grains are not easy to cultivate. However, the earlier types of these grains were more resistant to a cold climate (Kohler-Schneider, 2001, p. 127).

One of the most unpretentious types of grain is barley *(Hordeum sativum L. s. I.).* Charred leftovers document a similar dish than today's risotto containing barley, broomcorn millet and rye brome (*Bromus secalinus)* (Kohler-Schneider, 2001, p. 57, p. 130, p. 156).

1.1.1.5.2 Rare grains

Only a very small number of rye *(Secale cereale L.)* could be retrieved. This indicates, that it was not purposeful grown but can rather be seen as bad weed (Kohler-Schneider, 2001, p. 136).

1.1.1.5.3 Leguminous Plants

A relatively high appearance of lentils *(Lens culinaris Medikus)* indicates a high importance in the nutrition of the people in Stillfried. According to Kohler-Schneider (2001, p. 106, p. 136), it is likely, that lentils have also been cultivated in Stillfried.

Only a small number of peas (*Pisum sativum L.)* and only one seed of tickbeans *(Vicia faba L.)* were found in Stillfried. Due to that fact, the cultivation of peas and beans cannot certainly be proven (Kohler-Schneider, 2001, p. 65, p. 106, p. 138, p. 140).

The few findings of ervil *(Vicia ervilia L. Willd.)* in Stillfried do indicate an intended cultivation, since ervil often appears as bad weed. In Gars/Thunau on the contrary, the cultivation of ervil had be proven due to the finding of thousands of ervil seeds (Kohler-Schneider, 2001, p. 106, p. 140, p. 142).

1.1.1.5.4 Oleiferous fruits

The first archaeobotanical record of seeds of false flax *(Camelina sativa agg.)* origins from the Urnfield Period settlement in Stillfried. It is unclear whether false flax was only bad weed, gathered from somewhere else or intentionally cultivated. It is noticed, that it can always be found in context with broomcorn millet and barley (Kohler-Schneider, 2001, p. 143).

Only a small number of breadseed poppy *(Papaver somniferum L.)* was found during the flotation of soil. But since flax was not found in Stillfried, Kohler-Schneider (2001, p. 144) assumes that breadseed poppy was cultivated to gain linoleic acid which is essential for human health.

1.1.1.5.5 Vine

The record of cultivated vine in Stillfried *(Vitis vinifera L. ssp. vinifera)* is one of the oldest in middle Europe and the oldest record of cultivated vine in Austria. It dates back to 992-810 BC. However, it is unclear whether those grape seeds originate from Stillfried or if they were imported in some form. Tools that can be directly assigned to viniculture have not been found yet (Kohler-Schneider, 2001, p. 52, p. 149).

1.1.1.5.6 Agriculture

The visible spectrum of bad weeds shows an intense amount of soil cultivation. Kohler-Schneider (2001, p. 162f) concludes this due to the high amount of therophytes that were found in Stillfried. In her opinion, the fields for the cultivation of grains, leguminous plants and oleiferous fruits must have been located in the area of the hill country.

As for the summer grains, those must have been panicum, foxtail millet, breadseed poppy, lens, pea, ervil and tick-bean. Spelt and barley were probably grown as a winter grain. (Kohler-Schneider, 2001, p. 52, p. 166f, p. 183).

It is assumed, that a population which moves mostly afoot obtains its resources within a certain radius surrounding their settlement. In this case, Kohler-Schneider (2001, p. 185f) assumes a radius of 4-5 km. The acres might even have been situated within a radius of 1 km although the existence of carriages at that time has to be taken into consideration hence the acres could also have been located in a wider radius around the settlement. It has to be noted, that for hunting or gathering wild plants, people possibly might have also moved to areas further away (Kohler-Schneider, 2001, p. 186).

1.1.1.5.7 Fruits and berries

Remains of strawberries *(Fragaria sp.)*, apple or pear *(Malus/Pyrus)*, cherry or sour cherry *(Prunus avium/cerasus)*, black elder *(Sambucus nigra)*, dwarf elder *(Sambucus ebulus)*, bladder cherry *(Physalis alkekengi)* and European black nightshade *(Solanum nigrum)* were found in the settlement (Kohler-Schneider, 2001, p. 66, p. 169).

1.1.1.5.8 Vegetables

Wild carrots *(Daucus carota)* and melde *(Chenopodium album)* were found in the settlement. The latter were probably mostly used for something similar to spinach (Kohler-Schneider, 2001, p. 173).

1.1.1.5.9 Animal husbandry

Cattle, horses, pigs, sheep, goats, chicken and dogs were held in the settlement of Stillfried. Findings indicate, that cattle (40 %) and pigs (25%) were mainly used as food source. Horses on the other hand seem to have been mainly used for horseback riding or/and as pack animals (Pucher, 1982, p. 22, p. 147ff, Kohler-Schneider, 2001, p. 189). Rangelands must have been available for feeding those animals whereas during the winter they must have been fed from some sort of food stock. Therefore, the greenland as well as the forests might have been used as pasture ground (Kohler-Schneider, 2001, p. 52, p. 189f).

1.1.1.5.10 Hunting

Deer seems to have been one of the most hunted animals in Stillfried. During their seasonal movements, red deer spends the time during winter in floodplain forests and plain tracts. In Stillfried, those animals were probably hunted during the winter. They were most likely hunted for their fur which had its best quality during the winter season. Beavers, wolves, foxes and brown bears are also known to being hunted at that time (Pucher, 1982, p. 144, p. 146, Kohler-Schneider, 2001, p. 192).

As in the case of fishing, pike and carps could be accounted for in the archaeozoological record (Pucher, 1982, p. 146, Kohler-Schneider, 2001, p. 66, p. 192).

Furthermore, mussels and snails were also gathered, in all likelihood mainly during the summer months (Kohler-Schneider, 2001, p. 192).

1.1.1.6 The Burial Grounds of Stillfried

Burials of the cremated dead were custom at that time period (Felgenhauer, 1996, p. 15). The first settlers of the Urnfield Culture's settlement in Stillfried were buried in the burial ground '*Alter Mühlgraben'* (Neugebauer-Maresch, 1978, p. 45, Hellerschmid, 2006, p. 17, p. 22, Hellerschmid, Kern&Lochner, 2010, p. 287). The location of this burial ground was probably north of the municipality of Grub on the so called '*Haspelberg*'. The findings were collected during construction works in 1954 (Neugebauer-Maresch, 1978, p. 21, Hellerschmid, 2006, p. 22).

At the beginning of settlement phase II, people started to bury their dead in the burial ground '*In der Gans'* south of the settlement (Hellerschmid, 2006, p. 17, p. 21f, Hellerschmid, Kern&Lochner, 2010, p. 287, Hellerschmid, 2021, p. 73). It's estimated, that this burial ground contains roughly 2000 burials with an occupation time of about 100 years (Kaus, 1988, p. 113f, Felgenhauer, 1996, p. 15, Hellerschmid, Kern&Lochner, 2010, p. 287, Hellerschmid, 2021, p. 73). About 100 of those burials were excavated (Griebl&Hellerschmid, 2015, p. 183). According to Kaus (1988, p. 115), the cremated dead were mostly buried without an urn. In some of them, foreign influences can be detected. Those include horse-gear with eastern influences, ceramics from the Štítary area, a ceramic vessel of the Mirja Ruše group (Slovenia), ornaments from the west-bohemian Nynicer area and ceramics from the Silesian Culture (Kaus, 1984, p. 23ff, p. 39f, p. 49, Kaus, 1988, p. 118, Hellerschmid, 2006, p. 22, Griebl, 2021, p. 282).

1.1.2 The human and animal skeletal depositions

At the highest point of the fortified settlement, about 25 pits mostly containing complete remains of animals, some containing human remains, came to surface in the excavations by Felgenhauer (Griebl&Hellerschmid, 2015, p. 179).

Additional to the human skeletal depositions, the depositions of (almost) whole animal skeletons which show no signs of dismembering, but signs of captivation during their lifetime are a unique feature for the hillfort site in Stillfried (Pucher, 2018, p. 72).

For example, a deposited red deer seems to have been bridled for some time. Next to another deposited red deer, which died presumably due to a sepsis while having a miscarriage (red deer sign. 7473 (Pucher, 1982, p. 124 f, p. 145, Pucher, 2018, p. 82f)), an anthropoid bone-pendant was deposited (Felgenhauer, 1996, p. 14, Griebl, 2021, p. 307). These two red deer depositions and additional findings of deer parts led Felgenhauer (1996, p. 14) to the

assumption, that deer played the leading part in Stillfried's animal depositions. Nevertheless, there are also other deposited animals such as wolves, dogs, foxes, rabbits, pigs and others (Felgenhauer, 1996, p. 14, Pucher, 2018, p. 73). All in all, a total amount of 31 deposited animals from the 9th to 8th century BC were found during the excavations in Stillfried (Pucher, 2018, p. 73).

One of the deposited animals which we analysed in this study for its strontium isotopic ratio, is a dog found in the pit house V0601 whose remains showed many signs of abuse which partly started to heal again (Hellerschmid, 2006, p. 49f, Griebl&Hellerschmid, 2013, p. 334).

Many of the deposited animals show anomalies, growth disturbances caused by stress or skeletal traumas which were often healed (Pucher, 1988, p. 160f, Pucher, 2018, p. 74ff). According to Pucher (2018, p. 71, p. 75ff), the reduced brain capacity of the wolves as well as their congenital dental anomalies accord to those of zoo wolves. These are signs for the captivity of those wild animals during their whole lifetime (Griebl&Hellerschmid, 2015, p. 186, Pucher, 2018, p. 71).

As for the human depositions, Griebl&Hellerschmid (2013, p. 331) divide those in two different types. The first type includes depositions of only parts of human skeletons, mostly skull fragments. Seven deposited crania or fragments of such, dating to the Urnfield Period, have been found. One of those, the cranium of a girl (individual sign. 1377) will be discussed later on. Depositions of complete skeletons form the second group.

Apart from the later discussed skeletons of the pit V0841 and V1141, the skeleton of a woman, who was probably pushed into a burning house (V0601) was found. In the case of the latter, it was rather an accident than an intended deposition (Felgenhauer, 1996, p. 15, Hellerschmid, 2006, p. 49f, Griebl&Hellerschmid, 2013, p. 334).

Similar findings are for example those of three deposited individuals (male, female and child) in Thunau am Kamp and the skull of a child showing signs of violence found in Brno-Obřany (Griebl&Hellerschmid, 2015, p. 184, Wiltschke-Schotta&Renhart, 2021, p. 274). Furthermore, in Mannersdorf/Leithagebirge displaced human skeletal remains of a female were found (Wiltschke-Schotta&Renhart, 2021, p. 274). The remains of a human male individual werde found within a pit in Unterradlberg (Wiltschke-Schotta&Renhart, 2021, p. 274). In Pusztataskony-Ledence 1 (eastern Hungary), similar human depositions to those in pit V0841 could be found (Király, Sebők, Zoffmann et al., 2013, p. 307ff).

Earlier records of similar skeletal depositions can also be found in the bohemian Knovíz Culture of north and northwest Bohemia (Bz D–Ha B) (Griebl&Hellerschmid-Artner, 2012, p. 2).

1.1.2.1 Pit V1141 – 'The Seven from the pit'

During the excavation of the pit V1141 in 1976, the skeletons of seven human individuals came to surface (Felgenhauer, 1978a, p. 104). The former pit was located at the western part of the *'Kirchhügel'* near the western rampart. Until today, those skeletons are known as 'The seven from the pit' (Breitinger, 1980, p. 46, Breitinger, 1981, p. 3).

According to anthropological examinations, the seven individuals consisted of one approximately 30 years old male (Sk. 1, sign. 9023), two grown up females (Sk. 3 - approx. 40 years old and Sk. 5 - approx. 45 years old), one girl (Sk. 7 - approx. 9 years old) and three boys (Sk. 2 – approx. 3 years old, Sk. 4, sign. 9026 – approx. 8 years old and Sk. 6– approx. 6 years old). The analysis also showed, that anthropologically, there are no signs of *peri mortal* violence detectable (Breitinger, 1980, p. 70 ff, Breitinger, 1981, p. 3ff, p. 12). This led Eibner (1980, p. 133ff), (1988, p. 82f) to the conclusion, that the death of those individuals was the result of a political feud which probably resulted in poisoning (Szilvassy, Kritscher&Hauser, 1988, p. 56). The absence of severe diseases also led Eibner (1988, p. 84) to the assumption, that those people might have belonged to the upper-class of Stillfried.

According to morphometric analysis Breitinger (1981, p. 6f) concluded, that those individuals are related and a family of a father, two mothers and their children. Szilvassy, Kritscher&Hauser (1988, p. 55) however assign the kinship within this family differently. They assign all the children to one mother (Sk. 5), the second woman (Sk. 3) seems more likely to be the sister of the man (Sk. 1). Heiling-Schmoll (1985, p. 44) made the assumption, that this was a foreign family whose members were therefore buried differently. The results of $n(^{87}Sr)/n(^{86}Sr)$ isotope ratio analysis (chapter 1.4 explains this term in more detail) conducted by Teschler-Nicola, Irrgeher&Prohaska (2016, p. 165 f) disprove the kinship model by Szilvassy, Kritscher&Hauser (1988, p. 55). The birth place of two of the children (Sk. 6; 6 years and Sk. 7, 9 years) is allochthonous situated (=originating from a different place than where buried) (probably the same as the female Sk. 5 dedicated as the mother in the Szilvassy model) while the other two children (Sk. 2 - 3 years and Sk. 4 - 8

years) are autochthonous (= native) which all together interfers with the age of the children. With the exception of the 6-year old boy Sk. 6, the family model by Breitinger (1981, p. 6f) is in agreement with the individuals' origin determined by $n(^{87}Sr)/n(^{86}Sr)$ isotope-amount ratio analysis. Recent mtDNA-analysis shed further light on the question of genealogy. According to Parson, Eduardoff, Xavier et al. (2018, p. 150), only Sk. 5 (the 45 year old female) is maternally related to the boy Sk. 6.

There is the possibility, that the pit V1141 is connected to the male skull cap V2350, which was deposited on a horse bone, and the timber-clay construction V2274. Both were located above the pit. The construction V2274 in which's floor half of a vessel and the fragment of a loom weight had been inserted could have possible been a shrine for the seven deposited individuals (Hellerschmid, 2015, p. 217).

The pit V1141, V2274 and V2350 can be correlated with the first destruction of the rampart at the end of phase II or the beginning of phase III of the settlement. This responds to a time of about 900 BC – 850 BC (Ha B2 – Ha B3) (Hellerschmid, 2015, p. 228, Griebl, 2021, p. 304).

1.1.2.2 Pit V1133

The cranium of a 12-year old girl, which was found in a pit near the western part of the settlement (settlement Phase III/1) (Hellerschmid, 2006, p. 21), shows head injuries which indicate multiple hits to the head (Breitinger, 1976, p. 95ff). Similar injuries were also often found in deposited individuals of the Knovíz Culture (Breitinger, 1980, p. 89).

Furthermore, a possible widening of the *Foramen magnum* could be detected. Such a widening could indicate a brain removal after the girl's death (Breitinger, 1976, p. 98f). According to Teschler-Nicola, Irrgeher&Prohaska (2016, p. 162) however, the injury at the *Foramen magnum* is more likely a ring fracture than the result of removing the brain.

In addition, the remains of a young dog (about half a year old) were found in pit V1133. Its cervical vertebrae showed deformations (Griebl&Hellerschmid, 2013, p. 331).

The findings of burnt barley glumes (*Hordeum sp.*) (Sauter, Wurst&Hoke, 1976, p. 101, Sauter, 1988, p. 170, Griebl, 2021, p. 299) near the cranium of the girl, as well as fragments of a rare vessel, a so called *'Deckeldose',* indicate some cultic actions (Eibner, 1976, p. 77, Felgenhauer, 1985, p. 10, Griebl, 2021, p. 299). The burnt barley glumes were also found in oddly formed ovens near the pit. Near those ovens, another pit, which contained fragments of ceramics vessels was found. Those contained heated birch tar (Sauter, 1988,

p. 177, Felgenhauer, 1996, p. 15). A ceramic fragment of that pit, which, according to Felgenhauer (1996, p. 15), fits exactly to another fragment found in pit V1133, connects those two pits.

1.1.2.3 Pit V0841

The pit is located near the western hill fort of the settlement on the so called *'Hügelfeld'*. It can be assigned to the end of the Urnfield Period (Ha B3/C1a) which correlates to settlement phase III/2 around 850 – 800/780 BC (Ha B2 – Ha B3) (Hellerschmid, 2006, p. 293, Hellerschmid, 2015, p. 208). Griebl (2021, p. 305) on the other hand, assigns the deposition of those remains to the previous settlement phase III/1 (the last construction phase of rampart II). During the excavation of this pit, the remains of altogether 23 human individuals came to surface. Thereof, the bodies of 16 individuals were not cremated. Some of those un-cremated remains seem to have been deposited carefully, some do not. Furthermore, the remains of seven badly cremated individuals were found (Felgenhauer, 1988, p. 282f, Griebl&Hellerschmid, 2013, p. 334ff, Wiltschke-Schotta&Renhart, 2021, p. 271).

The individuals show anomalies and signs of diseases (e.g. four individuals possibly suffered from meningitis, others show *Cribra orbitalia,* many show deficiency symptoms) (Wiltschke-Schrotta, 2006, p. 414f, Griebl&Hellerschmid, 2013, p. 335 ff, Wiltschke-Schotta&Renhart, 2021, p. 276).

The first skeletal layer contained the remains of a woman (skeleton 13, sign. 9054, approx. 50 years old) and two children (skeleton 11, sign. 9052 - approx. 8 years old and skeleton 12 – approx. 8 years old). Afterwards in the second skeleton layer, the remains of a child with microcephaly (skeleton 10 , sign. 9051– approx. 3 – 4 years old), a subadult individual (skeleton 9), possibly male individual (skeleton 8, sign. 9049 – 15 - 18 years old), a woman (skeleton 14 – approx. 20 – 25 years old) and the upper body part of a child (skeleton 15 – approx. 3 – 4 years old) came to surface. It seems, that the individuals in the third skeletal layer were thrown carelessly in the pit. Bite marks of animals, diseases and signs of violence can be found on all of the skeletons. This layer contained the remains of an about 18 years old individual (skeleton 7) whose positions of arms and legs indicate captivation. Furthermore, the femur, pelvis and vertebrae of a female individual (skeleton 5/I – approx. 20 - 25 years old), the head and some ribs of a possibly male individual (skeleton 3 or here 9043), the torso of a female individual (skeleton 6, approx. 30 years old), the head of a child (skeleton 5/II, sign. 9046, approx. 10 – 12 years old) and the almost complete remains of

another child (skeleton 4, sign. 9044 – approx. 13 – 15 years old). The fact that all of the individuals of this layer have animal bite marks indicates that the bodies of those individuals were left unburied for a while. The head of skeleton 5/2 shows perimortal head strikes. In the fourth skeletal layer, badly cremated bones of seven individuals (skeletons 16 – 22) were found. Moreover, the skeletons of a male individual (skeleton 1, 40 – 60 years old) and a child (skeleton 2, sign. 9042, approx. 8 – 9 years old) were found in this skeleton layer. Except for skeleton 1, who carried a sharpening stone, a knife made of bronze and two fishing-hooks with him, none of the individuals carried objects with them (Griebl&Hellerschmid, 2013, p. 335ff, Griebl, 2021, p. 302ff, Wiltschke-Schotta&Renhart, 2021, p. 271).

1.2 Strontium isotopy and Human migration during the european Bronze Age

Previous studies showed a significant percentage of allochthonous individuals in bronze age settlements or burial sites. For example, during the early Bronze Age, about 20 % (20 % female, 22 % male individuals and 10 % individuals of unknown sex) of the 103 analysed inhumations in Franzhausen I were classified as allochthonous according to their *n* $n(^{87}Sr)/n(^{86}Sr)$ isotope-amount ratio analysis (Kreutz, 2011, p. 94). In Franzhausens Neolithic population however, only 12 % non-local individuals could be identified (Irrgeher, Teschler-Nicola, Leutgeb et al., 2012, p. 206).
The Bronze Age site of Hainburg/Donau consists of 86 % autochthonous and 14 allochthonous individuals according to their $n(^{87}Sr)/n(^{86}Sr)$ isotope-amount ratio. (Irrgeher, Weiß, Krenn-Leeb et al., 2011, p. 36).

In their study, Knipper, Fragata, Nicklisch et al. (2016, p. 510, p. 512) found no certain connection between deviant burials, (including settlement pits), and non-local inhumations during the Únětice Culture (early Bronze Age) in Central Germany. Out of the analysed burials, at Esperstedt 22.2 % (two out of nine analysed individuals) were allochthonous 21.1 % (four out of 19 individuals) were allochthonous in Karsdorf, 10 % (one out of ten individuals) at Röcken, 9.1 % (one of eleven individuals) at Plötzkau to none at all at Osterwieck, Leau, Brehna and Serbitz could be identified as allochthonous.

According to (Cavazzuti, Skeates, Millard et al., 2019, p. 36) preferentially women were identified as allochthonous. Furthermore, they detected large differences between smaller

settlements and larger central places concerning migration. Hence the latter showed significant more patterns of migration beyond regional boundaries, whereas the smaller settlements showed lesser spacious migrations.

Concerning the Urnfield Culture, about one third of adult inhumations could be identified as allochthonous at the burial site of Neckarsulm, Germany (Hallstatt A1 to Hallstatt A2). Furthermore, it became clear, that only 25 % of the allochthonous individuals, compared to nearly 50 % of autochthonous individuals had been buried in single graves (Wahl&Price, 2013, p. 302).

1.3 Teeth

1.3.1 Human teeth

Four different tissues form the human tooth. They can be divided into soft and calcified tissues. The soft tissue is located in the dental pulp which is located within the pulp cavity, the three calcified tissues are the dentine, enamel and cementum (Türp&Alt, 1998, p. 73) (see Fig. 3).

The dental pulp consists of the coronal pulp which is located in the pulp chamber, and the radicular pulp which is located in the root canals. The pulp contains blood and lymph vessels, nerve fibers and cells like fibroblasts, mesenchymal cells and odontoblasts. A layer of odontoblasts surrounds the pulp cavity (Türp&Alt, 1998, p. 73). The odontoblasts function is the lifelong dentinogenesis, meaning the formation of dentine alongside the pulp cavity throughout an individual's life (Hillson, 1996, p. 194).

Dentine consists of (by weight) 70 % inorganic matrix (mostly calcium and phosphate in hydroxyapatite crystals), 20 % organic matrix (collagen), and the remaining 10 % are water. (Türp&Alt, 1998, p. 73). Primary dentine is formed during tooth mineralisation. The formation of the thin layer of secondary dentine continues throughout an individual's lifespan. Irregular secondary dentine (or tertiary dentine) is formed to repair damage to the tooth such as caries (Hillson, 1996, p. 194).

Dental enamel coats the crown of each tooth with a mineralized layer that can be more than 2 mm thick (Hillson, 1996, p. 148). It is chemically composed of 95 % inorganic matrix, 1 % organic matrix and 4 % water by weight. It is formed by ameloblasts and consists of prisms built of hydroxyapatite crystals (Türp&Alt, 1998, p. 74). After its formation, dental enamel is not remodelled (Hillson, 1996, p. 118f).

The root cementum surrounds the root dentine (Türp&Alt, 1998, p. 74). It is formed by so called cementoblasts and has no blood or nervous supply. The cement also has no continuous turnover (like dentine or bone) but it can be remodelled by the activities of odontoclasts which are cement-destroying cells and cementoblasts, which can repair damaged areas (Hillson, 1996, p. 198). At the cervix of the tooth, the cementum is the thinnest and its thickness increases towards the apex of the root. By weight, it consists of 61 % inorganic matrix, 27 % organic matrix and 12 % water (Türp&Alt, 1998, p. 74).

The enamel formation of those teeth that were used in this thesis takes place at the following ages according to (AlQahtani, Hector&Liversidge, 2010, p. 5).The P1 gets formed between the age of 2.5 years and 5.5 years. At the age of 3.5years to 6.5 years the P2 is formed. As for the deciduous teeth, the formation period of the crown of the m1 starts at approx. 30 weeks *in utero* and ends at the age of 7.5 months. The deciduous canine is developed from 30 weeks *in utero* to the age of 7.5 months.

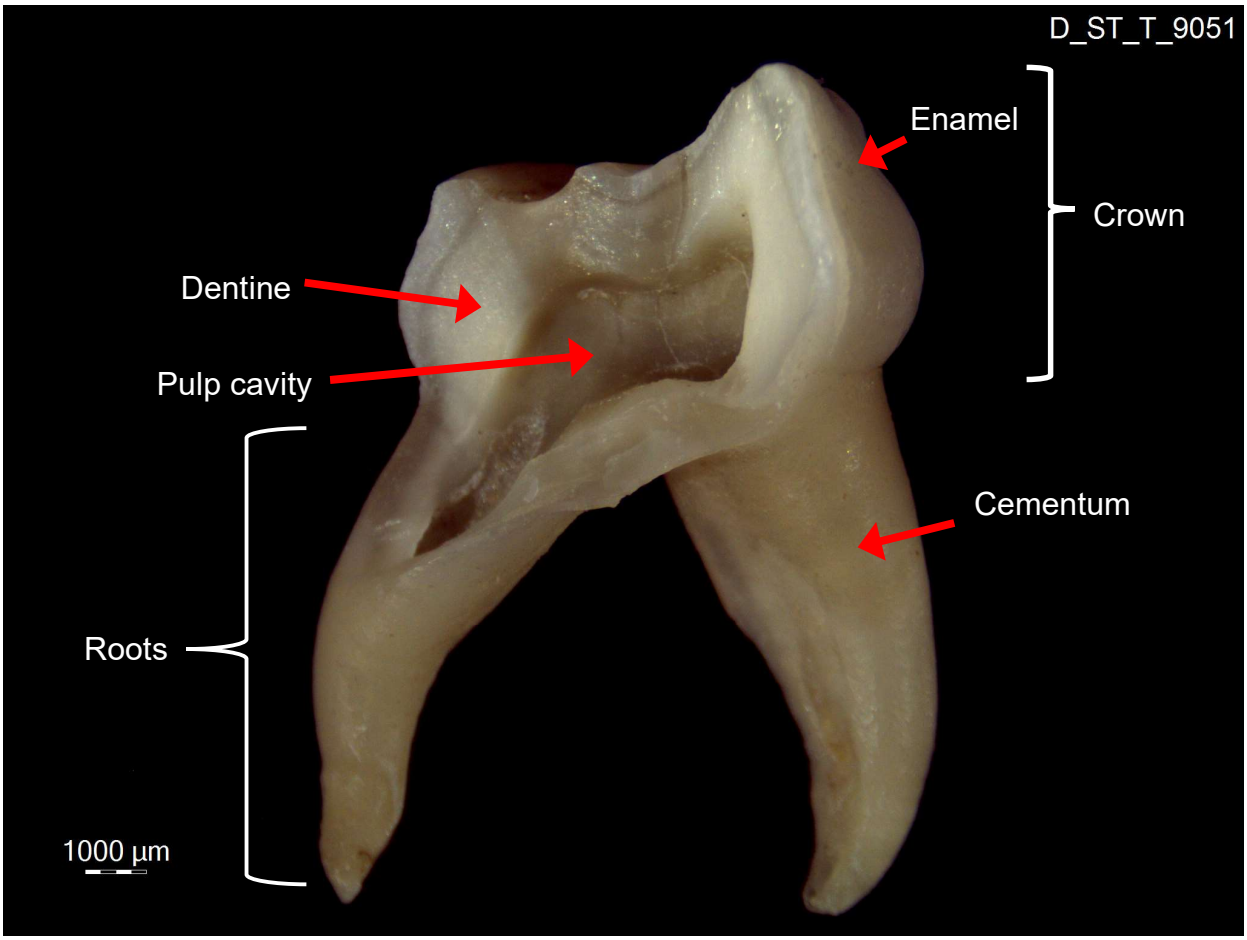

Figure 6 Compartments of a tooth on the example of the decidual tooth of skeleton 10 of pit V0841 (Picture: Anna-Maria Kriechbaum).

1.3.2 Animal teeth

The composition of many animal teeth is (almost) the same as the composition of human teeth (see Fig. 4).

The rodent tooth (in this thesis, the tooth of a beaver was analysed) on the other hand, shows a different composition. Only the outside part of the tooth is covered with enamel. At the inside part (ligual), the dentine is at the surface. The roots of the teeth are open. Furthermore, rodent teeth are permanently growing throughout the animals' life (Schmid, 1972, p. 78).

The canines of the male *Sus* are permanently growing and the root is open (see Fig. 5). The canines of the female *Sus* on the other hand, are smaller and the root is closed (Schmid, 1972, p. 80).

The occlusal surface of the molar teeth of herbivores shows enamel, dentine and cement (Fig. 4). All three form specific patterns (Schmid, 1972, p. 82).

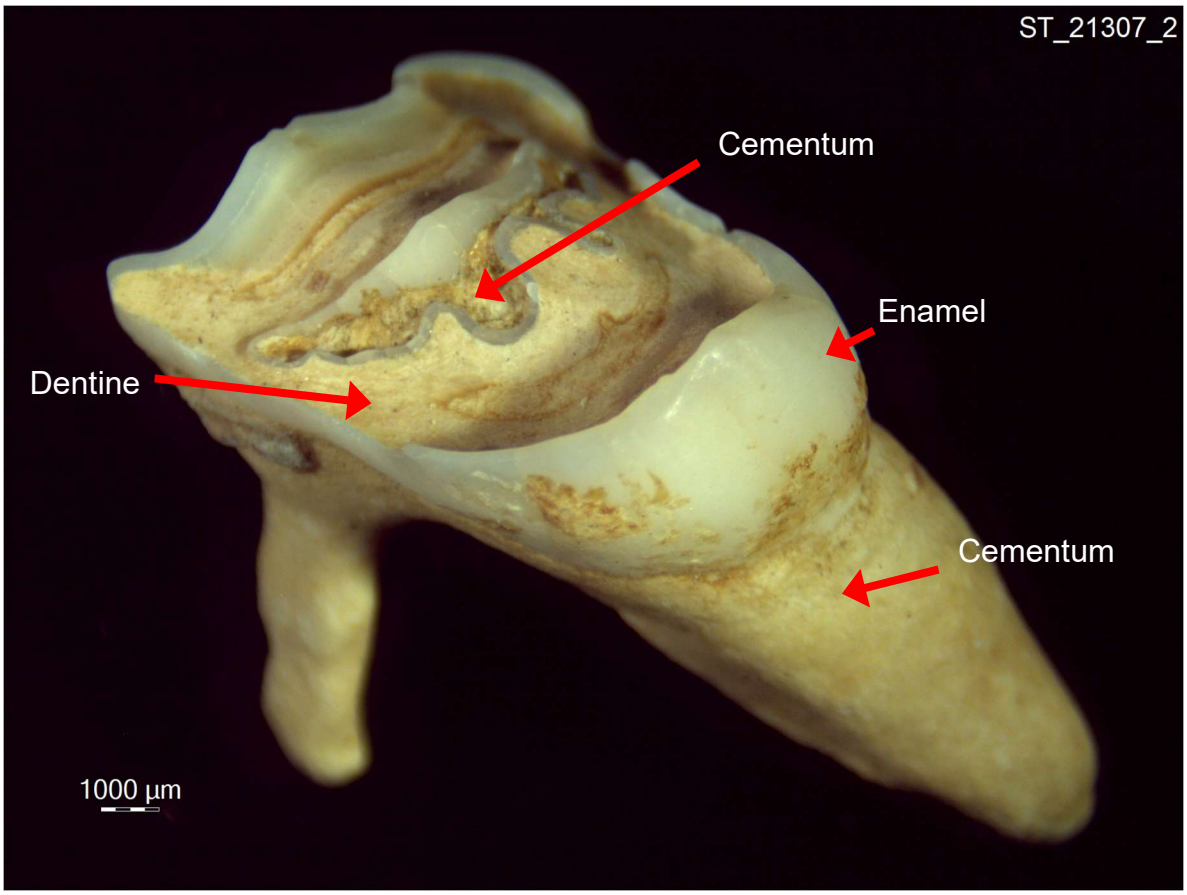

Figure 7 Composition of the tooth of the roe deer ST_21301 (Picture: Anna-Maria Kriechbaum)

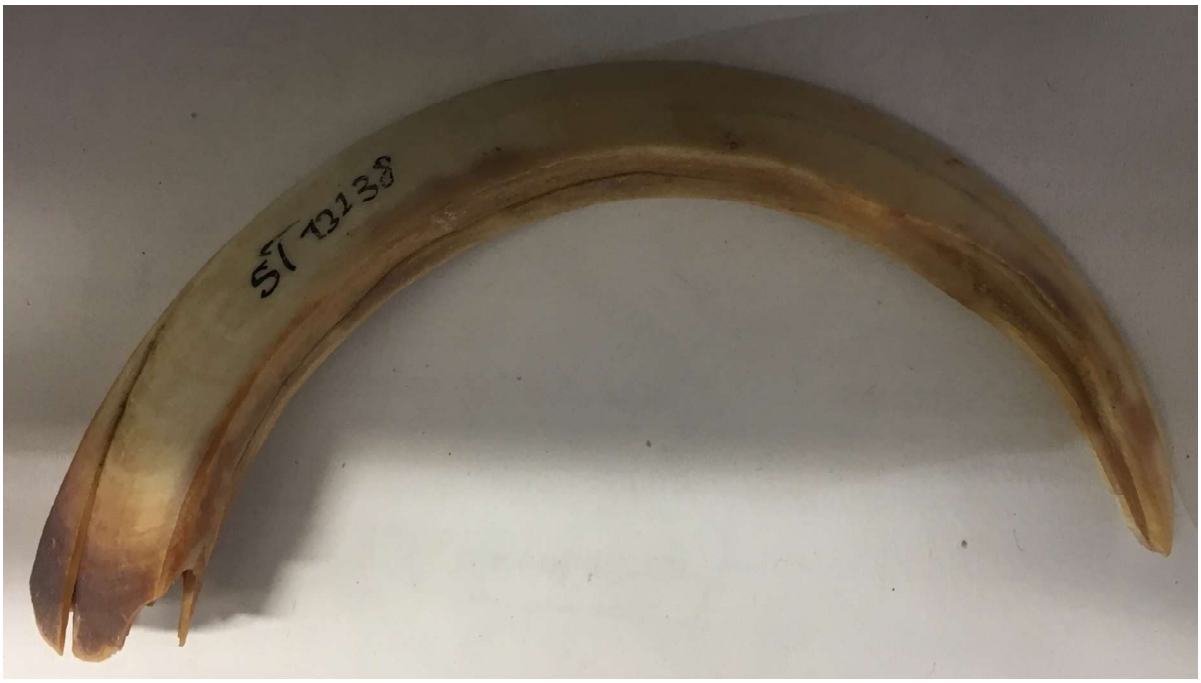

Figure 8 Complete canine of Sus scrofa ST_SS_13238, showing the open root on the left side. (Picture: Anna-Maria Kriechbaum)

1.4 $n(^{87}Sr)/n(^{86}Sr)$ isotope-amount ratio analysis as archaeometric tool

Archaeologists often explain the appearance of new or foreign features in the archaeological record as a result of migration (Price, Grupe&Schröter, 1998, p. 405). To determine migration in archaeological contexts, the usage of material diffusion or diffusion of knowledge can give a hint, but it is no definite proof for migration. Material and knowledge could just as easily be spread, by trade for example.

During the last decades, the analysis of incorporated environmental Strontium isotope ratios (often referred to as biosphere isotopic fingerprint (Montgomery, Evans&Wildman, 2006, p. 1626) in human and animal skeletal remains by either multi-collector inductively coupled plasma mass spectrometry (MC ICP-MS) or multi-collector thermal ionization mass spectrometry (MC TIMS) has been evolved as a key tool in archaeology to trace residential changes and to investigate migration (Ezzo, Johnson&Price, 1997, p. 447ff, Grupe, Price, Schröter et al., 1997, p. 519, Latkoczy, Prohaska, Stingeder et al., 1998, p. 561, Price, Grupe&Schröter, 1998, p. 405, Bendrey, Hayes&Palmer, 2009, p. 146, Montgomery, 2010, p. 325f, Price, Knipper, Grupe et al., 2013, p. 13, Bartelink&Chesson, 2019, p. 34).

Naturally, four stable Strontium isotopes occur: ^{84}Sr with an abundance of 0.56 %, ^{86}Sr (9.86 %), ^{87}Sr (7.00 %) and ^{88}Sr (82.58 %) (CIAAW). But the main interest lies in the natural $n(^{87}Sr)/n(^{86}Sr)$ isotope-amount ratio, which varies in the geosphere according to the radioactive decay of ^{87}Rb to ^{87}Sr with a half-life of approx. 4.9×10^{10} years. It is a conventional measure for the variability in nature as a function of geological age and the original Rb/Sr ratio (Faure, 1986, p. 117ff, Capo, Stewart&Chadwick, 1998, p. 199ff). The bioavailable Sr is released via weathering from the bedrock material and is transported throughout the biosphere. Due to its chemical similarity to Calcium, Sr is incorporated into plants and animals, and from there into the human organism as substitutes for Calcium (Bentley, 2006, p. 136, Tütken, 2010, p. 33, p. 41). Within the (animal and human) body, the majority of Sr is deposited in the hard tissue, e.g. teeth and bones (Price, Grupe&Schröter, 1998, p. 407). During the biological up-take no measurable fractionation of the environmental $n(^{87}Sr)/n(^{86}Sr)$ isotope signature takes place (Capo, Stewart&Chadwick, 1998, p. 215, Blum, Taliaferro, Weisse et al., 2000, p. 95).

1.4.1 Sr turnover of human hard tissue

In general, enamel only develops once during an individual's lifetime and hence shows no turnover afterwards (Tütken, 2010, p. 35f). The formation times of all dental enamel differ

depending on the type of tooth, but all enamel formations complete within the childhood years (approx. 15.5 years) (AlQahtani, Hector&Liversidge, 2010, p. 5). Consequently, after full mineralization of the enamel, the incorporated $n(^{87}Sr)/n(^{86}Sr)$ isotope-amount ratio is stable, even if the individual migrates to a place featuring a different $n(^{87}Sr)/n(^{86}Sr)$ isotope-amount ratio in its nutrition sources. Therefore, enamel serves as an 'archive of the childhood' (Grupe, 1998, p. 337)

The period of an individual's life potentially preserved in its dentine as biogenic Strontium is controversially discussed in literature. The primary dentine formation period exceeds those of enamel, potentially capturing information of places of residence during adolescence. Continuous formation of secondary dentine throughout adulthood potentially captures the $n(^{87}Sr)/n(^{86}Sr)$ isotope-amount ratio representing the last years of the individual's life (Hillson, 1996, p. 194).

Furthermore, bones can be used to determine the $n(^{87}Sr)/n(^{86}Sr)$ isotope-amount ratio of the individual's last years of life due to it's continuous remodelling throughout the individual's life. Nonetheless, due to the different turnover rates in bones, an exact assessment of the time of change cannot be accessed easily (Tütken, 2010, p. 34).

By comparing the $n(^{87}Sr)/n(^{86}Sr)$ isotope-amount ratio of an individual's enamel with the $n(^{87}Sr)/n(^{86}Sr)$ isotope-amount ratio of its dentine and/or, the residential changes between childhood, potentially adolescence and adult life are made visible (Tütken, 2010, p. 34ff).

1.4.2 Post-depositional alterations of human hard tissue

The term 'diagenesis' describes the biological, chemical and physical process that alters archaeological material in its surrounding environment of burial during deposition. This means, that a modification of the material's original chemical structure via the local chemical properties takes place. The buried remains may absorb the diagenetic Sr from its surroundings (e.g. soil, groundwater) which occurs in form of inorganic modifications and structural alterations, and may alter the biogenic Sr isotopic signature (Wilson&Pollard, 2002, p. 644 ff). Therefore it has to be taken into account while analysing and interpreting Sr isotopic results.

Indicators for diagenesis are elevated mass fractions of Al, Si, Ba (>10 $\mu g\ g^{-1}$ - 100 $\mu g\ g^{-1}$), the presence of elevated mass fractions of V, Fe and Mn and/or the presence of (ultra-) trace elements like REE, Y, Hf, Th and U (Kohn, SchoeninGer&Barker, 1999, p. 2739ff, Trueman, Palmer, Field et al., 2008, p. 153ff, Koenig, Rogers&Trueman, 2009, p. 513ff,

Benson, Kinsley, Willmes et al., 2013, p. 2991, Kohn&Moses, 2013, p. 419ff, Willmes, Kinsley, Moncel et al., 2016, p. 109ff, Kamenov, lofaro, Goad et al., 2018, p. 2f).

Due to its compacts structure, enamel is less susceptible to diagenetic alterations than dentine (Grupe, 1998, p. 338, Kohn, SchoeninGer&Barker, 1999, p. 2738, Lee-Thorp&Sponheimer, 2003, p. 214f, Dudás, Leblanc, Carter et al., 2016, p. 23), which makes enamel a reliable matrix for historic migration studies. Modern human Sr mass fractions in enamel range between 50 μg g^{-1} and 300 μg g^{-1}. They depend on the geological background and the individual's lifestyle. Elevated Sr mass fractions (> 250 μg g^{-1}) and depleted Sr mass fractions (< 100 μg g^{-1}) are seen as an indication for diagenetic modification in enamel and dentine (Montgomery, Evans&Cooper, 2007, p. 1510, Dudás, Leblanc, Carter et al., 2016, p. 27).

1.4.3 Interpretation of Sr isotopic ratios in human enamel

A reference Sr isotopic signature of the habitat under investigation is required for the identification of autochthonous[1] and allochthonous[2] individuals. This is commonly achieved by the estimation of the so-called local bioavailable Sr isotopic signature (Price, Burton&Bentley, 2002, p. 122ff, Montgomery, Evans&Wildman, 2006, p. 1626, Maurer, Galer, Knipper et al., 2012, p. 217, Söllner, Toncala, Hölzl et al., 2016, p. 123, Crowley, Miller&Bataille, 2017, p. 46, Lengfelder, Grupe, Stallauer et al., 2019, p. 247). Using $n(^{87}Sr)/n(^{86}Sr)$ isotope-amount ratio references of the local soil, water, fauna and/or flora, one can determine the local bioavailable $n(^{87}Sr)/n(^{86}Sr)$ isotope range and generate an isoscape of the area under investigation to which the $n(^{87}Sr)/n(^{86}Sr)$ isotope-amount ratio of the analysed individuals is compared. According to Price, Burton&Bentley (2002, p. 124f) the local fauna is a better proxy to determine the local biological $n(^{87}Sr)/n(^{86}Sr)$ isotope-amount ratio range compared to the local flora.

The autochthonous Sr isotopic signature can be calculated using a mixing model under consideration of different sources of stable Sr isotopes with different, diet-dependent amounts and contributions . In absence of archaeological samples from nutrition sources, the autochthonous Sr isotopic signature can be estimated using presumably locally raised (archaeological) animals and humans found at the site (Grupe, Price, Schröter et al., 1997,

[1] Native in the place where buried.
[2] Originating from a place other than where buried.

p. 518, Price, Burton&Bentley, 2002, p. 124f, Bentley&Knipper, 2005, p. 629, Irrgeher, Teschler-Nicola, Leutgeb et al., 2012, p. 200, Maurer, Galer, Knipper et al., 2012, p. 217). The autochthonous Sr isotopic reference allows for the determination whether an individual's $n(^{87}Sr)/n(^{86}Sr)$ isotope-amount ratio is supposedly autochthonous or allochthonous (Grupe, Price, Schröter et al., 1997, p. 518, Price, Grupe&Schröter, 1998, p. 407, Montgomery, 2010, p. 336, Tütken, 2010, p. 41, Price, Knipper, Grupe et al., 2013, p. 14).

1.5 Inductively coupled plasma mass spectrometry (ICP-MS)

A mass spectrometer separates charged ions based on their mass-to-charge ratio which can be done due to their different motions in an electrical or magnetic field. Then, it counts the separated ions (Prohaska, 2015, p. 29f).

The mass spectrometer consists of three essential parts, an ion source where the ions are generated from the sample, a mass separator which separates these ions by their mass-to-charge ratio and an ion detector for quantitatively detecting the separated ions according to their mass-to-charge ratio (Prohaska, 2015, p. 29).

In general, the sample in liquid form gets transferred into the sample introduction system via a peristaltic pump (Jakubowski, Horsky, Roos et al., 2015, p. 218f). The advantage of a peristaltic pump, is the insurance of a constant liquid flow (Thomas, 2001a, p. 56). Here, a nebuliser is used for generating an aerosol with the help of, in this case, argon gas flow. From there, the sample goes into the spray chamber from where just the smallest aerosol droplets enter the plasma (Jakubowski, Horsky, Roos et al., 2015, p. 218f, 271). The main function of the spray chamber is to ensure, that the large droplets (> 10 μm in diameter) exit through the drain tube and only small droplets (5-10 μm in diameter) can enter the plasma (Thomas, 2001a, p. 57). The plasma is generated electrodeless in Ar gas by applying high-frequency voltages to an induction coil located on the top of a plasma torch (Jakubowski, Horsky, Roos et al., 2015, p. 218). The torch consists of three concentric quarz tubes – the outer and middle tube and the sample injector (Thomas, 2001b, p. 28). Usually, three different Ar gas flows are used (a low Ar gas flow rate to transport the aerosol into the plasma, a higher rate of Ar gas as coolant gas and a third auxiliary gas flow for tuning the

plasma position within the torch). In the plasma, the particles in the aerosol get volatilised, atomised and finally ionised (Jakubowski, Horsky, Roos et al., 2015, p. 218f).

The ion beam then travels through the cooled sample and the skimmer cone. Directly behind the skimmer cone, an extraction lens is usually placed. Its task is to attract and accelerate ions leaving the extraction chamber. Then, the ions are separated due to their mass-to-charge ratio (m/z) in the mass analyser. (Jakubowski, Horsky, Roos et al., 2015, p. 208, 219ff).

A slit system is necessary to shape the ion beam which then gets transported to the detection system. Secondary electron multipliers and Faraday cups are mostly used for ion detection (Jakubowski, Horsky, Roos et al., 2015, p. 215). The detected signal is then often reported as counts per second (cps) or volts (Prohaska, 2015, p. 30).

1.5.1 Inductively Coupled Plasma – Quadrupole Mass Spectrometer (ICP-QMS)

In this thesis, an ICP-QMS was used for multi-element analysis (MEA). This type of ICP-MS uses a quadrupole for the ion separation (Prohaska, 2015, p. 35). Here, the quadrupole filters ions with a specific mass-to-charge ratio. Only those specific ions then get transferred to the ion detector, all other ions get eliminated. This means, that ions with a different mass-to-charge ratio cannot be detected simultaneously but only consecutively (Perkin Elmer, 2010, p. 19).

1.5.2 Multicollector - Inductively Coupled Plasma – Mass Spectrometer (MC-ICP-MS)

Here, a MC-ICP-MS was used for Sr isotope analysis. The benefit of a multicollector is the possibility to count multiple ion beams simultaneously on a set of detectors (Prohaska, 2015, p. 37). In the common geometry, the MC ICP-MS–consists of an electrostatic analyser followed by a magnetic sector. The ion beams are separated according their mass-to-charge ratio in the magnetic sector. The detector of these instruments usually consists of set of Faraday cups and ion counter units. Furthermore, the achievable precision via multicollector is significantly higher in case of isotope ratio analysis than it is using a single-collector instrument (Jakubowski, Horsky, Roos et al., 2015, p. 208, 213, 240).
In the case of isotope ratio analysis, the magnetic field for the ions separation is set for a range of isotopes and then kept constant. Instead of counts per second (cps), the measured signal is given in volts (but can be converted in cps) (Prohaska, 2015, p. 37).

2 Research Question

The significant differences in the mode of burial in the Urnfield Culture buarial site of Neckarsulm, Germany (Wahl&Price, 2013, p. 302) and the study of Knipper, Fragata, Nicklisch et al. (2016, p. 510) concerning deviant burials during the earlier Únětice Culture (early Bronze Age) (see chapter 1.2), led to the following research question:

Are the analysed inhumations, which are deposited deviant for the Urnfield Period, of allochthonous origin?

Strontium isotopic ratio analysis were used to answer this research question, consequently leading to get a better understanding of Stillfried's population structure and to enrich the debate about the funeral customs of the Urnfield culture.

3 Material and Methods

3.1 Samples

3.1.1 Archaeological Samples

The archaeological samples are human (Table 1) and animal teeth (Table 2), mussels (Table 2), straw (Table 3), wood (Table 3) and soil (Table 3) from the excavations at the late Urnfield Period site in Stillfried/March. The samples were provided by the Austrian Academy of Science and the Natural History Museum in Vienna.

In this study, the first premolar was preferentially used for sampling of human enamel and dentine. In three cases, another tooth was used - a second premolar, a deciduous first molar and a deciduous canine (see Table 1).

The animal teeth taken from species e.g. the wild boar and domesticated animals such as the dog, mussels and archaeological environmental samples were used to determine a local and autochthonous $n(^{87}Sr)/n(^{86}Sr)$ isotope signal. Furthermore, recent environmental samples were taken. This will be discussed in the following chapter.

Table 1 Sample list of the human teeth provided by the Natural History Museum Vienna

Sample ID	Pit	Interface	Sex and Age	Signature	Identification	Tooth (FDI)
ST_T_9042	V0841		Infans II, 8-9 years	9042	skeleton 2	14
ST_T_9043	V0841		Male ?, Adult, 25-35 years	9043	skeleton 3	15
ST_T_9044	V0841		Juvenis, 13-15 years	9044	skeleton 4	24
ST_T_9046	V0841		Infans II, 10-12 years	9046	skeleton 5/II	14
ST_T_9049	V0841	IF2079	Male? Juvenis, 15-18 years	9049	skeleton 8	14
ST_T_9051	V0841	IF2081	Infans I, 3-4 years	9051	skeleton 10	64
ST_T_9052	V0841	IF2082	Infans II, 8-10 years	9052	skeleton 11	14
ST_T_9054	V0841	IF2084	Female ? 40-60 years	9054	skeleton 13	14
ST_T_9023	V1141	IF2247	Male, Adult 30 years	9023	skeleton 1	14
ST_T_9026	V1141	IF2250	Male, 8 years	9026	skeleton 4	73
ST_T_1377	V1133		Female, 12 years	1377		14

Table 2 Sample list of animal teeth- and mussel samples provided by the Natural History Museum Vienna

Sample ID	**Pit**	**Animal**
ST_CE_7473	7653 (?)	red deer; *Cervus elaphus*
ST_M_13289	V0841	mussel
ST_CF_8855	V0601	dog, *Canis lupus f. familiaris*
ST_21307	V2784 - V3784	roe deer, *Capreolus capreolus*
ST_SS_13238	V0841	wild boar, *Sus scrofa*
ST_M_13238	V0841	mussel
ST_M_13272	V0841	mussel
ST_CF_13285	V0841	dog, *Canis lupus f. familiaris*
ST_CA_13286	V0841	beaver, *Castor fiber*
ST_M_13311	V0841	mussel
ST_SD_13332	V0841	pig, *Sus scrofa f. domesticus*

Table 3 Sample list of archaeological environmental samples

Sample ID / Find Number	**Sample Type**	**Object**	**Location**
ST_7649	straw	1154	western rampart, construction II
ST_9864	wood	1154	western rampart, construction II
ST_S_13307	soil	V0841	Hügelfeld
ST_S_13289	soil	V0841	Hügelfeld

3.1.2 Recent environmental samples

In addition to the archaeological samples, recent soil and water samples in a diameter of about 5 km around the settlement were taken from a depth of about 30 cm and analysed for their $n(^{87}Sr)/n(^{86}Sr)$ isotope-amount ratio for the determination of the local Sr signal (Table 4, Fig. 6). The water samples were taken in duplicates, with the exception of ST_W_P19. Cultivated land was not used for soil sampling.

Unfortunately, samples in Slovakia could not be taken, which means, that east of the settlement, samples were limited by the March river.

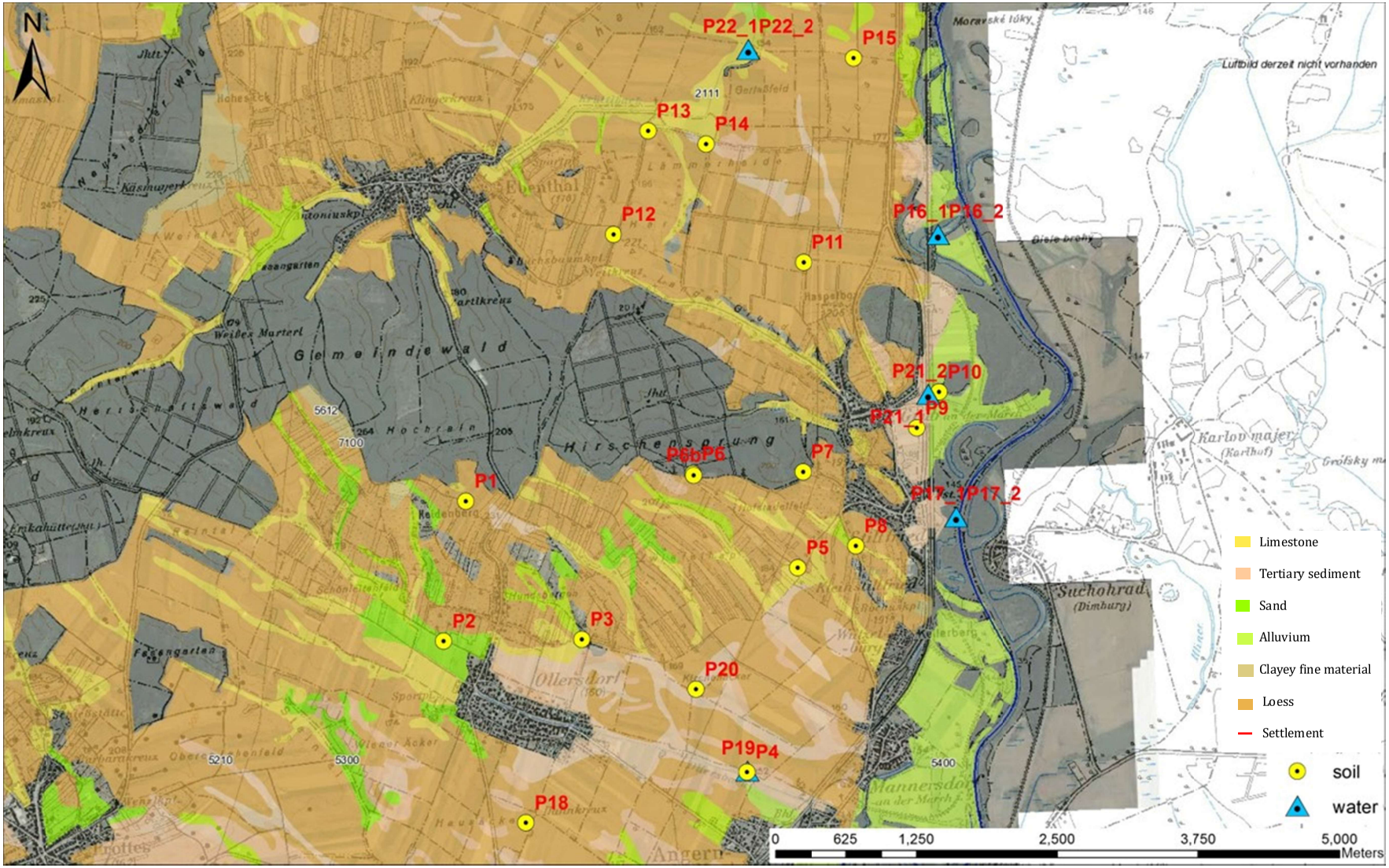

Figure 9 Map with all the sampling points. Soil samples are displayed in yellow, water samples in blue. (source: Digitale Bodenkarte von Österreich, 1km-Raster, Bundesforschungs- und Ausbildungszentrum für Wald, Naturgefahren und Landschaft (BFW))

Table 4 Sample list of recent water and soil samples

Sample ID	Sample type	Sample location	lat. (°N)	lon. (°E)
ST_S_ P18	soil	uncultivated land	48.38642	16.79686
ST_S_P2	soil	uncultivated land	48.40117	16.78802
ST_S_P1	soil	uncultivated land	48.41224	16.79142
ST_S_P3	soil	-	48.40083	16.80449
ST_W_P19	water	goit near P4	48.38973	16.82354
ST_S_P4	soil	uncultivated land	48.38968	16.8235
ST_S_P20	soil	-	48.39645	16.81791
ST_S_P5	soil	uncultivated land	48.40577	16.83062
ST_S_P6	soil	scarp	48.41362	16.8187
ST_S_P6b	soil	vineyard	48.41349	16.81878
ST_S_P7	soil	path next to vineyard	48.41338	16.8318
ST_S_P8	soil	uncultivated land	48.40728	16.83777
ST_W_P17_1	water	March river	48.40923	16.84986
ST_W_P17_2	water	March river	48.40923	16.84986
ST_S_P9	soil	plowed field	48.41646	16.84567
ST_S_P10	soil	wood land	48.41925	16.84852
ST_W_P21_1	water	creek near P10	48.41908	16.8472
ST_W_P21_2	water	creek near P10	48.41908	16.8472
ST_W_P16_1	water	backwater of the March near Hufeisenteich	48.43177	16.84924
ST_W_P16_2	water	backwater of the March near Hufeisenteich	48.43177	16.84924
ST_S_P11	soil	uncultivated land	48.43006	16.833002
ST_S_P12	soil	uncultivated land	48.43296	16.81046
ST_S_P13	soil	uncultivated land	48.44107	16.8152
ST_S_P14	soil	uncultivated land	48.43982	16.82202
ST_W_P22_1	water	Krüttlebach	48.44719	16.82752
ST_W_P22_2	water	Krüttlebach	48.44719	16.82752
ST_S_P15	soil	plowed field	48.44614	16.84012
ST_S_ P18	soil	uncultivated land	48.38642	16.79686

3.2 Sample preparation

Sample preparation, analysis and evaluation took place at the VIRIS Laboratory (University of Natural Resources and Life Sciences, Vienna) in a class 100,000 clean room.

3.2.1 Laboratory materials, reagents and standards

All laboratory vessels (except for Perfluoroalkoxy-alkanes-vessels (= PFA vessels)), funnel, syringes and pipette tips used were double acid washed before use. At first, they were left for 24 hours in nitric acid (*w*=10 %) then for another 24 hours in nitric acid (*w*=1%). Afterwards, the material was rinsed with high-quality (HQ) water and air dried. The PFA-vessels, which were used for sample digestion, were pre-cleaned in a two-stage steam wash procedure with concentrated nitric acid (*w*=65 %).

The nitric acid (*w*=65%, Merck- Millipore, Darmstadt, Germany) was purified by double sub-boiling before use. HQ-water (18 MΩ cm) (F+L GmbH, Vienna, Austria) and hydrochloric acid (*w*=30%, Merck-Millipore, Darmstadt, Germany) were further purified by sub-boiling. Sub-boiling was performed using a DST- 1000 sub-boiling distillation system (AHF Analysentechnik , Tübingen, Germany).

The diamond drilling head used for tooth and mussel sampling were pre-cleaned in an ultrasonic bath for 10 minutes using HQ-water. The spatulas used for soil sampling were first cleaned by rinsing with HQ-water, then with Isopropanol and nitric acid (*w=2%*) and finally again with HQ-water.

For the digestion, hydrogen peroxide (*w=30%*) was used in addition to concentrated nitric acid (*w*=65%).

The bioavailable metal fraction from the soil were extracted using 1 mol L^{-1} ammonium nitrate following the protocol DIN ISO 19730:1997-06 (Swoboda, Brunner, Boulyga et al., 2008, p. 489).

In case of the manual Sr/matrix separation, a Sr specific resin (TrisKem International, Bruz, France) was used. For the automated Sr/matrix separation via prepFAST-MC™, the unbranched DGA resin (TrisKem International) was used.

Indium single element standard (Merck-Millipore) was used as internal standard for MEA and the Rb/Sr screenings before isotopic analysis. Calibration curves for those analyses were established gravimetric using Merck ICP multi-element standard VI (Merck-Millipore). For quality control, an in-house solution, fabricated of a spiked Merck ICP multi-element standard VI (Merck-Millipore) solution was used.

The certified reference materials NIST SRM 1400 (consisting of Bone Ash; NIST, Gaithersburg USA) and NIST SRM 1486 (consisting of Bone Meal; NIST) were used as quality control for the digestion of teeth and mussel samples. The certified reference material NIST SRM 987 (highly purified $SrCO_3$, NIST) was used as reference value for Sr isotopic analysis.

3.2.2 Tooth and mussel samples

Before and after every cleaning and sampling step, the samples were photographed using a standard binocular microscope (S63T Trinocular Pod 8-50x) connected to digital camera (ProgRes CT3, Jenoptik, Jena, Germany) in 8- to 10-fold magnification.

3.2.2.1 Human tooth samples

The human tooth samples were cleaned with HQ-water using a tooth brush at first and afterwards cleaned in an ultrasonic bath for 10 minutes using HQ-water. In a second washing step, the teeth were cleaned in an ultrasonic bath for 10 minutes and afterwards soaked in isopropanol for 10 minutes. After each cleaning step, the teeth were air dried on sheets of clean room tissue.

For an easier reaching of the pulp dentine, the teeth were cut from the crown to the root using a low speed saw (IsoMet, Buehler, Lake Bluff, IL, USA) with a diamond-rim blade (Series 15LC IsoMet Wafering Blade, Buehler). This step was carried out in cooperation with a staff member of the Department for Anthropology of the Natural History Museum in Vienna (Bernhard Weinzinger). The teeth halves were again cleaned in an ultrasonic bath for 10 minutes using HQ-water and air dried.

To remove calculus and caries lesions and surface contaminations, the surface and the pulp cavity of the tooth was pre-cleaned using an electrical driller (Dremel Moto-Tool, Wisconsin, USA) combined with diamond drilling heads. The following step was cleaning in an ultrasonic bath for 10 minutes using HQ-water and air drying afterwards.

First, the enamel sample of each tooth was taken, using the electrical driller with a diamond drilling head. The sampled tooth powder was collected in Eppendorf test tubes. Before sampling of the dentine, the teeth were cleaned anew in an ultrasonic bath for 10 minutes

with HQ-water and then they were air dried. The pulp dentine adjusting to the pulp cavity was sampled in the same way as the enamel.
Between 6.9 and 18.2 mg enamel and dentine were taken for analysis from each human tooth (see Table 10 in the Appendix).

3.2.2.2 Animal tooth samples and mussels

The cleaning and sampling procedures for enamel, dentine and mussel samples were performed accordingly to those of the human teeth. Note, the animal teeth were not cut into halves. Nevertheless, the dentine samples were taken near the dental pulp.
As for the animal teeth and mussels, 7.0 mg to 13.1 mg enamel, dentine or mussel fragments were sampled (see Table 13 and 15 in the Appendix).

3.2.2.3 Digestion

The tooth and mussel powder were each weighted in a PFA vessels and merged with 2 mL concentrated double sub-boilded nitric acid (w=65%) and 1 mL hydrogen peroxide (*w*=30%). The samples then were digested on a hot plate at 150º C for 2.5 hours. Afterwards 8 mol L^{-1} nitric acid was added until a total weight of approximately 10 g was reached.

3.2.2.4 Sr/matrix separation

To be able to conduct Sr isotopic analysis, Sr has to be separated from isobaric and polyatomic interferences arising from matrix Rb and Ca. Hence, the teeth were manually separated according to a modified protocol of Swoboda, Brunner, Boulyga et al. (2008, p. 489). For this, about 0.5 mL of the suspended Sr specific resin (TrisKem International) was filled into columns. The resin was washed with 3 x 1 mL of 6 mol L^{-1} nitric acid, then with 3 x 1 mL of sub-boiled water. Afterwards the resin was washed with 2 x 1 mL of 6 mol L^{-1} hydrochloric acid and then again with 3 x 1 mL of sub-boiled water. For the conditioning, the resin was loaded with 3 x 1 mL of 8 mol L^{-1} nitric acid. In the case of the human teeth, 3 mL of enamel sample and 1 mL of dentine sample was loaded on the resin for separation. For the animal samples and mussels, 1 mL - 2 mL of sample was loaded on the resin, depending on the Sr mass fraction of each sample which was determined by MEA. The matrix was removed by adding 10 x 1 mL of 8 mol L^{-1} nitric acid. The purified Sr fraction was then eluted with 2 x 1 mL of sub-boiled water.

3.2.3 Environmental Samples

3.2.3.1 Soil samples

The soil samples were dried for seven days and then sieved (2 mm size). Note, the two soil samples directly from the excavation site were treated the same way as the recent soil samples.

The bioavailable metal fractions of the soil samples was extracted using NH_4NO_3 following the protocol DIN ISO 19730 (1997). For this, approximately 20 g of each soil sample was taken. The soil sample was then merged with 50 mL of 1 mol L^{-1} ammonium nitrate and shaken with an overhead shaker for three hours at 20 rpm. The suspension was filtered using folded filters (Munktell Ahlstrom, Falun, Sweden) and a PE funnel, whereas the first 3 mL were discarded, the rest of the filtrate was collected in previously weighted 50 mL Polyethylene (PE) bottles and then acidified with double sub-boilded concentrated nitric acid (*w*=65%) to a concentration of w=2 %.
Prior to the Sr/matrix separation, the samples were diluted by a factor of 10 with doubled sub-boiled concentrated nitric acid (w=65 %) and sub-boiled water to a final concentration of approx. 2 mol L^{-1} nitric acid.
The separated samples were preconcentrated by evaporation and re-dissolving to receive at least 200 ng g^{-1} Sr in 2 mL of nitric acid (*w*=2%) prior to Sr isotopic analysis,.

3.2.3.2 Water samples

The water samples were filtered with pre-cleaned 5 mL syringes and 0.45 µm filters (Sartorius, Göttingen, Germany) in previously weighted 50 mL PE bottles. Then they were acidified to 2% with double sub-boiled concentrated nitric acid (w=65 %).

To receive enough of Sr for the Sr/matrix separation, the water samples were evaporated in PFA vessels using a hot plate. After the samples were completely evaporated, they were re-dissolved in 1.5 mL of 2 mol L^{-1} nitric acid.

3.2.3.3 Archaeological wood and straw samples

The wood and straw sample were each prepared as triplicates. About 350 mg of the samples were transferred into Teflon vessels. Then 5 mL of nitric acid (*w*=65%) and 1 mL of hydrogen peroxide (*w*=30%) were added. The samples and additional blanks were then

microwave (Multiwave 3000, Anton Paar, Graz, Austria) digested. For the exact program data see Table 5 and Table 6. After sample digestion, the samples were transferred into pre-cleaned 50-mL PE bottles. Residual drops of the digest in the Teflon vessel were transferred with sub-boiled water.

Table 5 Microwave program details of straw samples

Phase	Power	Ramp	Hold	Fan
1	600	20	60	1
2	0		15	3

Table 6 Microwave program details of wood samples

Phase	Power	Ramp	Hold	Fan
1	600	20	35	1
2	0		15	3

3.2.3.4 Sr/matrix separation

Soil and water samples were automatically separated via prepFAST-MC™ (ESI, Omaha, USA) according to the protocol described by Retzmann, Zimmermann, Profrock et al. (2017, p. 5470 ff). First the column (1 mL DGA Resin) was conditioned with 5 mL of 2 mol L^{-1} nitric acid. Then the sample prepared in 2 mol L^{-1} nitric acid was loaded onto the column. The matrix was washed from the column with 6 mL of 2 mol L^{-1} nitirc acid. Subsequently, the Sr fraction was eluted with 5 mL of 0.2 mol L^{-1} nitric acid. Finally, the column was cleaned with 10 mL of 0.1 mol L^{-1} hydrochloric acid before the next separation took place.

The archaeological wood and straw samples were manually separated. The separation process was the same as it was for the teeth and mussels, already described in section 3.2.2.4. As for the sample loading, 2 mL of each sample were taken.

3.3 Measurements

3.3.1 Multi-elemental analysis (MEA)

For the MEA, the following elements/isotopes were measured: ^{7}Li, ^{9}Be, ^{10}B, ^{11}B, ^{23}Na, ^{24}Mg, ^{25}Mg, ^{26}Mg, ^{27}Al,^{31}P, ^{39}K, ^{42}Ca, ^{43}Ca, ^{44}Ca, ^{51}V, ^{52}Cr, ^{53}Cr, ^{54}Mn, ^{55}Mn, ^{56}Fe, ^{57}Fe, ^{58}Ni, ^{59}Co, ^{60}Ni, ^{63}Cu, ^{65}Cu, ^{66}Zn, ^{68}Zn, ^{69}Ga, ^{71}Ga, ^{75}As, ^{77}Se, ^{82}Se, ^{85}Rb, ^{88}Sr, ^{98}Mo, ^{107}Ag, ^{109}Ag, ^{111}Cd, ^{114}Cd, ^{115}In, ^{128}Te, ^{137}Ba, ^{138}Ba, ^{205}Tl, ^{206}Pb, ^{207}Pb, ^{208}Pb, ^{209}Bi, ^{238}U.

Not all of these elements were scope of this work, mainly Ca, Sr, Rb and those elements for the detection of diagenesis (V, Al, Ba, Mn, Fe, U).

The MEA measurements were carried out using a ICP-QMS Nexion 350D (Perkin Elmer, Waltham, USA) prior to Sr/matrix separation. It is equipped with an ESI autosampler (Elemental Scientific, Omaha, USA) Prior to the measurement, a daily performance check and the necessary tuning of the instrument were performed.

For the measurement, the sample digests and soil extracts were diluted with nitric acid (w=2%) or sub-boiled water, depending on the acidity of the sample. The tooth and mussel samples were diluted by a factor of 20 with sub-boiled water, the soil samples by a factor of 75 with nitric acid (w=2%), the water samples were directly measured. The archaeological straw and wood digests were diluted to a concentration of nitric acid (w=2%) using sub-boiled water. The triplicates of the straw samples were diluted by a factor of 8, 10 and 11. The triplicates of the wood samples were diluted by a factor of 7, 9 and 9. Previous to the dilution of the straw samples, they were filtered with pre-cleaned 5 mL syringes and 0.45 µm filters (Sartorius, Göttingen, Germany).

Multi-elemental quantification was accomplished using an external calibration in the range of 0.05 ng g^{-1} and 175 ng g^{-1}, gravimetrically prepared from Merck ICP multi-element standard VI. To each of the samples, standards and blanks 10 % Indium was spiked as internal standard (e.g. if the diluted sample had a volume of 3 mL, 0.3 mL of Indium were added). During the measurement, analysis blanks and in-house quality control samples were measured after every few samples.

3.3.2 Rb/Sr-Screening

After Sr/matrix separation, the samples were screened for Sr recovery and possible residual Rb and Ca. All separated samples were diluted by a factor of 20 with 2 % nitric acid (w/w).

To each of the samples, 10 % Indium was additionally added as internal standard. Quantification was accomplished using an external calibration in the range of 0.05 ng g^{-1} and 175 ng g^{-1}, gravimetrically prepared from Merck ICP multi-element standard VI.
The measurement process was the same as it was with the MEA as described above (section 3.3.1).
The Sr/matrix separations were successful with a Sr recovery of 60 % to 86 % for human teeth with a mean of 79 % for the dentine and 69 % for the enamel samples. The measured Sr mass fractions were, in case of the dentine, between 10 ng g^{-1} and 24 ng g^{-1} with a mean of about 16 ng g^{-1} and 2 ng g^{-1} to 11 ng g^{-1} with a mean of about 5 ng g^{-1} in case of the human enamel.

The recovery of the organic samples was 68 % to 98 %, with a mean of 79 %. The sample Sr mass fractions was between 664 ng g^{-1} and 1008 ng g^{-1} with a mean 856 ng g^{-1}.

In case of the prepFAST-MC^{TM} separated water samples, the recovery was 92 % to 108 % with a mean of 97 % and a Sr mass fractions of 101 ng g^{-1} to 198 ng g^{-1} and a mean of 138 ng g^{-1}.
The recovery rates for the soil samples are 92 % to 126 % with a mean of 105 %. The Sr mass fractions were between 111 ng g^{-1} and 647 ng g^{-1} with a mean of 398 ng g^{-1}.

In case of the animal teeth, the Sr recovery was about 42 % to 88 % with a mean of 64 % for the enamel samples and 60 % for the dentine samples. The Sr mass fractions were between 6 ng g^{-1} and 38 ng/g^{-1} with a mean of 14 ng g^{-1} for the enamel samples and 13 ng g^{-1} to 43 ng g^{-1} with a mean of 24 ng g^{-1} in case of the dentine.

The recovery of the mussel samples was 81 % to 120 % with a mean of 90 %. Their Sr mass fractions 16 ng g^{-1} to 26 ng g^{-1} with a mean of 19 ng g^{-1}.

3.3.3 $n(^{87}Sr)/n(^{86}Sr)$ isotope-amount ratio measurement

For the $n(^{87}Sr)/n(^{86}Sr)$ isotope-amount ratio measurement, a multicollector ICP-MS (Nu Instruments Ltd., Wrexham, UK) was used. It is coupled with an ESI autosampler (Elemental Scientific, Omaha, USA). The instrument is equipped with 12 Faraday cups and three ion counters. All measurements were performed in low mass resolution mode.

The instrument was optimized on a daily basis for torch position, nebulizer gas flow rates and peak shapes to gain the maximum Sr-stability and Sr-sensitivity. For this purpose, a solution of NIST SRM 987 (approx. 50 ng g^{-1}) in nitric acid (*w=2%*) was used.

The separated samples were diluted with nitric acid (*w=2%*) to a mass fraction of approx. 50 ng g^{-1}, based on the screening results. The isotopic analysis were performed with a signal intensity on ^{88}Sr of about 5 V.

Time-dependent instrumental isotopic fractionation during the isotopic analysis was corrected using an internal inter-elemental approach combining standard-sample bracketing (SSB) and external calibration by Zr following standard measurement protocols (Yang, Peter, Panne et al., 2008, p. 1271ff, Irrgeher, Prohaska, Sturgeon et al., 2013, p. 1690f, Irrgeher, Vogl, Santner et al., 2015, p. 141ff). Therefore, each separated sample (incl. method blanks) and NIST SRM 987 solution, used as SSB standard, were spiked with Zr for an internal inter-elemental correction of instrumental isotopic fractionation. Mass fraction of sample and SSB standard were matched within 10%.

All Sr isotopic data were collected using static multi-collection with a corresponding detector configuration with Mass 87 (^{87}Sr, ^{87}Rb) was measured as axial detector as shown in Table 7. Data collection was accomplished over a period of 300 s with an integration time of 10 s, resulting in a total of 60 measurements per sample. For blank correction, after every 5th sample, a blank (nitric acid (*w=2%*)) was measured using the 'measure zeros' method of the instrument software. The samples and the NIST SRM 987 standards were introduced into the plasma in the following sequence: standard1 - sample - standard2, to enable correction for instrumental isotopic fractionation.

The results were evaluated and the measurement uncertainty was calculated according to Horsky, Irrgeher&Prohaska (2016, p. 354ff) using a Microsoft Excel spreadsheet.

Table 7 Faraday Cup Setup

	F		F		F	F	F	F	F	F	F	IC	F	IC	F	IC	F
cup	**H6**		**H5**		**H4**	**H3**	**H2**	**H1**	**Ax**	**L1**	**L2**	**IC0**	**L3**	**IC1**	**L4**	**IC2**	**L5**
mass	91		90				88		87		86		85		84		
isotope	^{91}Zr		^{90}Zr				^{88}Sr		^{87}Sr, ^{87}Rb		^{86}Sr		^{85}Rb		^{84}Sr		

3.4 Determination of the 'local' and the autochthonous $n(^{87}Sr)/n(^{86}Sr)$ isotope-amount ratio ranges

To determine the local range, the $n(^{87}Sr)/n(^{86}Sr)$ ratios of the recent soil and water samples were used. First, the range of each category was determined by addition/subtraction of two times the standard deviation from each average. The total local range covers the whole span from the upper limit of the local water to the lower limit of the local soil range.

The autochthonous $n(^{87}Sr)/n(^{86}Sr)$ range was calculated in accordance to the local range but using the data from the archaeological animal enamel, the archaeological straw and wood data and the archaeological mussel as proxy for Sr as Sr nutrition sources, vegetation and drinking water sources.

3.5 Creation of isoscapes

For the creation of an isoscape, the $n(^{87}Sr)/n(^{86}Sr)$ isotope data and geographic coordinates of the soil and water samples were used. By using geological and soil maps (eBOD, Bundesministerium für Nachhaltigkeit und Tourismus) of Stillfried/March, a multi-layered isoscape was established via ArcGIS® 10.2 (ESRI, Redlands, CA, USA). The existing geomorphological data were assigned to the model.

4 Results

Some components of the results of this thesis are published in Retzmann, Kriechbaum, Griebl et al. (2020).

4.1 Multi-Elemental Analysis (MEA)

4.1.1 Human Teeth

The MEA shows a higher Sr mass fraction in the dentine than it is in the enamel of all human teeth samples. The enamel Sr mass fraction shows a variation of 71 ± 5 μg g^{-1} (Ind. 9051, Sk. 10, pit V0841) to 199 ± 13 μg g^{-1} (Ind. 9042, Sk. 2, pit V0841) whereas the dentin Sr mass fraction varies between 260 μg g^{-1} ± 17 μg g^{-1} (Ind. 9023, Sk. 1, pit V1141) and 621 ± 41 μg g^{-1} (Ind. 9026, Sk. 4, pit V1141) (see Fig. 7, Table 11). The Sr mass fractions of all enamel samples are neither elevated nor depleted (for further explanations, see chapter 1.4). Hence the enamel samples can be considered as biogenic and therefore show no signs of diagenesis.

The dentine of all individuals show elevated mass fractions in one or more of the following elements: V (Fig. 9), Mn (Fig. 10) , Sr (Fig. 7), Ba (Fig. 11) which indicate diagenetic alterations (for further explanations, see chapter 1.4) . Hence, the dentine samples were not considered as biogenetic and therefore not used to determine provenance. The approximation of biogenic Sr isotopic signatures from diagenetically altered dentine to gain additional insights on places of residence and population dynamic during a specific (later) period of life of these individuals is further discussed in Retzmann, Kriechbaum, Griebl et al. (2020, p. 67, p. 70, p. 80f)

It can be observed that the measured Ca mass fraction is generally higher in the enamel samples than the dentine (see Fig. 8), which can be explained by the fact, that enamel is composed of a hydroxyapatite (calcium phosphate) matrix with minor organic content (approx. *w*=1%) whereas dentine is composed of hydroxyapatite matrix with a larger organic content (approx. *w*=20%) (Hillson, 1996, p. 218, Kohn, SchoeninGer&Barker, 1999, p. 2738).

The mass fractions of all analysed elements can be seen in the Appendix (Table 11 – 18).

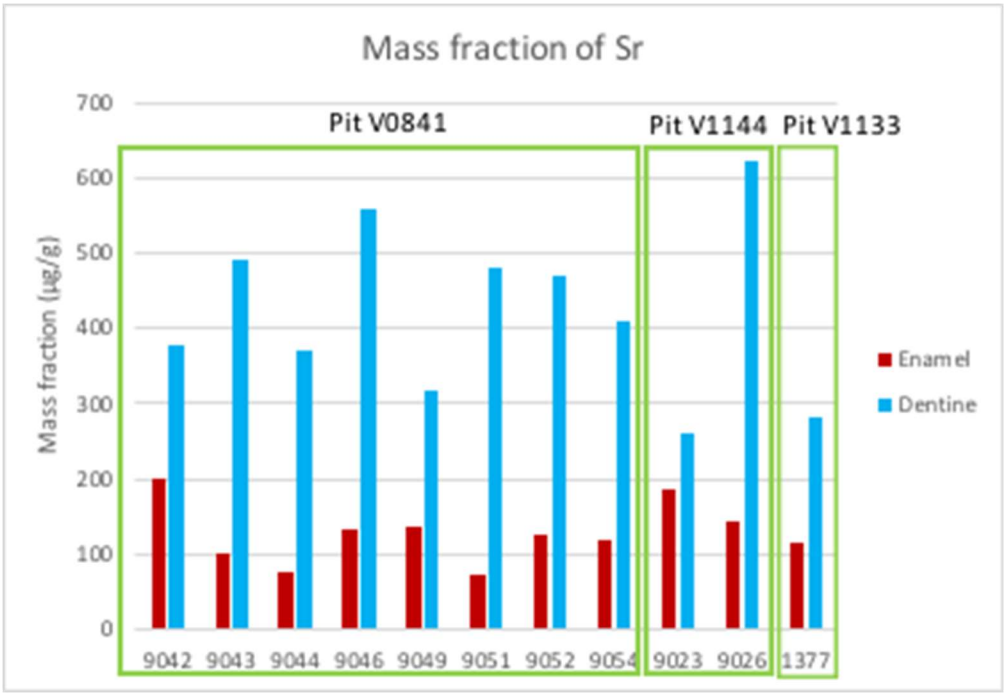

Figure 10 Mass fraction of Sr (µg g^{-1}) of human enamel and dentine samples

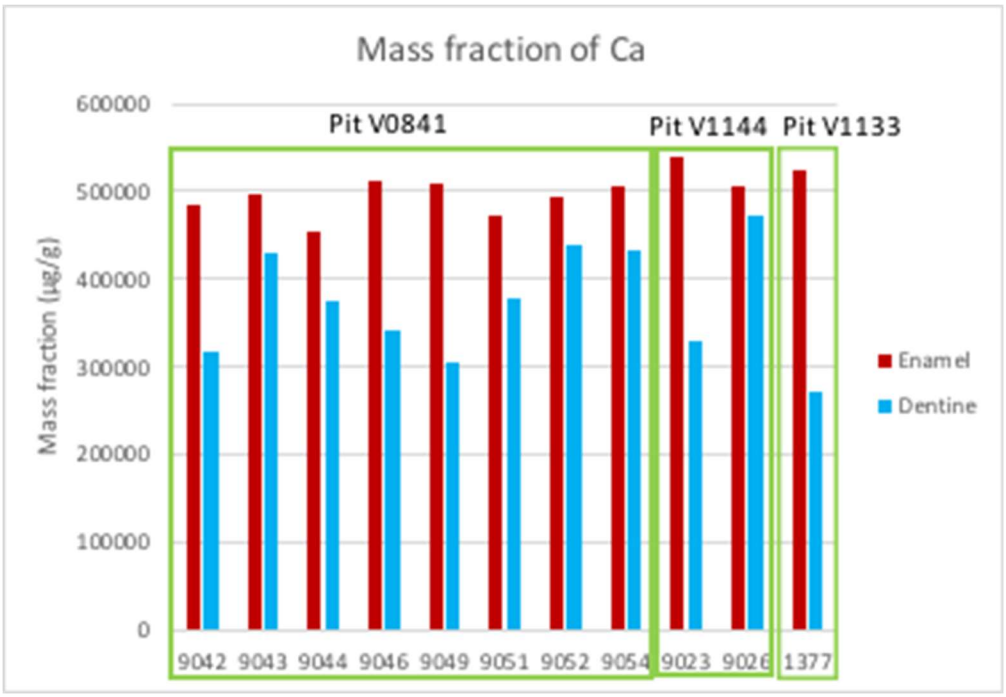

Figure 11 Mass fraction of Ca (µg g^{-1}) of human enamel and dentine samples

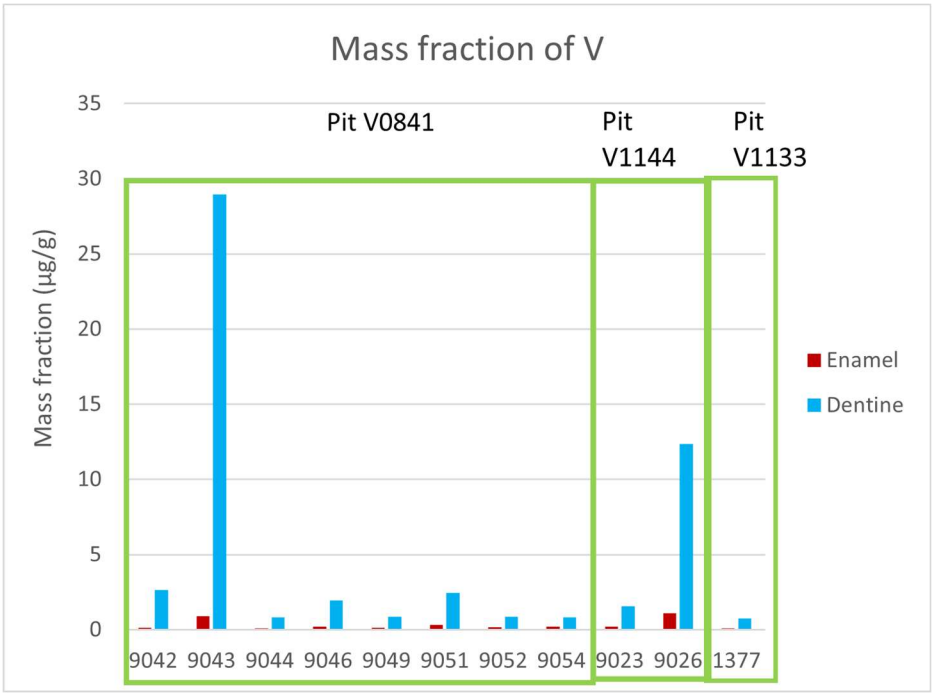

Figure 12 Mass fraction of V (µg g-1) of human enamel and dentine samples

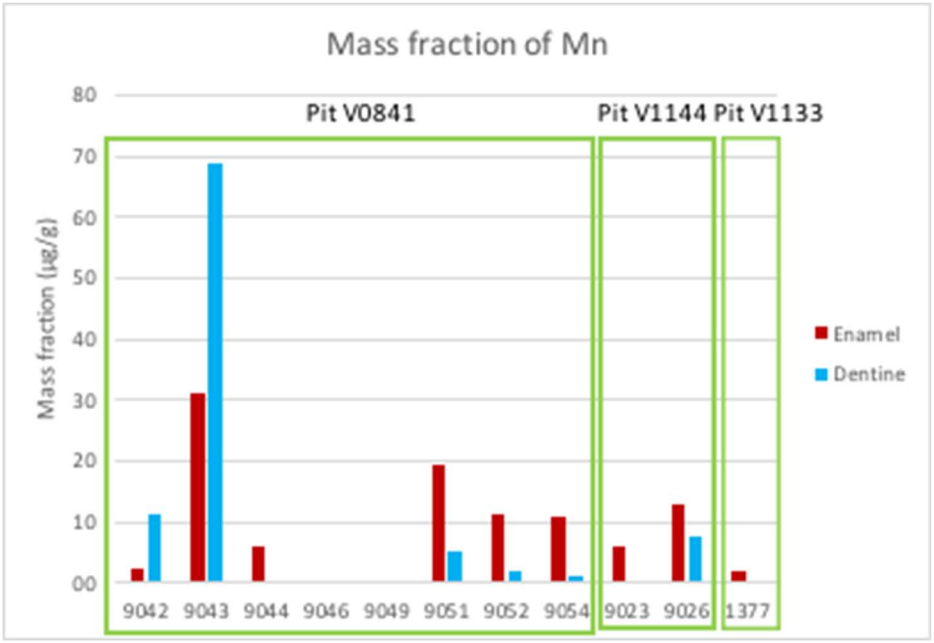

Figure 13 Mass fraction of Mn (µg g-1) of human enamel and dentine samples

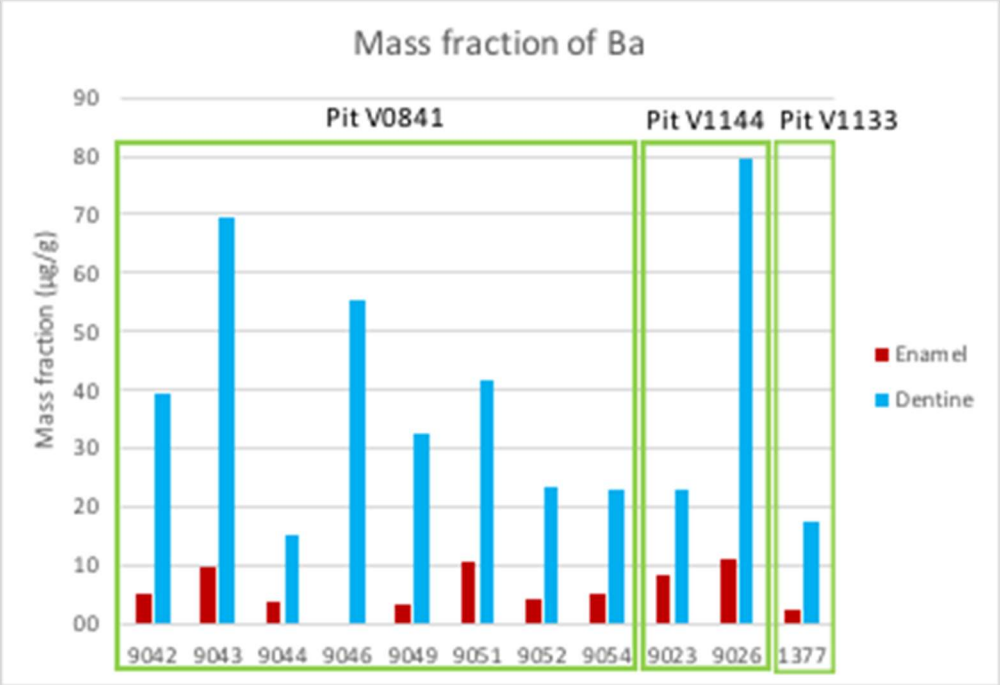

Figure 14 Mass fraction of Ba (µg g-1) of human enamel and dentine samples

4.1.2 Animal Teeth

The MEA of the animal teeth shows the same pattern as it does for the human teeth concerning Sr and Ca mass fractions. The dentine of the animal teeth is higher in its Sr mass fraction than the enamel except for the tooth of the beaver (sign. 13286) whose enamel shows a higher mass fraction of Sr (see Fig. 12). For cattle and porcine, a similar biogenic Sr mass fractions as for humans is found (Viner, Evans, Albarella et al., 2010, Madgwick, Mulville&Evans, 2012, p. 737, Minniti, Valenzuela-Lamas, Evans et al., 2014, p. 310), whereas for rodents, biogenic Sr mass fractions up to 450 µg g^{-1} have been reported (Copeland, Sponheimer, Le Roux et al., 2008, p. 3193). Only the Sr mass fraction in the tooth of the beaver (sign. 13286) exceeds this range but the Sr isotopic ratio agreed with those of the other animal enamel samples (see section 4.2.3). In comparison to the other animal enamel samples, no further indications for diagenesis have been found (see Table 21-25 in the Appendix, Fig. 12-18). Hence, all enamel samples can be considered as biogenic and therefore were included in the estimation of an autochthonous Sr range. Concerning Ca, the enamel shows in all cases a higher mass fraction than the dentine (see Fig. 13). This can again be explained by the fact, that enamel is composed of a hydroxyapatite (calcium phosphate) matrix with minor organic content (approx. *w*=1%)

whereas dentine is composed of hydroxyapatite matrix with a larger organic content (approx. *w*=20%) (Hillson, 1996, p. 218, Kohn, SchoeninGer&Barker, 1999, p. 2738).
The mass fractions of all analysed elements can be seen in the Appendix (Table 21-31).
The dentine of all animal individuals show elevated mass fractions in one or more of the following elements, as compared to the enamel: Al, V , Mn , Sr, Ba, U (see Fig. 12, 14-18) which indicate diagenetic alterations (for further explanations, see chapter 1.4) (see Table 26-31 in the Appendix). Hence, the dentine samples were not considered as biogenetic and therefore not used to determine the autochthonous Sr signal.
The mass fractions of all analysed elements can be seen in the Appendix (Table 21 – 31).

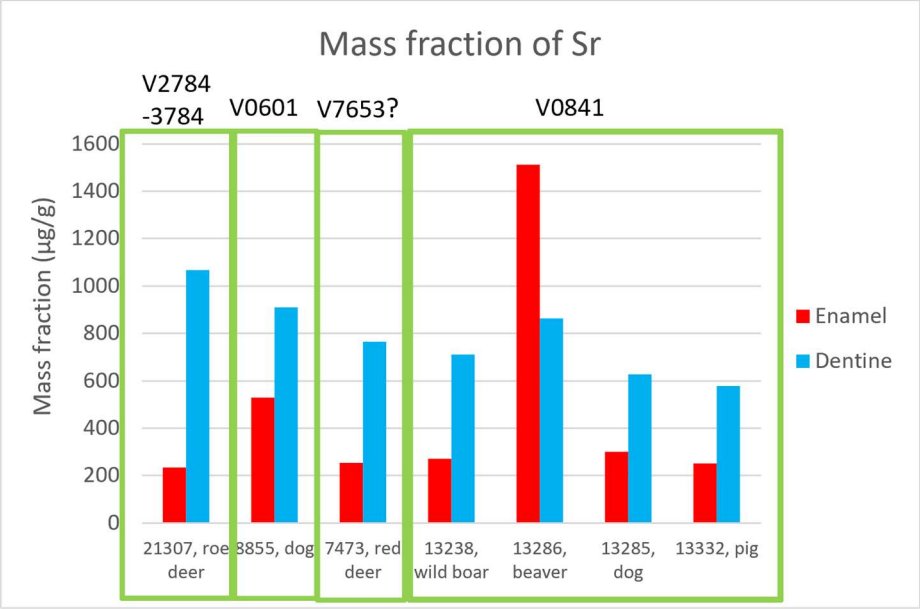

Figure 15 Mass fraction of Sr(µg g^{-1}) of animal enamel and dentine samples

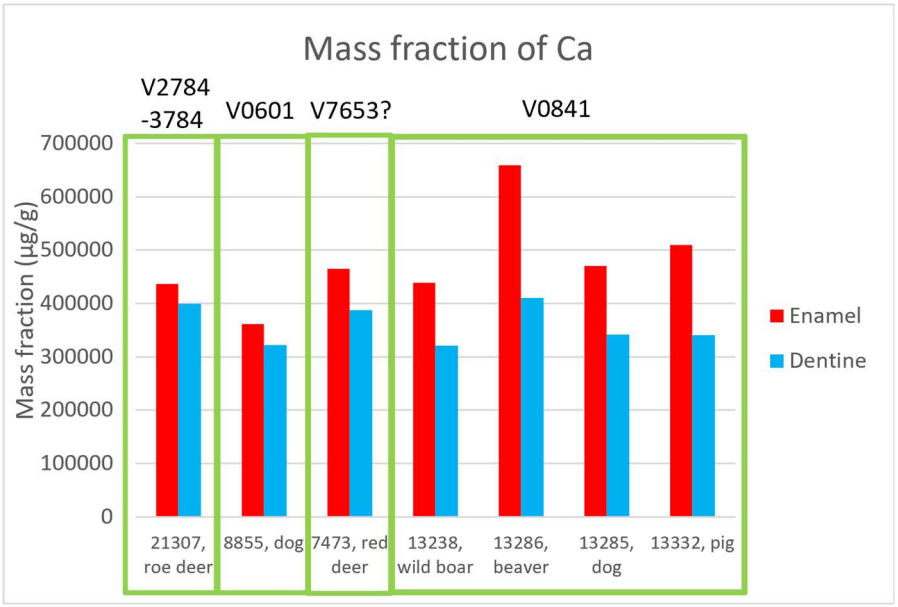

Figure 16 Mass fraction of Ca (µg g^{-1}) of animal enamel and dentine samples

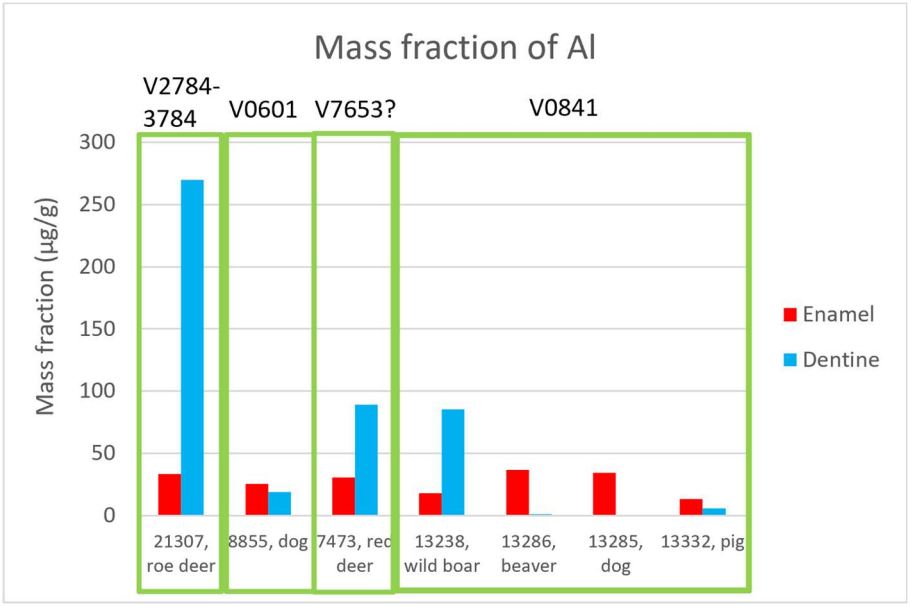

Figure 17 Mass fraction of Al (µg g^{-1}) of animal enamel and dentine samples

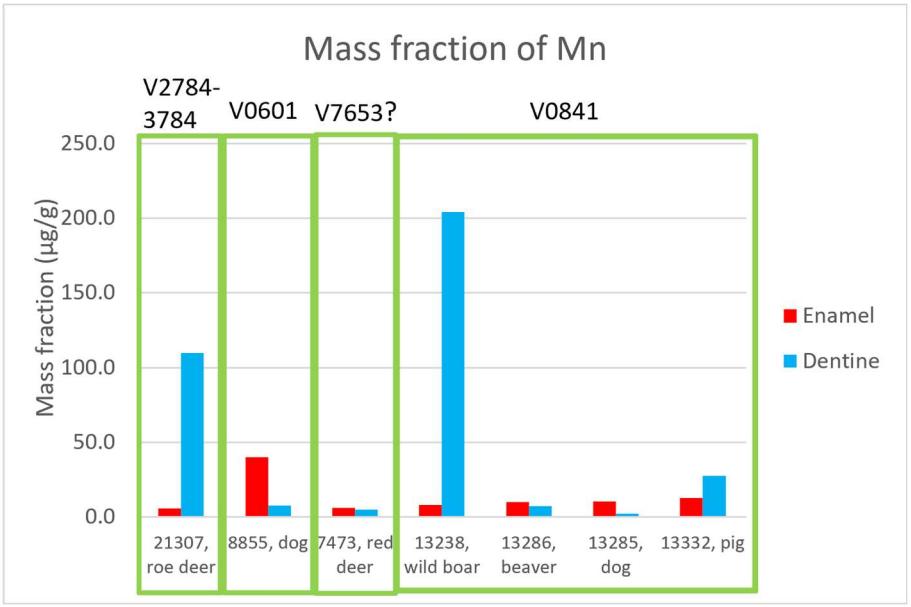

Figure 18 Mass fraction of Mn (µg g^{-1}) of animal enamel and dentine samples

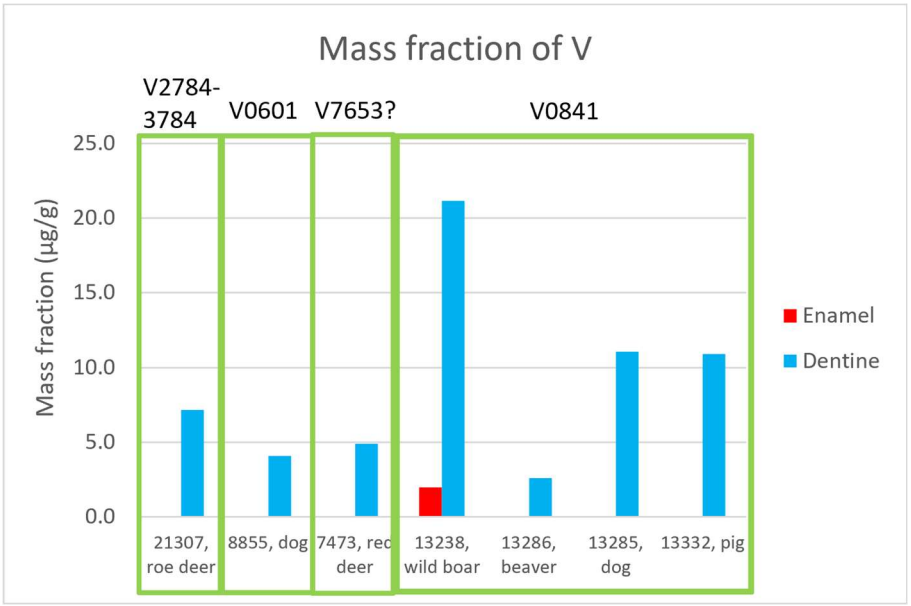

Figure 19 Mass fraction of V (µg g^{-1}) of animal enamel and dentine samples

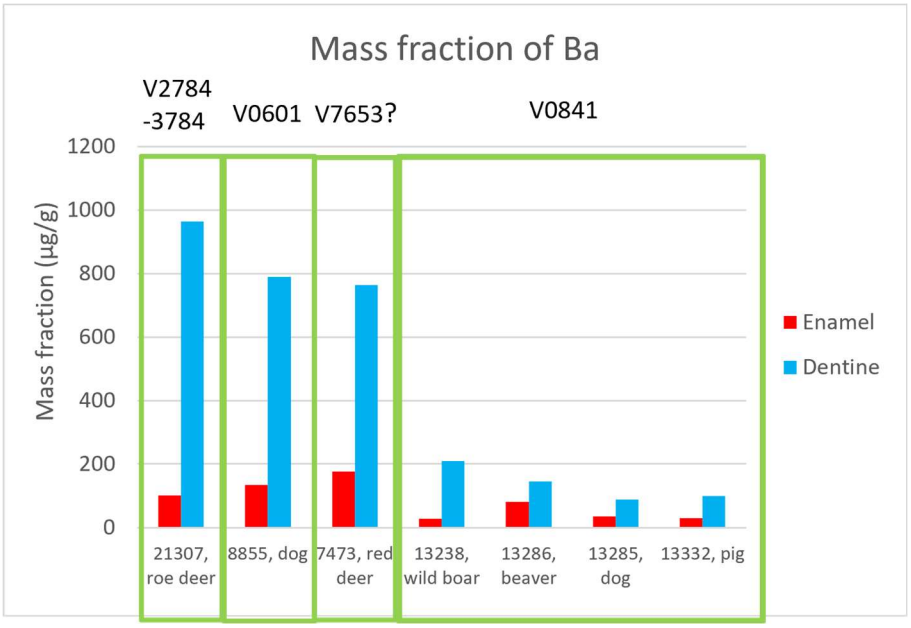

Figure 20 Mass fraction of Ba (µg g^{-1}) of animal enamel and dentine samples

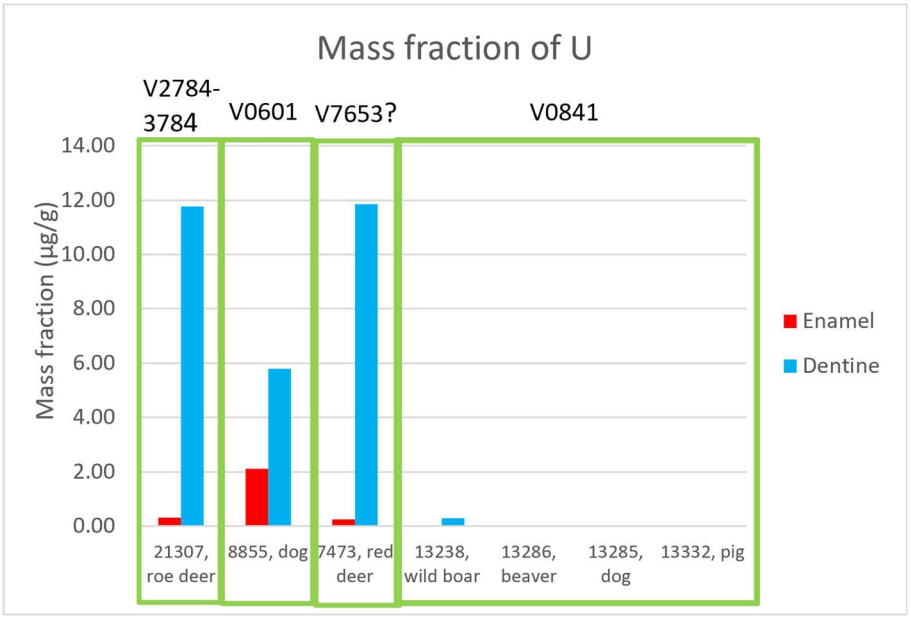

Figure 21 Mass fraction of U (µg g^{-1}) of animal enamel and dentine samples

4.1.3 Soil & Water Samples

Looking at the soil samples, the mass fraction of Sr is the highest within the settlement (Sample 13307, Pit V0841) with a mass fraction of 10.91 ± 1 μg g^{-1}. The lowest mass fraction can be found southwestern of the settlement (P2: 1.57 ± 0.17 μg g^{-1}, P3: 1.91 ± 0.13 μg g^{-1}, P18: 2.09 ± 0.14 μg g^{-1}) (see Fig. 19, Table 53 and 61 in the Appendix).

In the case of the water samples (Fig. 19, Table 69 in the Appendix), the lowest mass fraction of Sr can be found in the small streams (P 21: 0.255 ± 0.017 μg g^{-1}, P22: 0.270 ± 0.018 μg g^{-1}). The mass fraction of both samples taken in the March showed a mass fraction of 0.362 ± 0.024 μg g^{-1} (P16) and 0.339 ± 0.023 μg g^{-1} (P17). Sample P19 showed the highest Sr mass fraction (1.097 ± 0.079 μg g^{-1}).

The mass fractions of all analysed elements can be seen in the Appendix (Table 54 – 60, 41 – 46, 62 – 68).

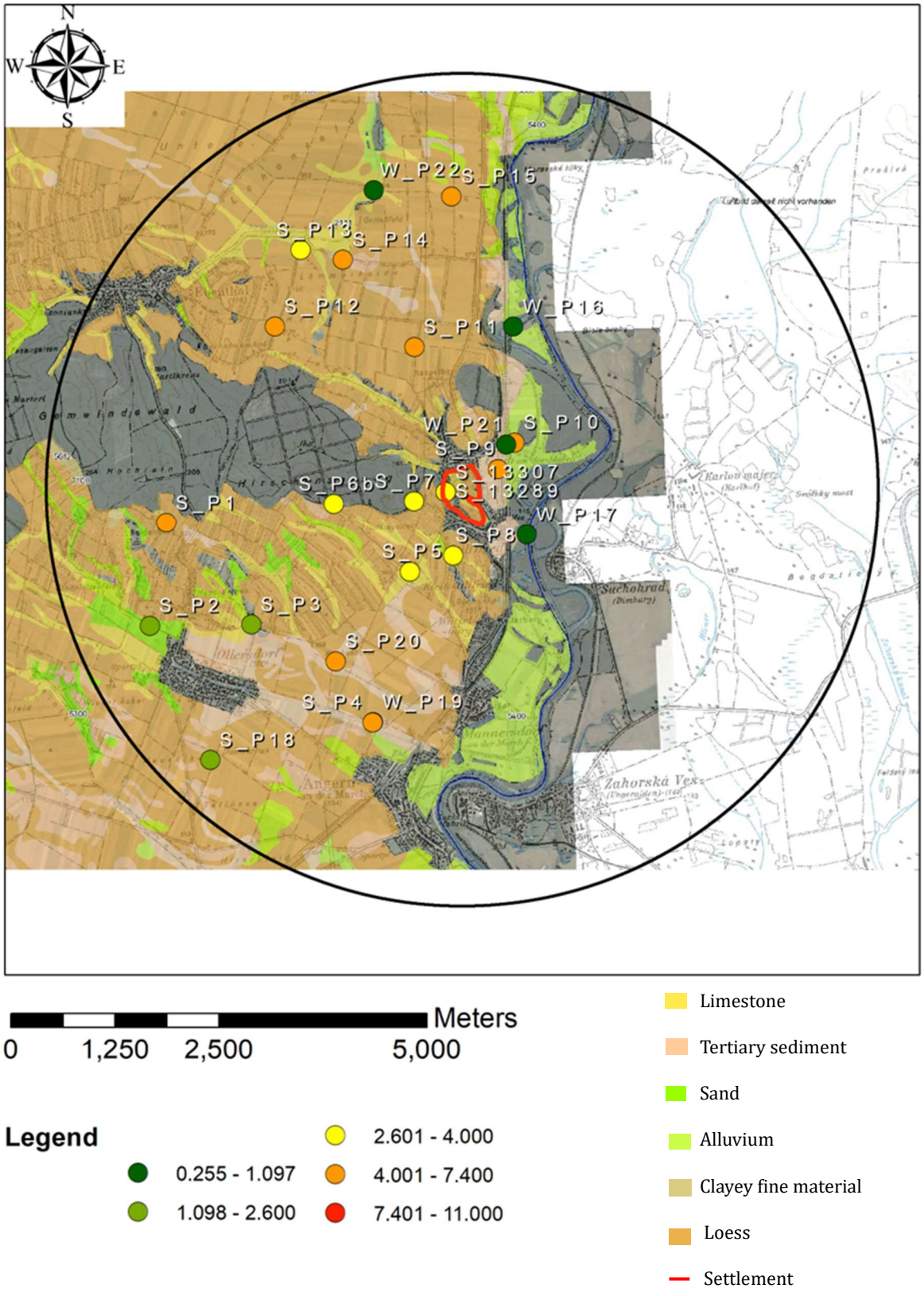

Figure 22 Geological map showing the Sr concentrations in µg g^{-1} (source: Digitale Bodenkarte von Österreich, 1km-Raster, Bundesforschungs- und Ausbildungszentrum für Wald, Naturgefahren und Landschaft (BFW))

4.2 $n(^{87}Sr)/n(^{86}Sr)$ isotope-amount ratio measurements

4.2.1 Local range

4.2.1.1 Soil and water samples

Figure 20 shows the results of the $n(^{87}Sr)/n(^{86}Sr)$ isotope-amount ratio analysis of the soil and water samples taken in the area of Stillfried. Due to the fact, that the $n(^{87}Sr)/n(^{86}Sr)$ isotope-amount ratios of the soil sample ST_S_P6 differs significantly from the soil sample ST_S_P6b, which was taken a few meters away, as well as the fact that ST_S_P6 also differs from all the other environmental samples, it was excluded from the calculation of the local range.

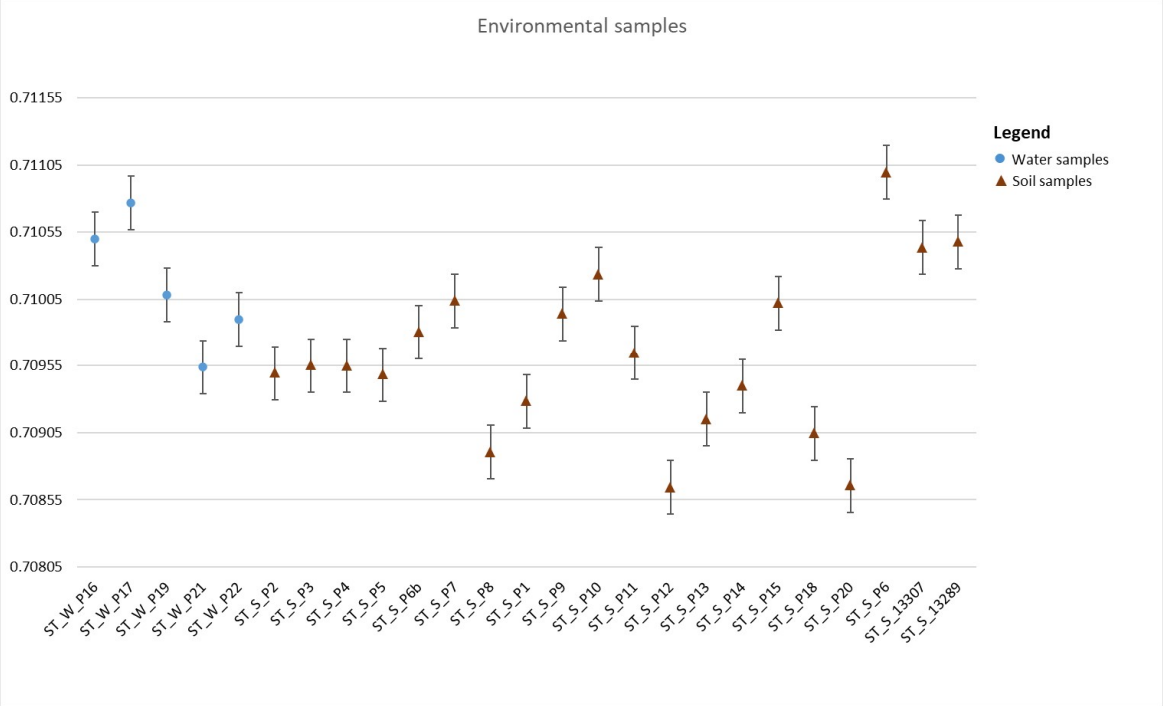

Figure 23 $n(^{87}Sr)/n(^{86}Sr)$ isotope-amount ratios of the soil and water samples from Stillfried

The $n(^{87}Sr)/n(^{86}Sr)$ isotope-amount ratios of the water and soil samples are relatively diverse (see Fig, 21). The ratios of the water samples range from 0.70954 ± 17 µg g^{-1} (P21) to 0.71077 ± 17 µg g^{-1} (P17). Even more diverse are the $n(^{87}Sr)/n(^{86}Sr)$ isotope-amount ratios of the recent soil samples which show a span from 0.70864 ± 17 µg g^{-1} (P12) to 0.71024 ± 17 µg g^{-1} (P10) (the excluded soil sample P6 was not taken into account). As a result of those different ratios, the local ranges differ slightly with the water range (0.70919-0.71113) being higher than the soil range (0.70852-0.71041). Therefore, the total combined local

range, shows a span from 0.70852-0.71113 (Fig. 21). This local range is also used in (Retzmann, Kriechbaum, Griebl et al., 2020, p. 67 ff).
For detailed $n(^{87}Sr)/n(^{86}Sr)$ isotope-amount ratios see Tables 61 and 69 in the appendix.

The $n(^{87}Sr)/n(^{86}Sr)$ ratio of the burial environments (soill samples sign. 13307 and 13289 taken during the excavations) was determined as 0.71046 ± 19 µg g^{-1} for pit V841 (see also (Retzmann, Kriechbaum, Griebl et al., 2020, p. 67)).

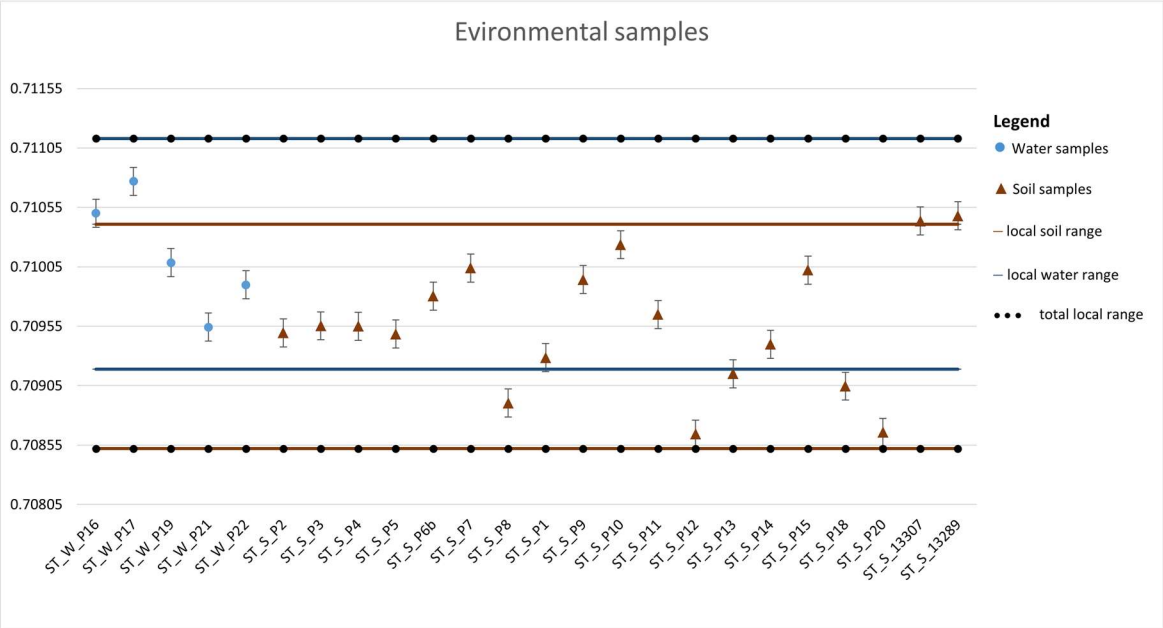

Figure 24 $n(^{87}Sr)/n(^{86}Sr)$ isotope-amount ratios of the environmental samples and the resulting local water (blue), soil range (brown) and total local range

As can be seen in the geological and the soil map (Fig. 22 and 23), the sampling spots near the Urnfield Culture settlement tend to show higher $n(^{87}Sr)/n(^{86}Sr)$ isotope-amount ratios than those further away.

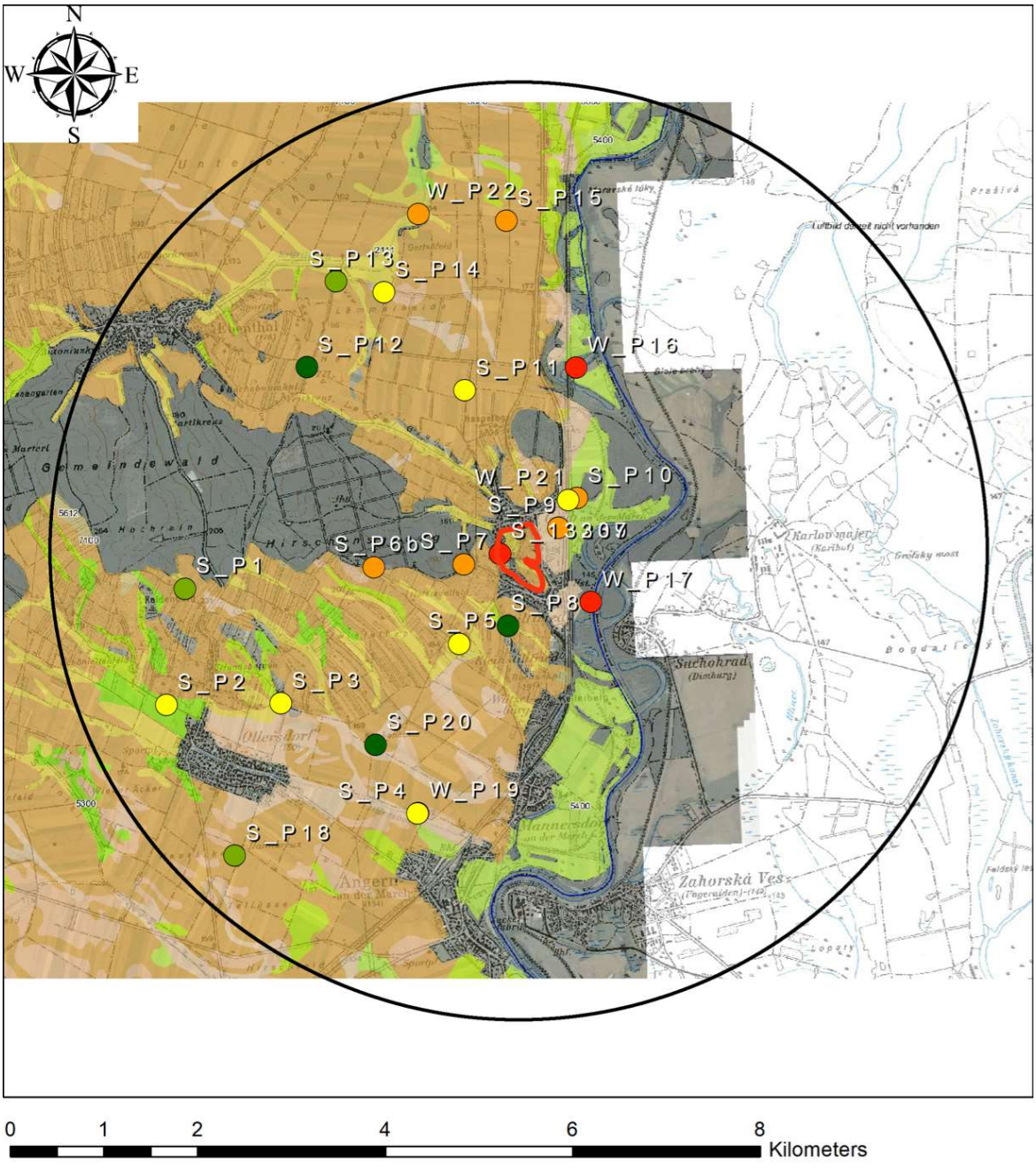

Figure 25 Geological Map showing the n(^{87}Sr)/n(^{86}Sr) isotope-amount ratios of the soil and water samples in a 5 km radius (source: Digitale Bodenkarte von Österreich, 1km-Raster, Bundesforschungs- und Ausbildungszentrum für Wald, Naturgefahren und Landschaft (BFW))

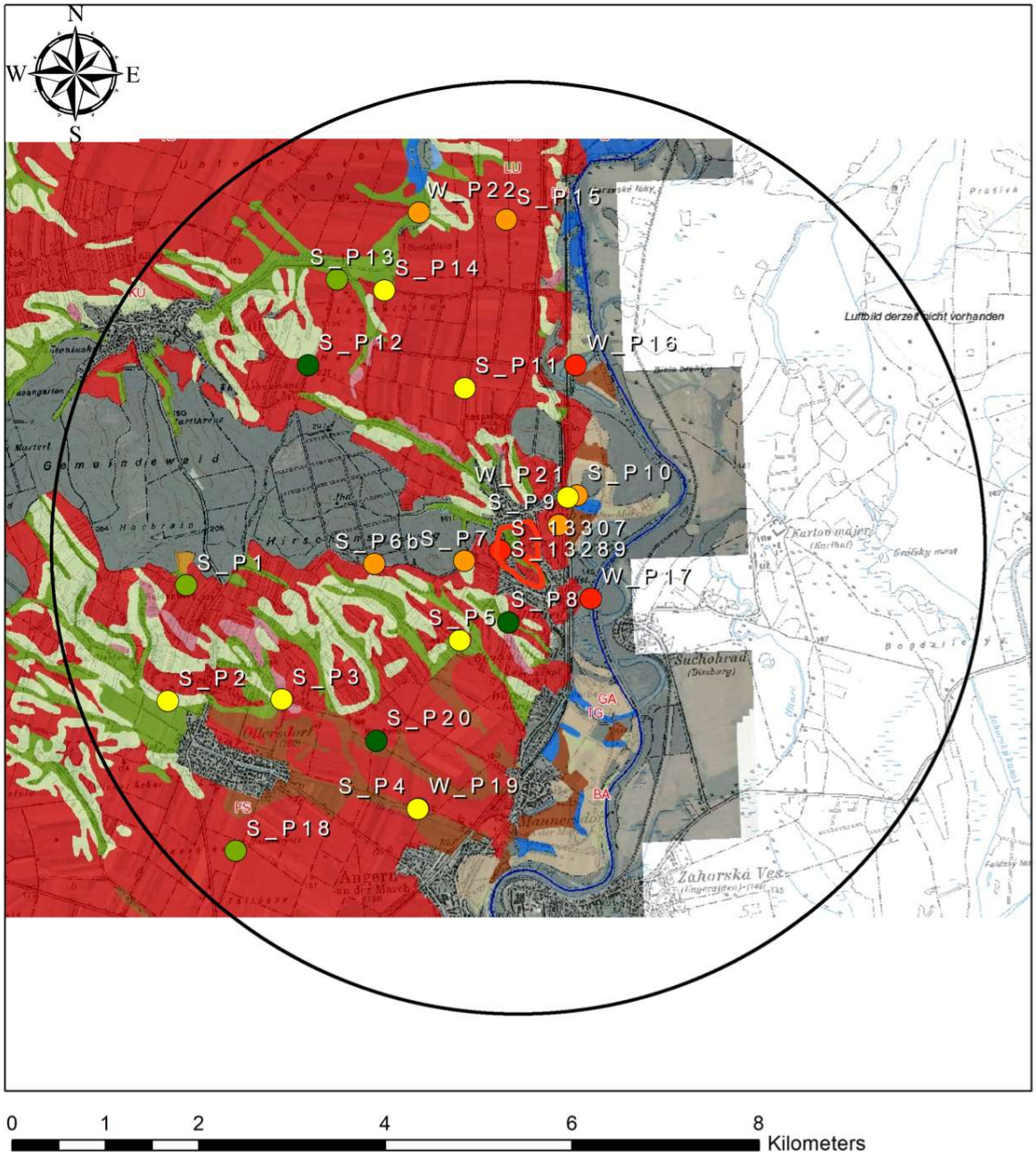

Legend Sr Ratios

- 0.70864 - 0.70890
- 0.70891 - 0.70929
- 0.70930 - 0.70965
- 0.70966 - 0.71024
- 0.71025 - 0.71074

- (KU) soil forming complex
- (LU) colluvium
- (TS) chernozem (arid)
- (LB) brown earth
- (FS) chernozem (humid)
- (TG) typical gley
- (BA) heavy weathered flood plain
- (GA) partially weathered flood plain
- (KU) eroded soil
- 5-kilometer-radius

Figure 26 Soil map showing the n(^{87}Sr)/n(^{86}Sr) isotope-amount ratios of the soil and water samples in a 5 km radius, (source: Digitale Bodenkarte von Österreich, 1km-Raster, Bundesforschungs- und Ausbildungszentrum für Wald, Naturgefahren und Landschaft (BFW))

4.2.2 Autochthonous Range

To determine the autochthonous environment, an autochthonous range was calculated. For this, the $n(^{87}Sr)/n(^{86}Sr)$ isotope-amount ratios of animal enamel (see below), mussel (see below) and archaeological straw and wood (see below) were used. The autochthonous signal ranges from 0.70987 to 0.71130. This range is also used in (Retzmann, Kriechbaum, Griebl et al., 2020, p. 67 ff).

4.2.3 Animal tooth samples

As can be seen in Fig. 25 the $n(^{87}Sr)/n(^{86}Sr)$ isotope-amount ratios of enamel and dentine of most of the animals overlap within their uncertainties (except the dog 13285 and the pig 13332). In case of both, the dog 13285 and the pig 13332, the $n(^{87}Sr)/n(^{86}Sr)$ isotope-amount ratio of the dentine is significantly lower than the $n(^{87}Sr)/n(^{86}Sr)$ isotope-amount ratio of the enamel.

The $n(^{87}Sr)/n(^{86}Sr)$ isotope-amount ratios of all analysed animals are relatively homogenous and in agreement with variability expected for local populations (Lengfelder, Grupe, Stallauer et al., 2019, p. 246f), the enamel signals lie between 0.70998 ± 36 µg g^{-1} and 0.71082 ± 27 µg g^{-1} (mean value 0.71049), the dentine signals are between 0.71008 ± 38 µg g^{-1} and 0.71074 ± 27 µg g^{-1} (mean value 0.71046) (Table 32 in the Appendix).

All of the animal tooth samples lie within the upper-half of the local range (Fig. 25) and can be seen as an indication for the autochthonous signal.

The $n(^{87}Sr)/n(^{86}Sr)$ isotope-amount ratios of the enamel are also mentioned in Retzmann, Kriechbaum, Griebl et al. (2020, p. 67).

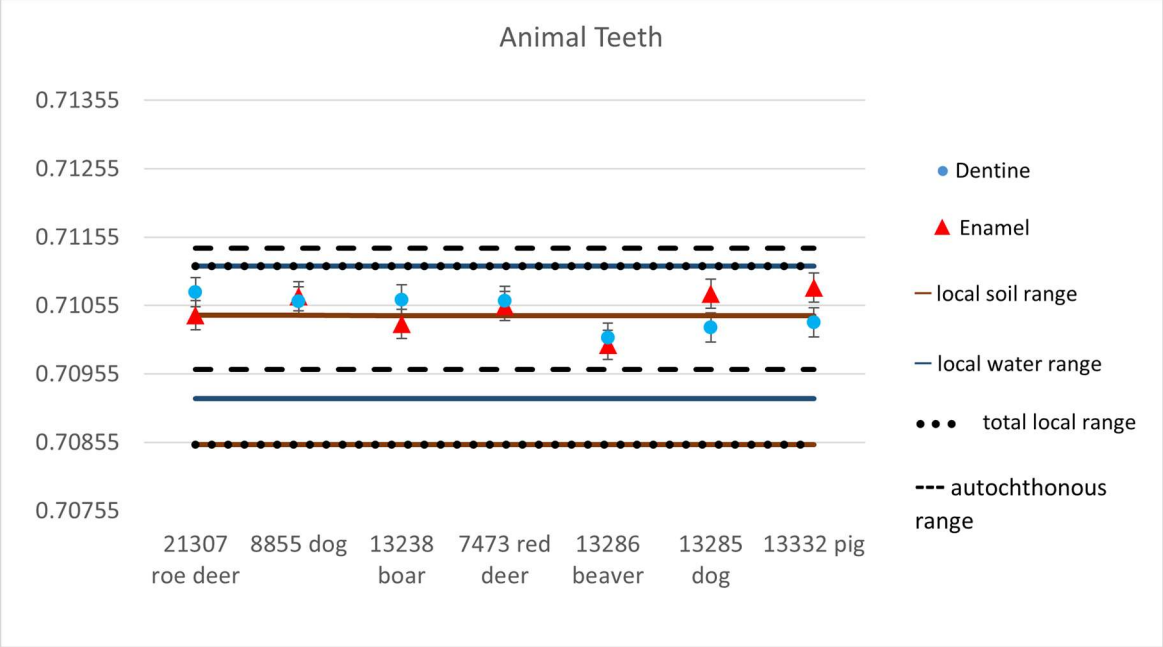

Figure 27 n(^{87}Sr)/n(^{86}Sr) isotope-amount ratios of enamel and dentine of the animal tooth samples compared to the local soil-, water-, total local- and autochthonous range

4.2.4 Mussel samples

Similar to the animal teeth, the mussel samples also lie within the local range, especially the local water range (except for sample ST_M_13272). Their $n(^{87}Sr)/n(^{86}Sr)$ isotope-amount ratios range from 0.71007 ± 24 µg g^{-1} to 0.71123 ± 24 µg g^{-1} with a mean value of 0.71050 (Table 40 in the Appendix). The samples all overlap within their uncertainties (see Fig. 26). The Sr isotopic ratios of mussel were included in the estimation of the autochthonous Sr signal as proxy for Sr drinking water source.

The $n(^{87}Sr)/n(^{86}Sr)$ isotope-amount ratios of the mussel samples are also mentioned in Retzmann, Kriechbaum, Griebl et al. (2020, p. 67).

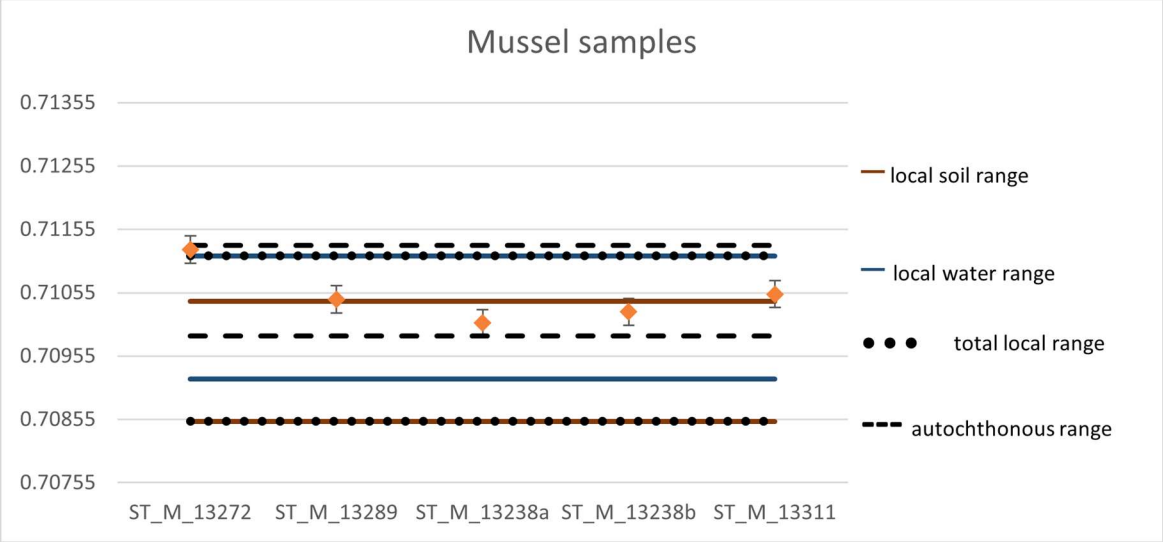

Figure 28 n(^{87}Sr)/n(^{86}Sr) isotope-amount ratios of the mussel samples compared to the local soil-, water-, total local- and autochthonous range

4.2.5 Archaeological environmental samples

Concerning the archaeological straw and wood samples, the mean value of each triplicate was taken. In the case of the straw sample, the mean $n(^{87}Sr)/n(^{86}Sr)$ isotope-amount ratio is 0.71116 ± 31µg g^{-1}, in the case of the wood sample the $n(^{87}Sr)/n(^{86}Sr)$ isotope-amount ratio is 0.71110 ± 35 µg g^{-1} (Table 53 in the Appendix). The samples overlap within their uncertainties. Both samples are on the upper limit of the local ranges.

Compared to the archaeological soil samples, taken from pit V0841 (Table 61 in the Appendix), both the straw and wood sample are higher in their Sr isotopic signature (Fig. 26). The Sr isotopic data of the archaeological straw and wood were included in the estimation of an autochthonous Sr range as proxy for Sr nutrition source (diet, vegetation). The $n(^{87}Sr)/n(^{86}Sr)$ isotope-amount ratios of those samples are also mentioned in Retzmann, Kriechbaum, Griebl et al. (2020, p. 67).

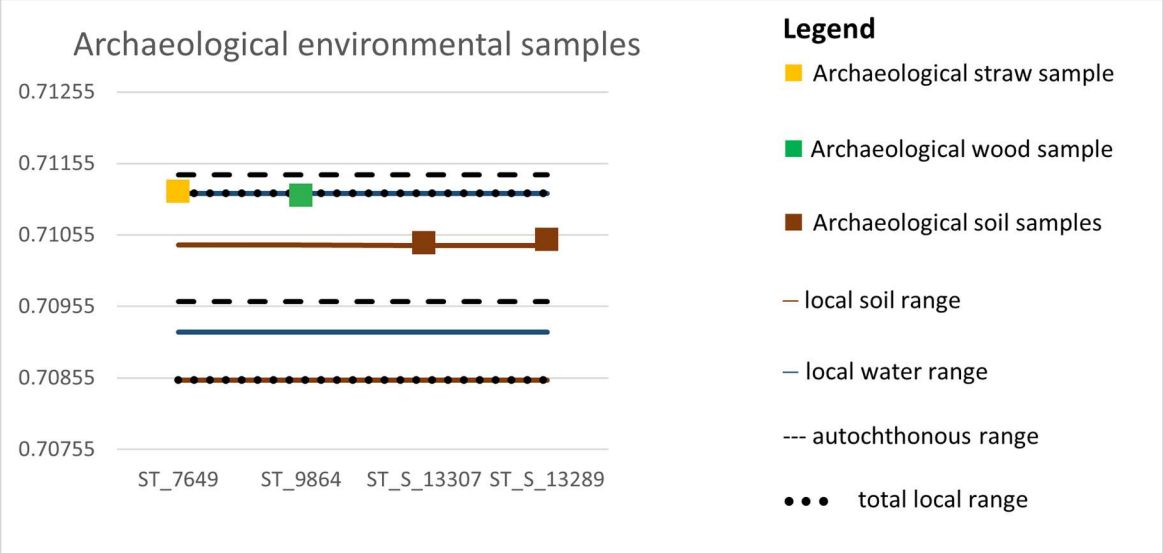

Figure 29 n(^{87}Sr)/n(^{86}Sr) isotope-amount ratios of the archaeological environmental samples, compared to the local soil, water-, autochthonous-, and total local range

4.2.6 Human tooth samples

Concerning diagenetic alterations, the biogenic $n(^{87}Sr)/n(^{86}Sr)$ ratios of the dentine samples were not calculated in this thesis. For those results see (Retzmann, Kriechbaum, Griebl et al., 2020, p. 67, p. 70). Here, the measured $n(^{87}Sr)/n(^{86}Sr)$ isotope-amount ratio of dentine was used.

4.2.6.1 Pit V1141

The enamel and dentine $n(^{87}Sr)/n(^{86}Sr)$ isotope-amount ratio of skeleton 1 (sign. 9023) do not lie within the local range and only the dentine value overlaps within uncertainty with the autochthonous Sr range (Fig. 27). The signals of enamel and dentine also do not overlap within their uncertainties. One can see a clear approach of the dentine signal to the local range which might indicate, that the individual had spent some time in Stillfried before its death or it is the result of diagenetic alteration.

The ratios of skeleton 4 (sign. 9026) lie within the local and autochthonous ranges and overlap within their uncertainties (Fig. 27). Therefore skeleton 4 is identified as supposedly autochthonous. For detailed $n(^{87}Sr)/n(^{86}Sr)$ isotope-amount ratios see Table 19 in the Appendix.

These results are also mentioned in Retzmann, Kriechbaum, Griebl et al. (2020, p. 70).

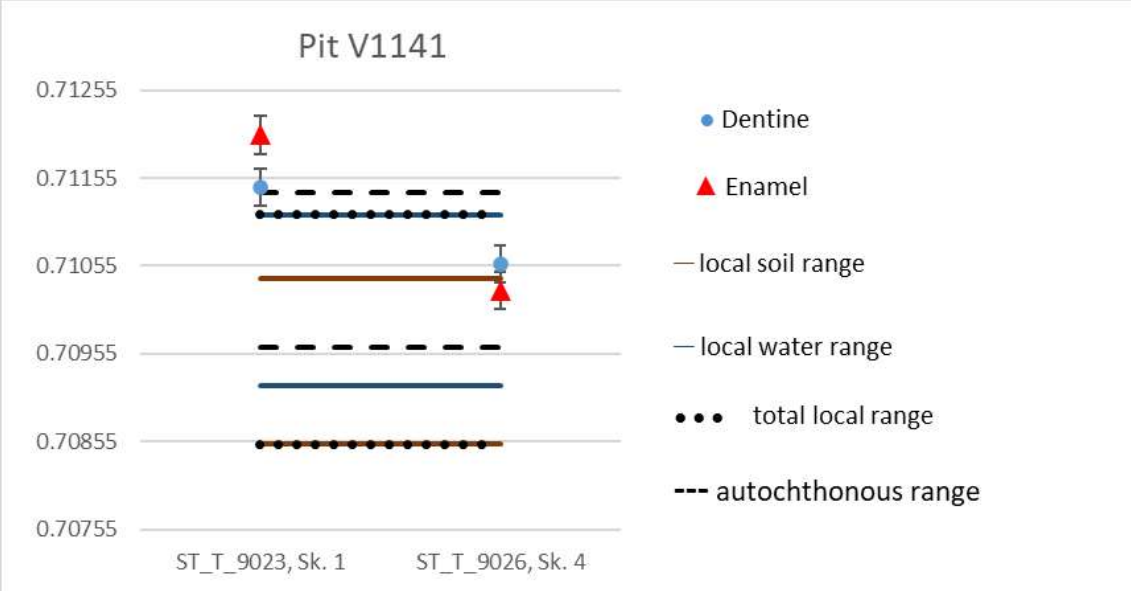

Figure 30 n(^{87}Sr)/n(^{86}Sr) isotope-amount ratios of enamel and dentine of the human tooth samples of pit V1141 compared to the local soil, water-, total local- and autochthonous range

4.2.6.2 Pit V1133

The child (sign. 1377) from pit V1133 shows $n(^{87}Sr)/n(^{86}Sr)$ isotope-amount ratios that lie within the local and autochthonous ranges. Nevertheless, one can see a significant difference between the enamel and dentine samples, since they do not overlap within their uncertainties. The enamel sample lies perfectly within the local range and at the lower area of the autochthonous range, whereas the dentine sample is located at the upper area of the local and autochthonous range (Fig. 28). Regardless, the girl is determined as supposedly autochthonous. For detailed $n(^{87}Sr)/n(^{86}Sr)$ isotope-amount ratios see Table 19 in the Appendix.

These results are also mentioned in Retzmann, Kriechbaum, Griebl et al. (2020, p. 74).

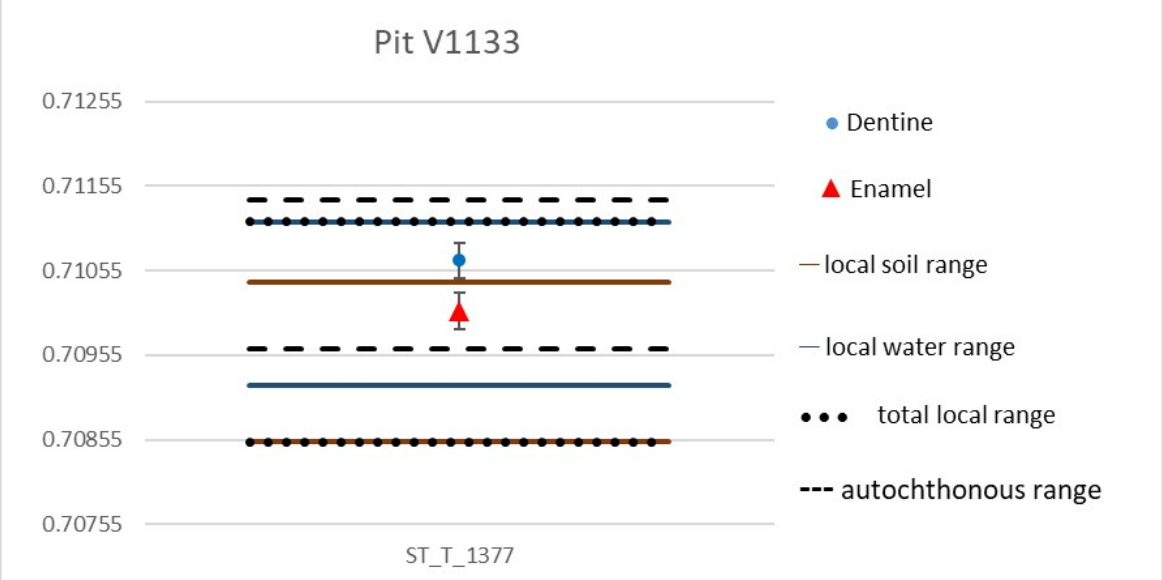

Figure 31 $n(^{87}Sr)/n(^{86}Sr)$ isotope-amount ratios of enamel and dentine of the human tooth samples of pit V1133 compared to the local soil, water-, total local and autochthonous range

4.2.6.3 Pit V0841

As can be seen in Fig. 29, all of the dentine samples clearly overlap within their uncertainties and lay within the upper-half of the local range. In contrast to that, only the enamel samples of skeleton 13 (sign. 9054), skeleton 11 (sign. 9052), skeleton 3 (sign. 9043) and skeleton 86-5/2 (sign. 9046) overlap within their uncertainties.

The enamel of skeleton 4 (sign. 9044) and skeleton 8 (sign. 9049) each shows a $n(^{87}Sr)/n(^{86}Sr)$ isotope-amount ratio clearly outside of the local and autochthonous Sr ranges (Fig 29). Hence, the skeleton 4 and 8 are determined as allochthonous individuals. The $n(^{87}Sr)/n(^{86}Sr)$ isotope-amount ratios of the dentine of those two individuals on the other hand, lie within the local ranges (the dentine $n(^{87}Sr)/n(^{86}Sr)$ isotope-amount ratio of skeleton 4 is at the upper area of the local and autochthonous ranges, but nevertheless within those ranges.

Still within the local soil and combined local range but nevertheless a completely different $n(^{87}Sr)/n(^{86}Sr)$ isotope-amount ratio shows the enamel of skeleton 2 (sign. 9042) which can be found at the lower area of those ranges and outside the autochthonous and water range (Fig. 29). Thus the individual is considered as probably allochthonous.

Even though the enamel and dentine $n(^{87}Sr)/n(^{86}Sr)$ isotope-amount ratio of skeleton 10 (sign. 9051) both lie within the local range, they differ significantly since their uncertainties do not overlap (see Fig. 29). Furthermore, the $n(^{87}Sr)/n(^{86}Sr)$ isotope-amount ratio of the

enamel of skeleton 10 does not overlap with the autochthonous Sr range and is significantly lower than the ratio of the dentine which overlaps in its uncertainty with the dentine ratios of the other individuals. This determines skeleton 10 as probably allochthonous (see Fig. 29).

As for the other analysed individuals of pit V0841, which are skeleton 3 (sign. 9043), skeleton 86-5/2 (sign. 9046), skeleton 11 (sign. 9052) and skeleton 13 (sign. 9054), those individuals $n(^{87}Sr)/n(^{86}Sr)$ isotope-amount ratio of the enamel and dentine overlap within their uncertainties and lie within the local and autochthonous ranges (see Fig. 29). Therefore those individuals can be classified as supposedly autochthonous.

For detailed $n(^{87}Sr)/n(^{86}Sr)$ isotope-amount ratios see Table 19 in the Appendix.

These results are also mentioned in Retzmann, Kriechbaum, Griebl et al. (2020, p. 74f).

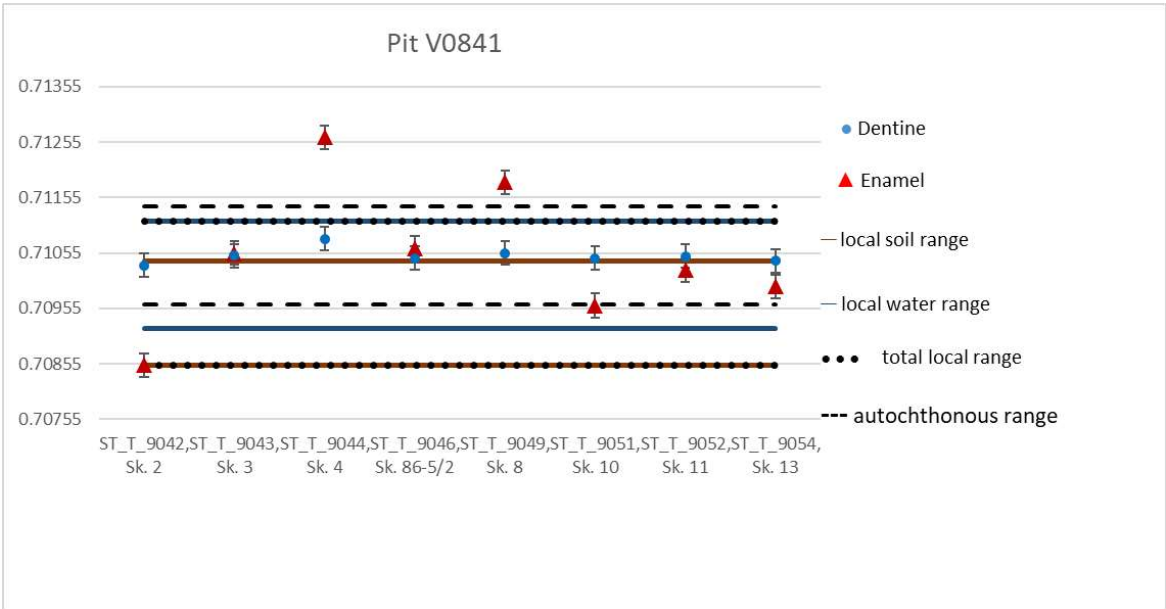

Figure 32 $n(^{87}Sr)/n(^{86}Sr)$ isotope-amount ratios of enamel and dentine of the human tooth samples of pit V0841 compared to the local soil, water-, total local- and autochthonous range

4.2.6.4 All human individuals – a comparison

Pit V1141 and Pit V0841 contain individuals with $n(^{87}Sr)/n(^{86}Sr)$ isotope-amount ratios that are outside the local and autochthonous range and therefore determined as allochthonous individuals. Nevertheless, about half of the individuals in all of the pits have $n(^{87}Sr)/n(^{86}Sr)$ isotope-amount ratios that are within the local and autochthonous ranges and hence are determined as supposedly autochthonous (Fig. 30).

For detailed $n(^{87}Sr)/n(^{86}Sr)$ isotope-amount ratios see Table 19 in the Appendix.

These results are also mentioned in Retzmann, Kriechbaum, Griebl et al. (2020, p. 70 ff).

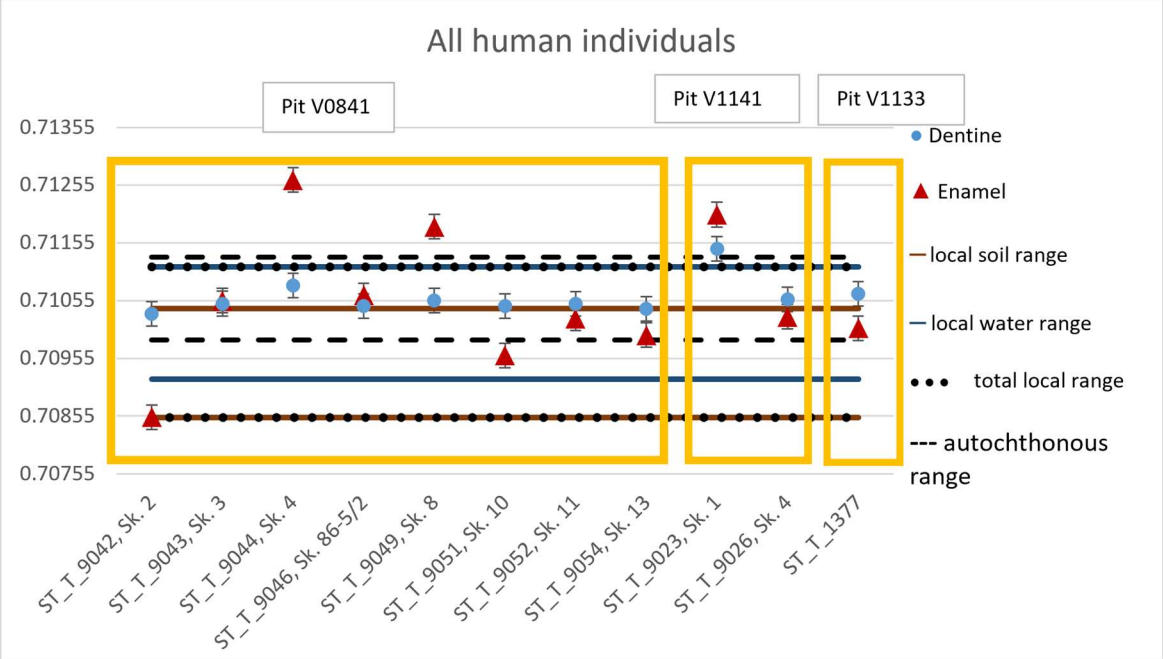

Figure 33 n(^{87}Sr)/n(^{86}Sr) isotope-amount ratios of enamel and dentine of all human individuals sorted by pits

5 Discussion

Some components of the discussion of this thesis are published in Retzmann, Kriechbaum, Griebl et al. (2020, p. 75 ff).

5.1 Local $n(^{87}Sr)/n(^{86}Sr)$ isotope range and autochthonous range

It has to be taken into consideration, that the reference samples for the determination of the local and autochthonous ranges could only be taken in the Austrian part of the settlements surroundings which means that the $n(^{87}Sr)/n(^{86}Sr)$ isotope-amount ratios in the March area of Slovakia remains unclear. This is a factor that weakens the determined ranges.

Teschler-Nicola, Irrgeher&Prohaska (2016, p. 165) got a broader autochthonous range in their study (0.70956 – 0.71159). They defined the range as mean human dentine $n(^{87}Sr)/n(^{86}Sr)$ plus-minus four times the standard deviation whereas here, the autochthonous range was defined as mean $n(^{87}Sr)/n(^{86}Sr)$ ratio of animal enamel, mussels and archaeological plant findings (straw and wood) plus-minus two times the standard deviation. Residential large vertebrates and omnivores (Price, Burton&Bentley, 2002, p. 132) and domesticated animals (dogs and pigs) fed presumably from the similar diet as humans were used. Therefore their $n(^{87}Sr)/n(^{86}Sr)$ isotope-amount ratio reflects the Sr source in plants that were ingested. The overlap of modern local water range and archaeological mussel samples strengthens the representativeness of the $n(^{87}Sr)/n(^{86}Sr)$ ratio for drinking water.

5.2 "The Seven from the Pit" V1141

The $n(^{87}Sr)/n(^{86}Sr)$ isotope-amount ratios of all the individuals found in pit V1141 have been analysed previously (Teschler-Nicola, Irrgeher&Prohaska, 2016, p. 159 ff). Comparing the results of Teschler-Nicola, Irrgeher&Prohaska (2016, p. 165 ff) with those of this thesis one can see slightly differing $n(^{87}Sr)/n(^{86}Sr)$ isotope-amount ratios. As one can see in Fig. 31, Table 8 and Table 9 the $n(^{87}Sr)/n(^{86}Sr)$ isotope-amount ratios of the enamel of skeleton 1 overlap within their uncertainties whereas the dentine samples of Sk. 1 (sign. 9023) do not. Based on what we can see in Fig. 31, the enamel neither of the M1 (Teschler-Nicola, Irrgeher&Prohaska, 2016, p. 166) nor the P1 of Sk. 1 lie within the local and autochthonous ranges which strengthens the classification of Sk. 1 as allochthonous. Its origin is most likely the Austrian part of the Bohemian Massif (Janousek, Rogers&Bowes,

1995, p. 520, Janousek, Finger, Roberts et al., 2004, p. 141). The dentine, on the other hand, is diverse. The $n(^{87}Sr)/n(^{86}Sr)$ ratio of the M1 lies within the local and autochthonous ranges, the ratio of the P1 on the other hand, does not. Both dentine $n(^{87}Sr)/n(^{86}Sr)$ isotope-amount ratios show an approach to the local range, in comparison to the dental enamel.

Neglecting differences in formation period of P1 and M1, the differences in Sr isotopic ratios between P1 and M1 of the same individual might indicate a different degree of diagenetic alteration. It is important to note, that in this thesis, the teeth were cut vertically for the first time which made it easier to only use the pulp dentine whereas Teschler-Nicola, Irrgeher&Prohaska (2016, p. 164) used root dentine. A Previous study suggests that circumpulpal dentine, as sampled from P1 in the present study, is less affected by diagenesis than root dentine, as sampled for the M1 (Bell, Boyde&Jones, 1991, p. 179). Nevertheless, the dentine in this study also shows indications for diagenesis. This is further discussed in our paper (Retzmann, Kriechbaum, Griebl et al., 2020, p. 67, p. 70).

Furthermore, pulp dentine exhibits a higher turnover than root dentine. This can be justified by the higher blood circulation within the pulp dentine which then results in a higher Strontium turnover. This means, that the root dentine sampled in the M1 preserves slightly older Sr isotopic information than the pulp dentine taken from the P1 (Theiner, 2011, p. 96). The $n(^{87}Sr)/n(^{86}Sr)$ isotope-amount ratios of enamel and dentine of Sk. 4 (sign. 9026) from this thesis and those determined by Teschler-Nicola, Irrgeher&Prohaska (2016, p. 166) overlap within uncertainties. Furthermore, they both clearly lie within the local and autochthonous range. This indicates, that the boy Sk. 4 is supposedly autochthonous.

Looking at these data, the assumptions of Breitinger (1981, p. 6f), that this is the deposition of a family, are theoretically possible in the case of Sk. 1 and Sk. 4. The other individuals of this pit and their $n(^{87}Sr)/n(^{86}Sr)$ isotope-amount ratios were analysed and discussed in Teschler-Nicola, Irrgeher&Prohaska (2016, p. 159).

Table 8 Comparison of the $n(^{87}Sr)/n(^{86}Sr)$ amount- ratios of the enamel of this thesis to those of Teschler-Nicola, Irrgeher&Prohaska (2016)

Individual	**Tooth** (Teschler-Nicola, Irrgeher&Prohaska, 2016, p. 166)	$n(^{87}Sr)/n(^{86}Sr)$ **ratio of the enamel** (Teschler-Nicola, Irrgeher&Prohaska, 2016, p. 166)	**Tooth** (this thesis)	$n(^{87}Sr)/n(^{86}Sr)$**of the enamel ratio** (this thesis)
SK.1 (9023)	left M1, Mandibula	0.71216 ± 18 µg g^{-1}	right P3, Maxilla	0.71204 ± 19 µg g^{-1}
SK.4 (9026)	left m2, mandibula	0.70990 ± 18 µg g^{-1}	left c, mandibula	0.71027 ± 19 µg g^{-1}

Table 9 Comparison of the the $n(^{87}Sr)/n(^{86}Sr)$ amount- ratios of the dentine of this thesis to those of Teschler-Nicola, Irrgeher&Prohaska (2016)

Individual	**Tooth** (Teschler-Nicola, Irrgeher&Prohaska, 2016, p. 166)	$n(^{87}Sr)/n(^{86}Sr)$ **ratio of the dentine** (Teschler-Nicola, Irrgeher&Prohaska, 2016, p. 166)	**Tooth** (this thesis)	$n(^{87}Sr)/n(^{86}Sr)$**of the dentine ratio** (this thesis)
SK.1 (9023)	left M1, Mandibula	0.71070 ± 18 µg g^{-1}	right P3, Maxilla	0.71144 ± 19 µg g^{-1}
SK.4 (9026)	left m2, mandibula	0.71018 ± 18 µg g^{-1}	left c, mandibula	0.71057 ± 19 µg g^{-1}

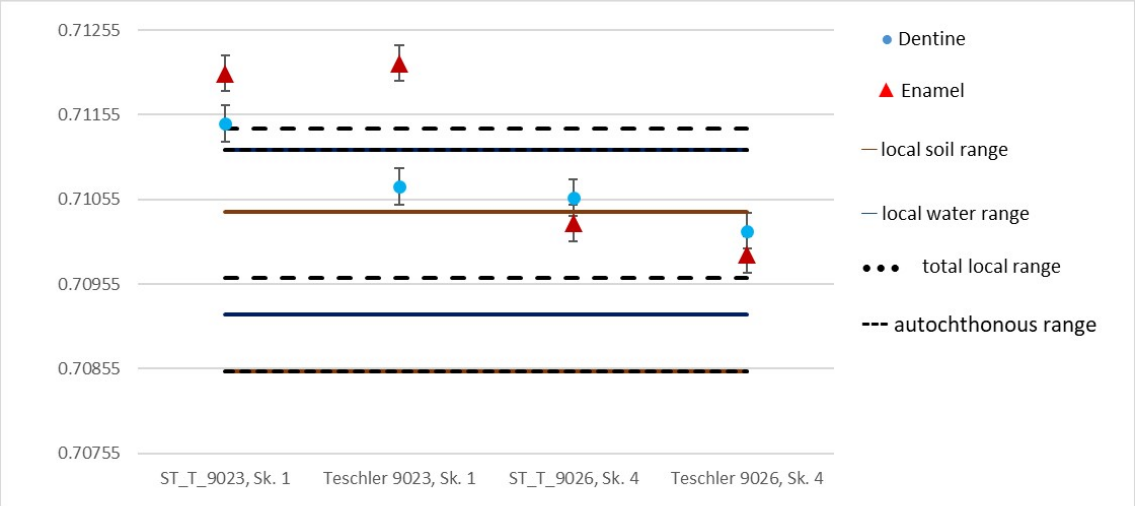

Figure 34 Comparison of the n(^{87}Sr)/n(^{86}Sr) amount-ratios of this thesis to those of Teschler-Nicola, Irrgeher&Prohaska (2016, p. 166)

5.3 The Calvarium of Pit V1133

Both, the enamel and dentine $n(^{87}Sr)/n(^{86}Sr)$ isotope-amount ratios of the child from pit V1133 are within the local and autochthonous $n(^{87}Sr)/n(^{86}Sr)$ range. However, they differ and do not overlap within their uncertainties. Such a variation in the $n(^{87}Sr)/n(^{86}Sr)$ isotope-amount ratios can either be the result of a change in nutrition or change of the resource of food supply or residential changes from an area with a similar $n(^{87}Sr)/n(^{86}Sr)$ isotope-amount ratio. Furthermore, it could also be the result of diagenetic alteration. Nevertheless, according to the results, this individual can be identified as autochthonous.

Parts of this subchapter are also mentioned in Retzmann, Kriechbaum, Griebl et al. (2020. p. 78).

5.4 Mass burial in Pit V0841

Parts of this subchapter are also mentioned in Retzmann, Kriechbaum, Griebl et al. (2020, p. 79).

The enamel of Sk. 4 (sign. 9044) and Sk. 8 (sign. 9049) shows a $n(^{87}Sr)/n(^{86}Sr)$ isotope-amount ratio which clearly lies outside the local and autochthonous Sr range whereas the dentine of both individuals shows a $n(^{87}Sr)/n(^{86}Sr)$ isotope-amount ratio within the local and autochthonous Sr range. This indicates a (similar) foreign origin of those two individuals. In accordance to Sk. 1 from pit V1141, their origin is most likely the Austrian part of the

Bohemian Massif (Janousek, Rogers&Bowes, 1995, p. 520, Janousek, Finger, Roberts et al., 2004, p. 141).

The enamel $n(^{87}Sr)/n(^{86}Sr)$ isotope-amount ratio of Sk. 10 is lower than the ratio of its dentine, and only overlaps with the enamel ratio of Sk. 13 in their uncertainties. It is important to note, that in case of Sk. 10 a deciduous tooth (left upper m1) was analysed. The enamel of this tooth is fully formed in utero to the age of approx. 7.5 months postpartum(AlQahtani, Hector&Liversidge, 2010). In general, the $n(^{87}Sr)/n(^{86}Sr)$ isotope-amount ratios of the enamel of Sk. 10 and Sk. 2 (9042) are different from the $n(^{87}Sr)/n(^{86}Sr)$ isotope-amount ratios of the other supposedly autochthonous and allochthonous individuals. Nevertheless, they are still within the local environmental $n(^{87}Sr)/n(^{86}Sr)$ range but below the autochthonous $n(^{87}Sr)/n(^{86}Sr)$ range. This could be the result of a different resource in nutrition during the childhood in comparison to the other individuals or residential changes from an area with a similar $n(^{87}Sr)/n(^{86}Sr)$ isotope-amount ratio. The latter seems to be more likely, since the autochthonous $n(^{87}Sr)/n(^{86}Sr)$ range was determined in particular from food and potential drinking water sources which represents most closely the autochthonous human $n(^{87}Sr)/n(^{86}Sr)$ amount-ratio of the hillfort site at Stillfried/March. This classifies both individuals as allochthonous individuals.

As it was in the case of the girl of pit V1133, the variation in the enamel and primary dentine $n(^{87}Sr)/n(^{86}Sr)$ ratio of Sk. 13 can either be the result of a change in nutrition, change in the resource of food supply or the result of diagenesis.

Comparing the three skeletal layers, a significant difference between those layers cannot be found. The sample size within the single layers is rather small, therefore is not possible to determine any significant differences between the three skeletal layers especially since not all 23 individuals were analysed.
Sk. 11 (sign. 9052) and Sk. 13 (sign. 9054) of skeletal layer 1, both are classified as autochthonous individuals (Fig. 32). In skeletal layer 2, skeleton 8 and 10 are classified as allochthonous individuals. In skeletal layer 3, Sk. 2 (sign. 9042) and Sk. 4 (sign. 9044) show different enamel $n(^{87}Sr)/n(^{86}Sr)$ isotope-amount ratios. Both are classified as allochthonous individuals. Sk. 3 (sign. 9043) and Sk. 86-5/2 (sign. 9046) are both classified as autochthonous individuals.

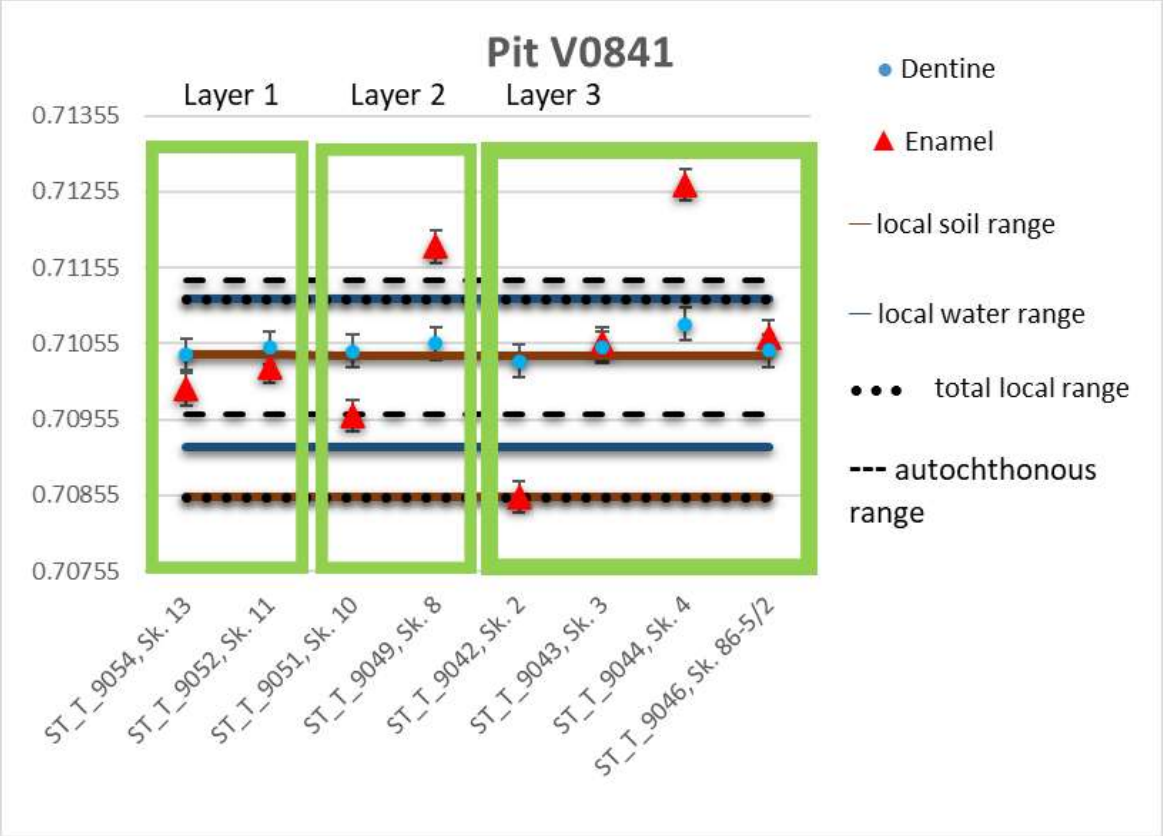

Figure 35 $n(^{87}Sr)/n(^{86}Sr)$ isotope-amount ratios of enamel and dentine of the human tooth samples of pit V0841 compared to the local soil, water-, combined- and autochthonous range sorted by layers (described in the introduction of this thesis)

5.5 Conclusion

A significant proportion of allochthonous individuals could be identified:

The enamel of three individuals (Sk. 4 and Sk. 8 of pit V0841 and Sk. 1 of pit V1141) shows a $n(^{87}Sr)/n(^{86}Sr)$ isotope-amount ratio higher than the local range. Those individuals were classified as allochthonous individuals. They could originate from a geologically similar region, probably the Bohemian Massif (Janousek, Rogers&Bowes, 1995, p. 520, Janousek, Finger, Roberts et al., 2004, p. 141). Sk. 2 and Sk. 10 of pit V0841 on the other hand show a Sr ratio in the enamel only overlapping with the local Sr range. They were also classified as allochthonous individuals, but their Sr ratios definitely originate from a different nutrition source than Sk. 4 (of pit V0841), Sk. 8 and Sk. 1. Their origin has not been determined yet, but is assumed to be nearby Stillfried. All other analysed individuals are classified as autochthonous.

A similar trend to previous studies for the late Bronze Age (Wahl&Price, 2013, p. 302, Knipper, Fragata, Nicklisch et al., 2016, p. 510, Cavazzuti, Skeates, Millard et al., 2019, p. 34ff) can be determined. Approx. 40 % of the investigated adult individuals (including those of the previous study from Teschler-Nicola, Irrgeher&Prohaska (2016, p. 166)) and more tha 50 % of the subadult individuals (including those of the previous study from Teschler-Nicola, Irrgeher&Prohaska (2016, p. 166)) from the settlement pits in Stillfried/March were classified as allochthonous.

The research question whether there is a clear indication that the inhumations in the settlement pits of Stillfried represent a distinct group of immigrated individuals could be answered. There seems to be no obvious connection between the the burial practice within the settlement and the individuals' origins. In order to further investigate a possible connection of differences in burial practice and an individual's origin, future studies should include $n(^{87}Sr)/n(^{86}Sr)$ isotope analysis of all human individuals recovered from the settlement pits as well as a representative sample of the cremated remains from the Urnfield culture burial site of Stillfried.

6 Abstract

In this thesis, the human skeletal depositions of the Late Urnfield Period Stillfried/March (Lower Austria) were analysed in respect of their residential origin. Therefore, enamel and dentine of mainly premolars of eleven deposited individuals were analysed for their $n(^{87}Sr)/n(^{86}Sr)$ amount-ratio using multi-collector inductively coupled plasma mass spectrometry (MC ICP-MS).

To differenciate between allochthonous and (supposeldly) autochthonous individuals, a local Sr isotopic range, based on environmental samples was defined. Furthermore an autochthonous range, based on archaeological findings of animals, mussels and plants (= proxy for Sr nutrion and drinking water sources) was defined.

The $n(^{87}Sr)/n(^{86}Sr)$ amount-ratios of the human enamel were compared to the local $n(^{87}Sr)/n(^{86}Sr)$ range as well to an autochthonous $n(^{87}Sr)/n(^{86}Sr)$ range. Five of the eleven analysed individuals could be classified as allochthonous. They indicate at least two different homelands. This diversity indicates high mobility of Strillfrieds population during the late Bronze Age which supports the classification of Stillfried as a ‘central site’.

The research question could be answered. There seems to be no obvious connection between the the burial practice within the settlement and the individuals’ origins. The reason for the different forms of burial remains undisclosed.

7 Zusammenfassung

Im Zuge dieser Masterarbeit wurden die menschlichen Skelettniederlegungen der späten Urnenfelderzeit in Stillfried an der March (Niederösterreich) im Hinblick auf ihre Herkunft analysiert. Hierfür wurden Enamel und Dentin von hauptsächlich Prämolaren von elf der Skelettniederlegungen beprobt und deren $n(^{87}Sr)/n(^{86}Sr)$ Verhältnis mittels Multikollektor Massenspektrometrie mit induktiv gekoppeltem Plasma (MC ICP-MS) untersucht.

Im Falle des Dentins wurde in dieser Arbeit nur Pulpendentin beprobt. Um an dieses zu gelangen, wurden die Zähne mit einer Säge in zwei Hälften geschnitten.

Weiters wurden die $n(^{87}Sr)/n(^{86}Sr)$ Verhältnisse des Enamels der menschlichen Zähne mit einem lokalen Bereich (berechnet aus Umweltproben) und einem autochthonen Bereich (basierend auf im Zuge der Grabungen vorgefundene tierische und pflanzliche Überreste) verglichen.

Fünf der untersuchten Individuen wurden als allochthon identifiziert. Drei davon wiesen ein höheres $n(^{87}Sr)/n(^{86}Sr)$ Verhältnis und zwei ein niedrigeres $n(^{87}Sr)/n(^{86}Sr)$ Verhältnis als der autochthone Bereich auf. Dieses Ergebnis deutet auf zumindest zwei unterschiedliche Herkunftsorte der allochthonen Individuen hin.

Die Forschungsfrage, ob die Skelettniederlegungen aufgrund einer unterschiedlichen Herkunft der in den Gruben deponierten Individuen basiert, kann beantwortet werden. Es scheint keinen klaren Zusammenhang zwischen der abweichenden Bestattungsform und der Herkunft der einzelnen Individuen zu geben. Der Grund für die abweichende Bestattungsform bleibt unbekannt.

8 Literature

ALQAHTANI, HECTOR & LIVERSIDGE, 2010

ALQAHTANI, S. J., HECTOR, M. P.&LIVERSIDGE, H. M. 2010. The London Atlas of Human Tooth Development and Eruption. *American Journal of Physical Anthropology,* 142**,** 481-490.

ANTL, 1985

ANTL, G. 1985. Die interdisziplinären Komponenten des Forschungsprojektes. *In:* WINDL, H. (ed.) *Ausgrabung in Stillfried. Stratigraphie von der Eiszeit bis zur Gegenwart.* Wien. Katalog des Niederösterreichischen Landesmuseums. Neue Folge 158. 15-18

ANTL-WEISER, 1985

ANTL-WEISER, W. 1985. Steinschläger-Werkstatt der Altsteinzeit. *In:* WINDL, H. (ed.) *Ausgrabung in Stillfried. Stratigraphie von der Eiszeit bis zur Gegenwart.* Wien. Katalog des Niederösterreichischen Landesmuseums. Neue Folge 158. 19-24

BARG, 1988

BARG, F. 1988. Wallstratigraphie und Siedlung von der Urnenfelderzeit bis ins Mittelalter. *In:* FELGENHAUER, F., J., S., KRITSCHER, H.&HAUSER, G. (eds.) *Stillfried: Archäologie - Anthropologie.* Wien. Veröffentlichungen des Museums für Ur- und Frühgeschichte in Stillfried. Sonderband 3. 97-104

BARTELINK & CHESSON, 2019

BARTELINK, E. J.&CHESSON, L. A. 2019. Recent applications of isotope analysis to forensic anthropology. *Forensic Sciences Research,* 4**,** 29-44.

BELL, BOYDE & JONES, 1991

BELL, L. S., BOYDE, A.&JONES, S. J. 1991. Diagenetic Alteration to Teeth In Situ Illustrated by Backscattered Electron Imaging. *Scanning,* 13**,** 173-183.

BENDREY, HAYES & PALMER, 2009

BENDREY, R., HAYES, T. E.&PALMER, M. R. 2009. Patterns of Iron Age Horse Supply: An Analysis of Strontium Isotope Ratios in Teeth. *Archaeometry,* 51**,** 140-150.

BENSON, KINSLEY, WILLMES et al. 2013

BENSON, A., KINSLEY, L., WILLMES, M., DEFLEUR, A., KOKKONEN, H., MUSSI, M.&GRÜN, R. 2013. Laser Ablation Depth Profiling of U-series and Sr Iso- topes in Human Fossils. *Journal of Archaeological Science,* 40**,** 2991-3000.

BENTLEY, 2006

BENTLEY, A. R. 2006. Strontium Isotopes from the Earth to the Archaeological Skeleton: A Review. *Journal of Archaeological Method and Theory,* 13**,** 135-187.

BENTLEY & KNIPPER, 2005

BENTLEY, R. A.&KNIPPER, C. 2005. Geographical patterns in biologically available strontium, carbon and oxygen isotope signatures in prehistoric SW Germany. *Archaeometry,* 47**,** 629-644.

BLUM, TALIAFERRO, WEISSE et al., 2000

BLUM, J. D., TALIAFERRO, E. H., WEISSE, M. T.&HOLMES, R. T. 2000. Changes in Sr/Ca, Ba/Ca and 87Sr/ 86Sr ratios between trophic levels in two forest ecosystems in the northeastern U.S.A. *Biogeochemistry,* 49**,** 87-101.

BREITINGER, 1976

BREITINGER, E. 1976. Das Kalvarium unter dem Späturnenfelderzeitlichen Wall von Stillfried an der March. *Forschungen in Stillfried,* 2**,** 86-100.

BREITINGER, 1980

BREITINGER, E. 1980. Skelette aus einer späturnenfelderzeitlichen Speichergrube in der Wallburg von Stillfried an der March, NÖ. *Forschungen in Stillfried,* 4**,** 45-106.

BREITINGER, 1981

BREITINGER, E. 1981. Die Sieben aus der Speichergurube. *Veröffentlichungen des Museums für Ur- und Frühgeschichte Stillfried,* 2/1981**,** 1-12.

CAPO, STEWART & CHADWICK, 1998

CAPO, R. C., STEWART, B. W.&CHADWICK, O. A. 1998. Strontium isotopes as tracers of ecosystem processes: theory and methods. *Geoderma,* 82**,** 197-225.

CAVAZZUTI,SKEATES, MILLARD et al., 2019

CAVAZZUTI, C., SKEATES, R., MILLARD, A. R., NOWELL, G., PETERKIN, J., BERNABÒ BREA, M., CARDARELLI, A.&SALZANI, L. 2019. Flows of people in villages and large

centres in Bronze Age Italy through strontium and oxygen isotopes. *PLOS ONE,* 14**,** e0209693.

CIAAW, 2020

CIAAW. *Strontium* [Online]. Available: https://www.ciaaw.org/strontium.htm [Accessed 20.08. 2020].

COPELAND, SPONHEIMER, LE ROUX et al., 2008

COPELAND, S. R., SPONHEIMER, M., LE ROUX, P. J., GRIMES, V., LEE-THORP, J. A., DE RUITER, D. J.&RICHARDS, M. P. 2008. Strontium isotope ratios (87Sr/86Sr) of tooth enamel: a comparison of solution and laser ablation multicollector inductively coupled plasma mass spectrometry methods. *Rapid Communications in Mass Spectrometry,* 22**,** 3187-3194.

CROWLEY, MILLER & BATAILLE, 2017

CROWLEY, B. E., MILLER, J. H.&BATAILLE, C. P. 2017. Strontium isotopes ((87) Sr/(86) Sr) in terrestrial ecological and palaeoecological research: empirical efforts and recent advances in continental-scale models. *Biol Rev Camb Philos Soc,* 92**,** 43–59.

DUDÁS, LEBLANC, CARTER et al., 2016

DUDÁS, F. Ö., LEBLANC, S. A., CARTER, S. W.&BOWRING, S. A. 2016. Pb and Sr concentrations and isotopic compositions in prehistoric North American teeth: A methodological study. *Chemical Geology,* 429**,** 21-32.

EIBNER, 1974

EIBNER, A. 1974. Zum Befund einer hallstattzeitlichen Webgrube aus Stillfried. *Forschungen in Stillfried,* 1**,** 76-84.

EIBNER, 1976

EIBNER, C. 1976. Eine Späturnenfelderzeitliche Grube unter den Aufschüttungen des Westwalles von Stillfried. Zum Befund einer Schädeldeposition. *Forschungen in Stillfried,* 2**,** 70-85.

EIBNER, 1980

EIBNER, C. 1980. Die Mehrfachbestattung aus einer Grube unter dem urnenfelderzeitlichen Wall in Stillfried an der March, NÖ. *Forschungen in Stillfried,* 4**,** 107-142.

EIBNER, 1985

EIBNER, C. 1985. Die urnenfelderzeitliche Wallburg und das Gräberfeld ("In der Gans"/Burenberg). *In:* WINDL, H. (ed.) *Ausgrabungen in Stillfried. Stratigraphie von der Eiszeit bis zur Gegenwart.* Wien. Katalog des Niederösterreichischen Landesmuseums. Neue Folge 158. 31-37

EIBNER, 1988

EIBNER, C. 1988. Die Mehrfachbestattung aus Stillfried an der March aus archäologischer Sicht. *In:* FELGENHAUER, F., SZILVÁSSY, J., KRITSCHER, H.&HAUSER, G. (eds.) *Stillfried: Archäologie – Anthropologie.* Wien. Veröffentlichungen des Museums für Ur- und Frühgeschichte in Stillfried. Sonderband 3. 77-87

ELMER, 2010

ELMER, P. 2010. NexION 300-Hardwarehandbuch.

EZZO, JOHNSON & PRICE, 1997

EZZO, J. A., JOHNSON, C. M.&PRICE, T. D. 1997. Analytical Perspectives on Prehistoric Migration: A Case Study From East-Central Arizona. *Journal of Archaeological Science,* 24**,** 447–466.

FAURE, 1986

FAURE, G. 1986. *Principles of Isotope Geology,* NewYork/Chichester/Brisbane/Toronto/Singapore, John Wiley & Sons.

FELGENHAUER, 1973

FELGENHAUER, F. 1973. Fundberichte aus Österreich, 1972. *Fundberichte aus Österreich.* Wien. Bundesdenkmalamt, Abteilung für Bodendenkmalpflege. 11. 56-57

FELGENHAUER, 1978a

FELGENHAUER, F. 1978a. Arbeitsbericht Stillfried 1972, 1973, 1974, 1975, 1976. *Forschungen in Stillfried,* 3**,** 96-106.

FELGENHAUER, 1980a

FELGENHAUER, F. 1980a. Arbeitsbericht Stillfried 1977, 1978, 1979, 1980. *Forschungen in Stillfried,* 4**,** 177-192.

FELGENHAUER, 1980b

FELGENHAUER, F. 1980b. Ein jungpaläolithisches Steinschlägeratelier aus Stillfried an der March, Niederösterreich. Zur Herstellungstechnik von Mikrogravettespitzen. *Forschungen in Stillfried,* 4**,** 7-40.

FELGENHAUER, 1985

FELGENHAUER, F. 1985. Erforschung des Lebens- und Kulturraumes Stillfried an der March von der Eiszeit bis zur Gegenwart. *In:* WINDL, H. (ed.) *Ausgrabung in Stillfried. Stratigraphie von der Eiszeit bis zur Gegenwart.* Wien. Katalog des Niederösterreichischen Landesmuseums. Neue Folge 158. 11-12

FELGENHAUER, 1988

FELGENHAUER, F. 1988. Arbeitsbericht Stillfried, 1986,1987. *Forschungen in Stillfried.* 8. 281-288

FELGENHAUER, 1996

FELGENHAUER, F. 1996. Lebensraum des Menschen seit 30.000 Jahren. Archäologischer Fundplatz von internationaler Bedeutung. Objekt interdisziplinärer Forschung von bedeutendem Rang. Ergebnisse der Ausgrabungen und Forschungen 1969 - 1989. *Forschungen in Stillfried,* 9/10**,** 9-29.

FELGENHAUER, 1978b

FELGENHAUER, S. 1978b. Ein mittelalterlicher Speicher aus Stillfried. *Forschungen in Stillfried,* 3**,** 58-61.

FELGENHAUER-SCHMIEDT, 1985

FELGENHAUER-SCHMIEDT, S. 1985. Die mittelalterliche Besiedlung der Wallanlage. *In:* WINDL, H. (ed.) *Ausgrabung in Stillfried. Stratigraphie von der Eiszeit bis zur Gegenwart.* Wien. Katalog des Niederösterreichischen Landesmuseums. Neue Folge 158. 55-62

FINK, 1954

FINK, J. 1954. Die fossilen Böden im österreichischen Löß. *Quartär,* 6**,** 85-107.

FORDINÁL, MAGLAY, ELEČKO et al., 2012

FORDINÁL, K., MAGLAY, J., ELEČKO, M., NAGY, A., MORAVCOVÁ, M., VLAČIKY, M., KUČERA, M., POLÁK, M., PLAŠIENKA, D., FILO, I., OLŠAVSKÝ, M., BUČEK, S.,

HAVRILA, M., KOHÚT, M., BEZÁK, V.&NÉMETH, Z. 2012. *Geologická mapa Záhorskej nížiny*. http://apl.geology.sk/gm50js/.

FRANK, 1990

FRANK, C. 1990. Pleistozäne und holozäne Molluskenfaunen aus Stillfried an der March: Ein Beitrag zur Ausgrabungsgeschichte von Stillfried und des Buhuberges nördlich von Stillfried. *Wissenschaftliche Mitteilungen des Niederösterreichischen Landesmuseum,* 7**,** 7-272.

GRIEBL, 2021

GRIEBL, M. 2021. Gesellschaft, Kult und Religion. *In:* LOCHNER, M. (ed.) *Brandbestattung und Bronzemetallurgie.* Archäologie Niederösterreichs 5. Wien. Österreichische Akademie der Wissenschaften. 282-333

GRIEBL, BIEDERER, JACHS et al., 2017

GRIEBL, M., BIEDERER, B., JACHS, T.&PETSCHKO, I. 2017. Aktuelle Forschungen zu den Speichergruben auf der späturnenfelderzeitlichen Wallanlage von Stillfried an der March. *Beiträge zum Tag der Niederösterreichischen Landesarchäologie 2017 : Festschrift für Ernst Lauermann***,** 195-206.

GRIEBL & HELLERSCHMID, 2011

GRIEBL, M.&HELLERSCHMID, I. 2011. Mensch- und Tierdepositionen. Kult in Stillfried? *Tag der Niederösterreichischen Landesarchäologie 2011***,** 39-40.

GRIEBL & HELLERSCHMID, 2013

GRIEBL, M.&HELLERSCHMID, I. 2013. Menschenknochen und Menschenniederlegungen in Siedlungsgruben der befestigten Höhensiedlung von Stillfried an der March, Niederösterreich: Gängige Praxis der Totenbehandlung in der jüngeren Urnenfelderkultur? In: MÜLLER-SCHEESSE, N., ed. ‚Irreguläre' Bestattungen in der Urgeschichte: Norm, Ritual, Strafe ...? Akten der Internationalen Tagung in Frankfurt a. M. vom 3. bis 5. Februar 2012, Kolloquien zur Vor- und Frühgeschichte 19. 327-346.

GRIEBL & HELLERSCHMID, 2015

GRIEBL, M.&HELLERSCHMID, I. 2015. Arbeitsgrube und Kultgrube? Verfärbung V0479 der späturnenfelderzeitlichen Wallanlage von Stillfried, Niederösterreich. *Archaeologia Austriaca,* 99**,** 179-201.

GRIEBL & HELLERSCHMID-ARTNER, 2012

GRIEBL, M.&HELLERSCHMID-ARTNER, I. 2012. Menschenknochen und Menschenniederlegungen in Siedlungsgruben der befestigten Höhensiedlung von Stillfried a.d. March, Niederösterreich. Gängige Praxis der Totenbehandlung in der späten Urnenfelderzeit (1000-750 v.Chr.)? *Forum Archaeologiae — Zeitschrift für klassische Archäologie,* 63**,** 1-2.

GRUPE, 1998

GRUPE, G. 1998. 'Archives of Childhood' - The Research Potential of Trace Element Analysis of Ancient Human Dental Enamel. *In:* ALT, K. W., RÖSING, F. W.&TESCHLER- NICOLA, M. (eds.) *Dental Anthropology - Fundamentals, Limits and Prospects.* Vienna. Springer-Verlag. 337-347

GRUPE, PRICE, SCHRÖTER et al. 1997

GRUPE, G., PRICE, T. D., SCHRÖTER, P., SOLLNER, F., JOHNSON, C. M.&BEARD, B. L. 1997. Mobility of Bell Beaker people revealed by strontium isotope ratios of tooth and bone: a study of southern Bavarian skeletal remains. *Applied Geochemistry,* 12**,** 517-525.

HEILING-SCHMOLL, 1985

HEILING-SCHMOLL, I. 1985. Sonderbestattungen und Tierdepositionen. *In:* WINDL, H. (ed.) *Ausgrabung in Stillfried. Stratigraphie von der Eiszeit bis zur Gegenwart.* Wien. Katalog des Niederösterreichischen Landesmuseums. Neue Folge 158. 43-48

HEISS, ANTOLÍN, BERIHUETE AZORÍN et al., 2019

HEISS, A. G., ANTOLÍN, F., BERIHUETE AZORÍN, M., BIEDERER, B., ERLACH, R., GAIL, N., GRIEBL, M., LINKE, R., LOCHNER, M., MARINOVA, E., OBERNDORFER, D., STIKA, H.-P.&VALAMOTI, S. M. 2019. The Hoard of the Rings. “Odd” annular bread-like objects as a case study for cereal-product diversity at the Late Bronze Age hillfort site of Stillfried (Lower Austria). *PLOS ONE,* 14**,** e0216907.

HELLERSCHMID, 2004

HELLERSCHMID, I. 2004. *Die urnenfelder-/hallstattzeitliche Wallanlage von Stillfried an der March. Ergebnisse der Ausgrabungen 1969-1989 unter besonderer Berücksichtigung des Kulturwandels an der Epochengrenze Urnenfelder-/Hallstattkultur.* Dissertation. GEKU Fakultät, Universität Wien.

HELLERSCHMID, 2006

HELLERSCHMID, I. 2006. *Die urnenfelder-/hallstattzeitliche Wallanlage von Stillfried an der March, 63,* Wien, Mitteilungen der Prähistorischen Kommission Wien.

HELLERSCHMID, 2015

HELLERSCHMID, I. 2015. Mord oder Opferung? Die Niederlegung der „Sieben" in Grube V1141 am Kirchhügel von Stillfried. *Archaeologia Austriaca,* 8**,** 203-232.

HELLERSCHMID, 2021

HELLERSCHMID, I. 2021. Höhensiedlung Stillfried an der March. *In:* LOCHNER, M. (ed.) *Brandbestattung und Bronzemetallurgie.* Archäologie Niederösterreichs 5. Wien. Österreichische Akademie der Wissenschaften. 71-76

HELLERSCHMID, KERN & LOCHNER, 2010

HELLERSCHMID, I., KERN, D.&LOCHNER, M. 2010. Oberleiserberg - Stillfried - Thunau. Drei Höhensiedlungen der mitteldonauländischen Urnenfelderkultur im Vergleich. *In:* GEDIGA, B. (ed.) *Rola głównych centrów kulturowych w kształtowaniu oblicza kulturowego Europy środkowej we wczesnych okresach epoki żelaza.* Biskupin. 283-298

HILLSON, 1996

HILLSON, S. 1996. *Dental Anthropology,* Cambridge, UK, Cambridge University Press.

HORSKY, IRRGEHER & PROHASKA, 2016

HORSKY, M., IRRGEHER, J.&PROHASKA, T. 2016. Evaluation strategies and uncertainty calculation of isotope amount ratios measured by MC ICP-MS on the example of Sr. *Anal Bioanal Chem,* 408**,** 351-367.

IRRGEHER, PROHASKA, STURGEON et al., 2013

IRRGEHER, J., PROHASKA, T., STURGEON, R. E., MESTER, Z.&YANG, L. 2013. Determination of strontium isotope amount ratios in biological tissues using MC-ICPMS. *Analytical Methods,* 5**,** 1687.

IRRGEHER, TESCHLER-NICOLA, LEUTGEB et al., 2012

IRRGEHER, J., TESCHLER-NICOLA, M., LEUTGEB, K., WEIS, C., KERN, D.&PROHASKA, T. 2012. Migration and mobility in the latest Neolithic of the Traisen Valley, Lower

Austria: Sr isotope analysis. *In:* KAISER, E., BURGER, J.&SCHIER, W. (eds.) *Population Dynamics in Prehistory and Early History. New Approaches Using Stable Isotopes and Genetics.* Berlin/Boston. De Gruyter. 199-212

IRRGEHER; VOGL; SANTNER et al., 2015

IRRGEHER, J., VOGL, J., SANTNER, J.&PROHASKA, T. 2015. CHAPTER 8 measurement strategies. *In:* PROHASKA, T., IRRGEHER, J., A., Z.&N., J. (eds.) *Sector field mass spectrometry for elemental and isotopic analysis. .* Cambridge. The Royal Society of Chemistry. 126-151

IRRGEHER, WEIS, KRENN-LEEB et al., 2011

IRRGEHER, J., WEIS, C., KRENN-LEEB, A., TESCHLER-NICOLA, M.&PROHASKA, T. 2011. Lokal oder fremd? *Archäologie Österreichs***,** 33-37.

JAKUBOWSKI, HORSKY, ROOS et al., 2015

JAKUBOWSKI, N., HORSKY, M., ROOS, P. H., VANHAECKE, F.&PROHASKA, T. 2015. Inductively Coupled Plasma Mass Spectrometry. *Sector Field Mass Spectrometry for Elemental and Isotopic Analysis.* New Developments in Mass Spectrometry. [Cambridge]. Royal Society of Chemistry. 208-318

JANOUSEK, FINGER, ROBERTS et al., 2004

JANOUSEK, V., FINGER, F., ROBERTS, M.&FRYDA, J. 2004. Deciphering the petrogenesis of deeply buried granites: whole-rock geochemical constraints on the origin of largely undepleted felsic granulites from the Moldanubian Zone of the Bohemian Massif. *Earth and Environmental Science Transactions of the Royal Society of Edinburgh* 95**,** 141–159.

JANOUSEK, ROGERS & BOWES, 1995

JANOUSEK, V., ROGERS, G.&BOWES, D. R. 1995. Sr-Nd isotopic constraints on the petrogenesis of the Central Bohemian Pluton, Czech Republic. *Geologische Rundschau,* 84**,** 520–534.

KAMENOV, LOFARO, GOAD et al., 2018

KAMENOV, G. D., LOFARO, E. M., GOAD, G.&KRIGBAUM, J. 2018. Trace Elements in Modern and Archaeological Human Teeth: Implications for Human Metal Exposure and Enamel Diagenetic Changes. *Journal of Archaeological Science,* 99**,** 27-34.

KAUS, 1984

KAUS, M. 1984. Das Gräberfeld der jüngeren Urnenfelderzeit von Stillfried an der March. Ergebnisse der Ausgrabungen 1975 - 1977. *Forschungen in Stillfried,* 6**,** 1-208.

KAUS, 1988

KAUS, M. 1988. Das Stillfrieder Gräberfeld. *In:* FELGENHAUER, F., J., S., KRITSCHER, H.&HAUSER, G. (eds.) *Stillfried: Archäologie - Anthropologie.* Wien. Veröffentlichungen des Museums für Ur- und Frühgeschichte in Stillfried. Sonderband 3. 113-119

KIRÁLY, SEBŐK, ZOFFMANN et al., 2013

KIRÁLY, A., SEBŐK, K., ZOFFMANN, Z.&KOVÁCS, G. 2013. Early Iron Age 'Mass Graves' in the Middle Tisza Region: Investigation and Interpretation. In: MÜLLER-SCHEESSE, N., ed. ‚Irreguläre' Bestattungen in der Urgeschichte: Norm, Ritual, Strafe ...? Akten der Internationalen Tagung in Frankfurt a. M. vom 3. bis 5. Februar 2012, Kolloquien zur Vor- und Frühgeschichte 19, Frankfurt a. M., 307-326.

KNIPPER, FRAGATA, NICKLISCH et al., 2016

KNIPPER, C., FRAGATA, M., NICKLISCH, N., SIEBERT, A., SZÉCSÉNYI-NAGY, A., HUBENSACK, V., METZNER-NEBELSICK, C., MELLER, H.&ALT, K. W. 2016. A distinct section of the Early Bronze Age society? Stable isotope investigations of burials in settlement pits and multiple inhumations of the Únětice culture in central Germany. *American journal of physical anthropology,* 159**,** 496-516.

KOENIG, ROGERS & TRUEMAN, 2009

KOENIG, E., ROGERS, R. R.&TRUEMAN, C. N. 2009. Visualizing Fossilization Using Laser Ablation– Inductively Coupled Plasma–Mass Spectrometry Maps of Trace Elements in Late Cretaceous Bones. *Geology,* 37**,** 511-515.

KOHLER-SCHNEIDER, 2001

KOHLER-SCHNEIDER, M. 2001. *Verkohlte Kultur- und Wildpflanzenreste aus Stillfried an der March als Spiegel spätbronzezeitlicher Landwirtschaft im Weinviertel, Niederösterreich, Mitteilungen der Prähistorischen Kommission Wien, 37*.

KOHN & MOSES, 2013

KOHN, M. J.&MOSES, R. J. 2013. Trace Element Diffusivities in Bone Rule Out Simple Diffusive Uptake During Fossilization but Explain In Vivo Uptake and Release. *PNAS,* 110**,** 419-424.

KOHN, SCHOENINGER & BARKER, 1999

KOHN, M. J., SCHOENINGER, M. J.&BARKER, W. W. 1999. Altered States: Effects of Diagenesis on Fossil Tooth Chemistry. *Geochimica et Cosmochimica Acta,* 63**,** 2737-2747.

KREUTZ, 2011

KREUTZ, D. 2011. *Elemental and isotopic analysis by (multiple collector) – inductively coupled plasma mass spectrometry in human teeth from the Early Bronze Age excavation site Franzhausen I (Lower Austria) for the investigation of population dynamics and dietary patterns.* Diplomarbeit. Fakultät für Chemie. Universität Wien.

LANGENECKER, 1988

LANGENECKER, U. 1988. Hallstatt- und latenezeitliche Webgruben in Stillfried. *In:* FELGENHAUER, F., J., S., KRITSCHER, H.&HAUSER, G. (eds.) *Stillfried: Archäologie - Anthropologie.* Wien. Veröffentlichungen des Museums für Ur- und Frühgeschichte in Stillfried. Sonderband 3. 121-128

LATKOCZY, PROHASKA; STINGEDER et al., 1998

LATKOCZY, C., PROHASKA, T., STINGEDER, G.&TESCHLER- NICOLA, M. 1998. Strontium isotope ratio measure- ments in prehistoric human bone samples by means of high-resolution inductively coupled plasma mass spec- trometry (HR-ICP-MS). *Journal of Analytical Atomic Spectrometry,* 13**,** 561-566.

LEE-THORP & SPONHEIMER, 2003

LEE-THORP, J.&SPONHEIMER, M. 2003. Three case studies used to reassess the reliability of fossil bone and enamel isotope signals for paleodietary studies. *Journal of Anthropological Archaeology,* 22**,** 208-216.

LENGFELDER, GRUPE, STALLAUER et al., 2019

LENGFELDER, F., GRUPE, G., STALLAUER, A., HUTH, R.&SÖLLNER, F. 2019. Modelling strontium isotopes in past biospheres - Assessment of bioavailable (87)Sr/(86)Sr

ratios in local archaeological vertebrates based on environmental signatures. *The Science of the total environment,* 648**,** 236–252.

MADGWICK, MULVILLE & EVANS, 2012

MADGWICK, R., MULVILLE, J.&EVANS, J. 2012. Investigating diagenesis and the suitability of porcine enamel for strontium (87Sr/86Sr) isotope analysis. *Journal of Analytical Atomic Spectrometry,* 27**,** 733-742.

MAURER, GALER, KNIPPER et al., 2012

MAURER, A. F., GALER, S. J., KNIPPER, C., BEIERLEIN, L., NUNN, E. V., PETERS, D., TUTKEN, T., ALT, K. W.&SCHONE, B. R. 2012. Bioavailable 87Sr/86Sr in different environmental samples--effects of anthropogenic contamination and implications for isoscapes in past migration studies. *Sci Total Environ,* 433**,** 216-29.

MINNITI, VALENZUELA-LAMAS, EVANS et al., 2014

MINNITI, C., VALENZUELA-LAMAS, S., EVANS, J.&ALBARELLA, U. 2014. Widening the market. Strontium isotope analysis on cattle teeth from Owslebury (Hampshire, UK) highlights changes in livestock supply between the Iron Age and the Roman period. *Journal of Archaeological Science,* 42**,** 305-314.

MONTGOMERY, 2010

MONTGOMERY, J. 2010. Passports from the past: Investigating human dispersals using strontium isotope analysis of tooth enamel. *Ann Hum Biol,* 37**,** 325-46.

MONTGOMERY, EVANS & COOPER, 2007

MONTGOMERY, J., EVANS, J. A.&COOPER, R. E. 2007. Resolving archaeological populations with Sr-isotope mixing models. *Applied Geochemistry,* 22**,** 1502-1514.

MONTGOMERY, EVANS & WILDMAN 2006

MONTGOMERY, J., EVANS, J. A.&WILDMAN, G. 2006. 87Sr/86Sr isotope composition of bottled British mineral waters for environmental and forensic purposes. *Applied Geochemistry,* 21**,** 1626-1634.

MUSEUM-STILLFRIED, 2017a

MUSEUM-STILLFRIED. 2017a. Bronzezeit. *http://www.museumstillfried.at/virtueller-rundgang/bronzezeit/* [Online]. [Accessed 20.08. 2017].

MUSEUM-STILLFRIED, 2017b

MUSEUM-STILLFRIED. 2017b. Stillfried zur Zeit der Römer. *http://www.museumstillfried.at/virtueller-rundgang/roemer/* [Online]. [Accessed 07.03. 2017].

NEUGEBAUER-MARESCH, 1978

NEUGEBAUER-MARESCH, C. 1978. Die ur- und frühgeschichtliche Fundstelle "Alter Mühlgraben" beim Haspelberg, Grub a. d. March, NÖ. Unter besonderer Berücksichtigung des urnenfelderzeitlichen Gräberfeldes. *Forschungen in Stillfried,* 3**,** 21-50.

PARSON, EDUARDOFF, XAVIER et al., 2018

PARSON, W., EDUARDOFF, M., XAVIER, C., BERTOGLIO, B.&TESCHLER-NICOLA, M. 2018. Resolving the matrilineal relationship of seven Late Bronze Age individuals from Stillfried, Austria. *Forensic Science International: Genetics,* 36**,** 148-151.

POPOVTSCHAK, HEISS & DRESCHER-SCHNEIDER, 2021

POPOVTSCHAK, M., HEISS, A. G.&DRESCHER-SCHNEIDER, R. 2021. Zur Umwelt. *In:* LOCHNER, M. (ed.) *Brandbestattung und Bronzemetallurgie. Die Urnenfelderkultur in Niederösterreich.* Archäologie Niederösterreichs 5. Wien. Österreichische Akademie der Wissenschaften. 28-45

PRICE, BURTON & BENTLEY, 2002

PRICE, T. D., BURTON, J. H.&BENTLEY, R. A. 2002. The Characterization of Biologically Available Strontium Isotope Ratios for the Study of the Prehistoric Migration. *Archaeometry,* 44**,** 117-135.

PRICE, GRUPE & SCHRÖTER, 1998

PRICE, T. D., GRUPE, G.&SCHRÖTER, P. 1998. Migration in the Bell Beaker period of central Europe. *Antiquity* 72**,** 405-411.

PRICE, KNIPPER, GRUPE et al., 2013

PRICE, T. D., KNIPPER, C., GRUPE, G.&SMRCKA, V. 2013. Strontium Isotopes and Prehistoric Human Migration: The Bell Beaker Period in Central Europe. *European Journal of Archaeology,* 7**,** 9-40.

PROHASKA, 2015

PROHASKA, T. 2015. General Overview. *In:* PROHASKA, T. (ed.) *Sector Field Mass Spectrometry for Elemental and Isotopic Analysis.* New Developments in Mass Spectrometry. [Cambridge]. Royal Society of Chemistry. 29-43

PROHASKA, LATKOZY, SCHULTHEIS et al., 2002

PROHASKA, T., LATKOCZY, C., SCHULTHEIS, G., TESCHLER-NICOLA, M.&STINGEDER, G. 2002. Investigation of Sr isotope ratios in prehistoric human bones and teeth using laser ablation ICP-MS and ICP-MS after Rb/Sr separation. *Journal of Analytical Atomic Spectrometry,* 17**,** 887-891.

PUCHER, 1982

PUCHER, E. 1982. *Tierknochenfunde aus Stillfried an der March.* Dissertation. NaWi Fakultät, Universität Wien.

PUCHER, 1988

PUCHER, E. 1988. Tierskelette aus den urnenfelderzeitlichen Gruben von Stillfried. *In:* FELGENHAUER, F., J., S., KRITSCHER, H.&HAUSER, G. (eds.) *Stillfried: Archäologie - Anthropologie.* Wien. Veröffentlichungen des Museums für Ur- und Frühgeschichte in Stillfried. Sonderband 3. 159-166

PUCHER, 2018

PUCHER, E. 2018. Krumme Hirsche und zahnlose Wölfe – bronzezeitliche Wildtierhaltung in Stillfried. *Beiträge zur Archäozoologie und Prähistorischen Anthropologie,* 11**,** 71-92.

RETZMANN, KRIECHBAUM, GRIEBL et al., 2020

RETZMANN, A., KRIECHBAUM, A.-M., GRIEBL, M., WILTSCHKE-SCHOTTA, K., TESCHLER-NICOLA, M., IRRGEHER, J.&PROHASKA, T. 2020. Sr Isotope Analysis of Human Remains from Settlement Pits at Stillfried/March – Reassessing Diagenetic Changes. *Archaeologia Austriaca,* 104**,** 53-87.

RETZMANN, ZIMMERMANN, PROFROCK et al. 2017

RETZMANN, A., ZIMMERMANN, T., PROFROCK, D., PROHASKA, T.&IRRGEHER, J. 2017. A fully automated simultaneous single-stage separation of Sr, Pb, and Nd using DGA Resin for the isotopic analysis of marine sediments. *Anal Bioanal Chem,* 409**,** 5463-5480.

RIEGLER & PETICZKA, 2004

RIEGLER, D.&PETICZKA, R. 2004. Typuslokalität Stillfried an der March – Ausgangssituation. *In:* PETICZKA, R. (ed.) *Beiträge zur Quartärforschung und Landschaftsökologie: Gedenkschrift zum 60. Geburtstag von Spyridon Verginis.* Institut für Geographie und Regionalforschung Universität Wien. 41-46

RÖGL & SUMMESBERGER, 1978

RÖGL, F.&SUMMESBERGER, H. 1978. Die geologische Lage von Stillfried an der March. *Forschungen in Stillfried,* 3**,** 76-86.

RÖGL & SUMMESBERGER, 1988

RÖGL, F.&SUMMESBERGER, H. 1988. Der geologische Rahmen von Stillfried an der March. *In:* FELGENHAUER, F., J., S., KRITSCHER, H.&HAUSER, G. (eds.) *Stillfried: Archäologie - Anthropologie.* Veröffentlichungen des Museums für Ur- und Frühgeschichte in Stillfried. Sonderband 3. 148-158

SAUTER, 1988

SAUTER, F. 1988. Chemie im Dienst der Archäologie. Ergebnisse chemischer Untersuchungen. *In:* FELGENHAUER, F., J., S., KRITSCHER, H.&HAUSER, G. (eds.) *Stillfried: Archäologie - Anthropologie.* Wien. Veröffentlichungen des Museums für Ur- und Frühgeschichte in Stillfried. Sonderband 3. 167-182

SAUTER, WURST & HOKE, 1976

SAUTER, F., WURST, F.&HOKE, E. 1976. Inhaltsuntersuchung einer späturnenfelderzeitlichen Deckeldose aus Stillfried. *Forschungen in Stillfried,* 2**,** 35-39.

SCHMID, 1972

SCHMID, E. 1972. *Atlas of Animal Bones. For Prehistorians, Archaeologists and Quaternary Geologists.,* Amsterdam - London - New York, Elsevier Publishing Company.

SÖLLNER, TONCALA, HÖLZL et al. 2016

SÖLLNER, F., TONCALA, A., HÖLZL, S.&GRUPE, G. 2016. Determination of geo-dependent bioavailable 87Sr/86Sr isotopic ratios for archaeological sites from the Inn Valley (Austria): A model calculation. *In:* GRUPE G.&G., M. (eds.) *Isotopic Landscapes in Bioarchaeology.* Berlin, Heidelberg. 123–140

SPRAFKE, 2016

SPRAFKE, T. 2016. *Löss in Niederösterreich - Archiv quartärer Klima- und Landschaftsveränderungen.* Würzburg University Press.

STROHSCHNEIDER, 1974

STROHSCHNEIDER, M. 1974. Die Bronzetasse aus Stillfried. *Forschungen in Stillfried,* 1**,** 61-68.

SWOBODA, BRUNNER, BOULYGA et al., 2008

SWOBODA, S., BRUNNER, M., BOULYGA, S. F., GALLER, P., HORACEK, M.&PROHASKA, T. 2008. Identification of Marchfeld asparagus using Sr isotope ratio measurements by MC-ICP-MS. *Anal Bioanal Chem,* 390**,** 487-94.

SZILVASSY, KRITSCHER & HAUSER, 1988

SZILVASSY, J., KRITSCHER, H.&HAUSER, G. 1988. Eine urnenfelderzeitliche Mehrfachbestattung in Stillfried an der March, NÖ. *In:* FELGENHAUER, F., J., S., KRITSCHER, H.&HAUSER, G. (eds.) *Stillfried: Archäologie - Anthropologie.* Wien. Veröffentlichungen des Museums für Ur- und Frühgeschichte in Stillfried. Sonderband 3. 9-76

TESCHLER-NICOLA, IRRGEHER & PROHASKA, 2016

TESCHLER-NICOLA, M., IRRGEHER, J.&PROHASKA, T. 2016. Wohnsitz und Geneaologie der sieben Menschen aus der späturnenfelderzeitlichen Vorratsgrube V1141 von Stillfried an der March - eine archäometrische Ergänzung anlässlich eines "Schauplatzwechsels". *Mitteilungen der Anthropologischen Gesellschaft,* 146**,** 159-168.

THEINER, 2011

THEINER, S. 2011. *The use of strontium isotope ratio measurements by MC-ICP-MS for fundamental studies on diagenesis and for the reconstruction of animal migration at the Celtic excavation site Roseldorf.* Diplomarbeit. Fakultät für Chemie, Universität Wien.

THOMAS, 2001a

THOMAS, R. 2001a. A Beginner's Guide to ICP-MS. Part II: The sample Introduction System. *Spectroscopy,* 16**,** 56-60.

THOMAS, 2001b

THOMAS, R. 2001b. A Beginner's Guide to ICP-MS. Part III: The Plasma Source. *Spectroscopy,* 16**,** 26-30.

TRNKA, 1978

TRNKA, G. 1978. Früh- und mittelbronzezeitliche Funde aus dem Museum Stillfried. *Forschungen in Stillfried,* 3**,** 15-20.

TRUEMAN, PALMER, FIELD et al., 2008

TRUEMAN, C. N., PALMER, M. R., FIELD, J., PRIVAT, K., LUDGATE, N., CHAVAGNAC, V., EBERTH, D. A., CIFELLI, R.&ROGERS, R. R. 2008. Comparing Rates of Recrystallisation and the Potential for Preservation of Biomolecules from the Distribution of Trace Elements in Fossil Bones. *Comptes Rendus Palevol,* 7**,** 145-158.

TÜRP, ALT, 1998

TÜRP, J. C.&ALT, K. W. 1998. Anatomy and Morphology of Human Teeth. *In:* ALT, K. W., RÖSING, F. W.&TESCHLER- NICOLA, M. (eds.) *Dental Anthropology - Fundaments, Limits and Prospects.* Vienna. Springer-Verlag. 71-94

TÜTKEN, 2010

TÜTKEN, T. 2010. Die Isotopenanalyse fossiler Skelettreste – Bestimmung der Herkunft und Mobilität von Menschen und Tieren. In: MELLER, H.&ALT, K. W., eds. Anthropologie, Isotopie und DNA - biografische Annäherung an namenlose vorgeschichtliche Skelette?, 2. Mitteldeutscher Archäologentag vom 08. bis 10. Oktober 2009 in Halle (Saale), Tagungen des Landesmuseums für Vorgeschichte Halle, Halle (Saale). 33-51.

URBAN, 1985

URBAN, O. 1985. Kelten, Römer und Germanen. *In:* WINDL, H. (ed.) *Ausgrabung in Stillfried. Stratigraphie von der Eiszeit bis zur Gegenwart.* Wien. Katalog des Niederösterreichischen Landesmuseums. Neue Folge 158. 49-54

VINER, EVANS, ALBARELLA et al., 2010

VINER, S., EVANS, J., ALBARELLA, U.&PARKER PEARSON, M. 2010. Cattle mobility in prehistoric Britain: strontium isotope analysis of cattle teeth from Durrington Walls (Wiltshire, Britain). *Journal of Archaeological Science,* 37**,** 2812-2820.

WAHL & PRICE, 2013

WAHL, J.&PRICE, T. D. 2013. Local and foreign males in a late Bronze Age cemetery at Neckarsulm, south-western Germany: strontium isotope investigations. *Anthropol Anz,* 70**,** 289-307.

WEISER, 1978

WEISER, W. 1978. Die paläolithischen Funde aus Stillfried 1879 - 1977 *Forschungen in Stillfried,* 3**,** 5-14.

WILLMES, KINSLEY, MONCEL et al. 2016

WILLMES, M., KINSLEY, L., MONCEL, M. H., ARMSTRONG, R. A., AUBERT, M., EGGINS, S.&GRÜN, R. 2016. Improvement of Laser Ablation In Situ Micro analysis to Identify Diagenetic Alteration and Measure Strontium Isotope Ratios in Fossil Human Teeth. *Journal of Archaeological Science,* 70**,** 102-116.

WILSON & POLLARD, 2002

WILSON, L.&POLLARD, M. 2002. Here Today, Gone Tomorrow? Integrated Experimentation and Geochemical Modeling in Studies of Archaeological Diagenetic Change. *Accounts of Chemical Research,* 35**,** 644-651.

WILTSCHKE-SCHROTTA & RENHART, 2021

WILTSCHKE-SCHOTTA, K.&RENHART, S. 2021. Der Mensch - eine anthropologische Spurensuche. *In:* LOCHNER, M. (ed.) *Brandbestattung und Bronzemetallurgie. Die Urnenfelderkultur in Niederösterreich (1300-800 v. Chr.).* Archäologie Niederösterreichs 5. Wien. Österreichischen Akademie der Wissenschaften. 260-281

WILTSCHKE-SCHROTTA, 2006

WILTSCHKE-SCHROTTA, K. 2006. Stillfried - Grube V841 (1985/86), eine anthropologisch, detektivische Herausforderung. *In:* HELLERSCHMID, I. (ed.) *Die urnenfelder-/hallstattzeitliche Wallanlage von Stillfried an der March.* Mitteilungen der Prähistorischen Kommission. Wien. Mitteilungen der Prähistorischen Kommission Wien. 63. 414-415

YANG, PETER, PANNE et al., 2008

YANG, L., PETER, C., PANNE, U.&STURGEON, R. E. 2008. Use of Zr for mass bias correction in strontium isotope ratio determinations using MC-ICP- MS. *J Anal At Spectrom,* 23**,** 1269–74.

9 Appendix

9.1 Human Teeth

Table 10 Amount of sampled enamel and dentine in mg in human teeth

Sample ID	Amount enamel (mg)	Amount dentine (mg)
ST_T_1377	18.2	9.3
ST_T_9052	16.1	10.4
ST_T_9054	9.8	12.1
ST_T_9042	16.1	10.3
ST_T_9043	6.9	11.6
ST_T_9049	10.6	10.3
ST_T_9046	10.4	10.0
ST_T_9023	14.8	9.6
ST_T_9051	9.3	9.9
ST_T_9044	11.0	9.9
ST_T_9026	9.4	10.6

Table 11 MEA results of human enamel (part 1)

Enamel	**^{7}Li**	**^{9}Be**	**^{10}B**	**^{11}B**	**^{23}Na**	**^{24}Mg**	**^{25}Mg**	**^{26}Mg**	**^{27}Al**	**^{39}K**	**^{43}Ca**	**^{44}Ca**
Unit [µg g^{-1}]												
Urel (k=2)	15%	15%	15%	15%	15%	15%	15%	15%	15%	15%	15%	15%
LOD	0.02	0.02	0.81	0.82	36.03	49.64	50.12	50.82	2,26	65.22	410.47	404.43
9042	3	LOD	12	12	7524	2691	2684	2670	72	552	481909	484277
9043	2	LOD	15	16	7442	3215	3233	3195	30	641	484847	496295
9044	3	LOD	11	11	5984	2519	2536	2492	6	459	450276	454368
9046	2	LOD	12	12	6229	3414	3417	3369	LOD	496	510086	510658
9049	2	LOD	13	14	7710	2965	2972	2939	11	600	509275	509279
9051	3	LOD	14	15	6678	2905	2877	2828	28	636	467219	473416
9052	2	LOD	12	12	6354	2895	2905	2879	19	570	481828	493871
9054	2	LOD	11	12	7572	3531	3539	3480	LOD	573	521230	507215
9023	5	LOD	11	11	8389	3975	3990	3931	27	773	529532	539881
9026	2	LOD	9	8	7203	2909	2868	2856	LOD	566	497895	506952
1377	6	LOD	17	17	8244	3373	3393	3319	24	790	520502	523898

Table 12 MEA results of human enamel (part 2)

Enamel	^{51}V	^{52}Cr	^{55}Mn	^{56}Fe	^{57}Fe	^{58}Ni	^{59}Co	^{60}Ni	^{63}Cu	^{65}Cu	^{66}Zn	^{68}Zn
Unit [µg g^{-1}]												
Urel (k=2)	15%	15%	15%	15%	15%	15%	15%	15%	15%	15%	15%	15%
LOD	0.06	0.35	2.23	56.07	19.80	36.59	0.04	36.57	99.79	100.54	71.69	71.43
9042	0.14	0.6	2	328	1228	LOD	0.47	LOD	LOD	LOD	253	254
9043	0.89	1.3	31	611	1335	163	0.71	171	LOD	LOD	367	366
9044	0.10	0.9	6	404	1166	214	0.45	223	LOD	LOD	452	443
9046	0.22	1.5	LOD	616	1333	80	0.49	88	LOD	LOD	1075	1064
9049	0.11	2.3	LOD	835	1342	109	0.53	121	LOD	LOD	339	340
9051	0.32	1.6	19	756	1307	LOD	0.48	LOD	LOD	LOD	176	169
9052	0.15	0.6	11	405	1286	250	0.50	256	LOD	LOD	506	493
9054	0.21	1.0	11	607	1339	163	0.53	178	LOD	LOD	284	281
9023	0.21	2.1	6	655	1448	33	0.59	42	LOD	LOD	307	306
9026	1.10	1.5	13	810	1414	LOD	0.51	LOD	LOD	LOD	164	166
1377	0.08	1.0	2	470	1400	77	0.55	85	LOD	LOD	284	283

Table 13 MEA results of human enamel (part 3)

Enamel	^{69}Ga	^{75}As	^{77}Se	^{82}Se	^{85}Rb	^{88}Sr	^{98}Mo	^{107}Ag	^{109}Ag	^{111}Cd	^{114}Cd	^{128}Te	^{137}Ba	^{138}Ba
Unit [µg g^{-1}]														
Urel (k=2)	15%	15%	15%	15%	15%	15%	15%	15%	15%	15%	15%	15%	15%	15%
LOD	0.07	0.13	1.13	1.20	0.04	0.37	0.36	0.01	0.01	0.03	0.02	0.03	1.68	1.65
9042	0.17	0	LOD	LOD	0.12	199	1.49	0	0	LOD	LOD	LOD	5.1	5.0
9043	0.38	LOD	LOD	LOD	0.17	99	0.83	LOD	0	LOD	0	LOD	9.8	9.8
9044	0.15	LOD	LOD	LOD	0.14	78	0.65	LOD	LOD	LOD	LOD	LOD	4.0	4.0
9046	LOD	LOD	LOD	LOD	0.08	132	0.73	LOD	LOD	LOD	0	LOD	LOD	LOD
9049	0.11	LOD	LOD	LOD	0.14	136	LOD	0	0	LOD	LOD	LOD	3.6	3.5
9051	0.37	0	LOD	LOD	0.14	71	LOD	0	0	LOD	LOD	LOD	10.8	10.7
9052	0.14	LOD	LOD	LOD	0.14	127	0.41	LOD	LOD	LOD	LOD	LOD	4.2	4.2
9054	0.19	LOD	LOD	LOD	0.14	120	LOD	LOD	LOD	LOD	LOD	LOD	5.2	5.3
9023	0.30	0	LOD	LOD	0.18	185	0.41	LOD	0	LOD	0	LOD	8.3	8.2
9026	0.44	0	LOD	3	0.08	143	LOD	LOD	LOD	LOD	LOD	LOD	11.1	11.2
1377	0.08	LOD	LOD	LOD	0.14	113	LOD	LOD	LOD	LOD	LOD	0	2.4	2.4

Table 14 MEA results of human enamel (part 4)

Enamel	**^{205}Tl**	**^{206}Pb**	**^{207}Pb**	**^{208}Pb**	**^{209}Bi**	**^{238}U**
Unit [µg g^{-1}]						
Urel (k=2)	15%	15%	15%	15%	15%	15%
LOD	0.00	1.81	1.62	1.69	0.01	0.001
9042	0	LOD	LOD	LOD	0	0.051
9043	LOD	LOD	LOD	LOD	LOD	0.024
9044	LOD	LOD	LOD	LOD	LOD	0.008
9046	LOD	LOD	LOD	LOD	LOD	LOD
9049	LOD	LOD	LOD	LOD	LOD	0.008
9051	LOD	LOD	LOD	LOD	LOD	0.040
9052	LOD	LOD	LOD	LOD	LOD	0.010
9054	LOD	LOD	LOD	LOD	LOD	0.017
9023	LOD	LOD	LOD	LOD	0	0.021
9026	LOD	LOD	LOD	LOD	LOD	0.014
1377	LOD	LOD	LOD	LOD	LOD	0.006

Table 15 MEA results of human dentine (part 1)

Dentine	**^{7}Li**	**^{9}Be**	**^{10}B**	**^{11}B**	**^{23}Na**	**^{24}Mg**	**^{25}Mg**	**^{26}Mg**	**^{27}Al**	**^{39}K**	**^{43}Ca**	**^{44}Ca**
Unit [µg g^{-1}]												
Urel (k=2)	15%	15%	15%	15%	15%	15%	15%	15%	15%	15%	15%	15%
LOD	0.02	0.03	2.67	3.18	79.55	13.35	14.51	12.79	14.53	757.96	582.98	553.03
9042	9	LOD	24	24	2653	3082	3129	3069	LOD	LOD	319183	317528
9043	13	LOD	41	44	3551	6033	6093	6035	58	LOD	429463	429098
9044	8	LOD	38	39	4305	5632	5693	5616	LOD	LOD	373969	374607
9046	5	LOD	52	54	3705	4872	4947	4818	LOD	LOD	335232	341676
9049	7	LOD	34	35	2868	4743	4744	4726	LOD	LOD	304521	304923
9051	8	LOD	61	62	3633	9598	9673	9904	LOD	LOD	370443	379155
9052	9	LOD	61	64	4374	8166	8223	8039	27	LOD	430931	437919
9054	8	LOD	44	45	3840	9775	9841	9905	LOD	LOD	434570	432403
9023	6	LOD	27	27	4258	8234	8229	8363	LOD	2098	325559	330302
9026	11	LOD	29	29	2594	7511	7609	7578	LOD	LOD	471841	471918
1377	7	LOD	58	60	2760	6543	6528	6456	LOD	LOD	268733	272014

Table 16 MEA results of human dentine (part 2)

Dentine	**^{51}V**	**^{52}Cr**	**^{55}Mn**	**^{56}Fe**	**^{57}Fe**	**^{58}Ni**	**^{59}Co**	**^{60}Ni**	**^{63}Cu**	**^{65}Cu**	**^{66}Zn**	**^{68}Zn**
Unit [µg g^{-1}]												
Urel (k=2)	15%	15%	15%	15%	15%	15%	15%	15%	15%	15%	15%	15%
LOD	0.03	1.01	0.68	496.97	27.56	79.41	0.04	80.41	2.22	2.28	146.25	147.99
9042	3	LOD	11	LOD	834	LOD	0	LOD	3	3	LOD	LOD
9043	29	5	69	LOD	1153	LOD	1	LOD	13	14	403	395
9044	1	LOD	LOD	LOD	932	LOD	0	LOD	LOD	LOD	LOD	LOD
9046	2	LOD	LOD	LOD	830	LOD	0	LOD	LOD	LOD	LOD	LOD
9049	1	LOD	LOD	LOD	740	LOD	0	LOD	16	16	LOD	LOD
9051	2	5	5	LOD	897	137	0	138	14	14	LOD	LOD
9052	1	LOD	2	LOD	1073	LOD	0	LOD	LOD	LOD	257	260
9054	1	LOD	1	LOD	1005	LOD	0	LOD	3	3	217	215
9023	2	LOD	LOD	LOD	723	LOD	0	LOD	4	4	LOD	LOD
9026	12	2	8	LOD	1101	LOD	0	LOD	15	16	162	165
1377	1	LOD	LOD	LOD	633	LOD	0	LOD	LOD	LOD	LOD	LOD

Table 17 MEA results of human dentine (part 3)

Dentine	**^{69}Ga**	**^{75}As**	**^{77}Se**	**^{82}Se**	**^{85}Rb**	**^{88}Sr**	**^{98}Mo**	**^{107}Ag**	**^{109}Ag**	**^{111}Cd**	**^{114}Cd**	**^{128}Te**	**^{137}Ba**	**^{138}Ba**
Unit [µg g^{-1}]														
Urel (k=2)	15%	15%	15%	15%	15%	15%	15%	15%	15%	15%	15%	15%	15%	15%
LOD	0.03	0.31	2.18	1.01	0.07	0.57	0.67	0.01	0.02	0.03	0.02	0.22	0.69	0.75
9042	1	2	LOD	3	LOD	379	44	0	0	0	0	LOD	39	39
9043	2	3	4	6	LOD	491	58	0	0	1	1	LOD	70	70
9044	1	1	LOD	2	LOD	370	3	LOD	LOD	LOD	0	LOD	15	15
9046	2	3	LOD	1	LOD	559	9	LOD	LOD	LOD	LOD	LOD	55	55
9049	1	2	LOD	LOD	LOD	316	5	LOD	LOD	LOD	LOD	LOD	33	32
9051	1	2	LOD	2	0	481	1	0	LOD	LOD	LOD	LOD	42	42
9052	1	1	LOD	LOD	0	470	6	LOD	LOD	LOD	LOD	LOD	23	23
9054	1	1	LOD	LOD	LOD	411	3	LOD	LOD	LOD	LOD	LOD	23	23
9023	1	2	LOD	2	LOD	260	LOD	LOD	LOD	LOD	LOD	LOD	23	23
9026	3	9	2	2	LOD	621	4	0	0	0	0	LOD	80	78
1377	1	1	LOD	LOD	0	283	1	LOD	LOD	LOD	LOD	LOD	17	17

Table 18 MEA results of human dentine (part 4)

Dentine	**^{205}Tl**	**^{206}Pb**	**^{207}Pb**	**^{208}Pb**	**^{209}Bi**	**^{238}U**
Unit [µg g^{-1}]						
Urel (k=2)	15%	15%	15%	15%	15%	15%
LOD	0.01	0.80	0.77	0.80	0.01	0.001
9042	LOD	LOD	LOD	LOD	0	0.039
9043	LOD	LOD	LOD	LOD	LOD	0.012
9044	LOD	LOD	LOD	LOD	LOD	0.022
9046	LOD	LOD	LOD	LOD	LOD	0.062
9049	LOD	1	1	1	LOD	0.004
9051	LOD	1	1	1	LOD	0.280
9052	LOD	LOD	LOD	LOD	LOD	0.045
9054	LOD	LOD	LOD	LOD	LOD	0.005
9023	LOD	4	4	4	LOD	0.015
9026	LOD	LOD	LOD	LOD	LOD	0.274
1377	LOD	LOD	LOD	LOD	LOD	0.112

Table 19 n(*^{87}Sr*)/n(*^{86}Sr*) *ratios of the human teeth, D=dentine, E= enamel*

Sample ID	$n(^{87}Sr)/n(^{86}Sr)$ isotope-amount ratio	*U(k=2)*	U_{rel} *(k=2)*	Sr mass fraction [µg g^{-1}]	*U (k=2)*	U_{rel} *(k=2)*
E_ST_T_ 9042	0.70853	0.00019	0.027 %	199	13	15 %
D_ST_T_9042	0.71032	0.00019	0.027 %	379	25	15 %
E_ST_T_9043	0.71055	0.00019	0.027 %	99	7	15 %
D_ST_T_ 9043	0.71050	0.00019	0.027 %	491	33	15 %
E_ST_T_ 9044	0.71264	0.00019	0.027 %	78	5	15 %
D_ST_T_ 9044	0.71081	0.00019	0.027 %	370	25	15 %
E_ST_T_ 9046	0.71064	0.00019	0.027 %	132	9	15 %
D_ST_T_ 9046	0.71046	0.00019	0.027 %	559	37	15 %
E_ST_T_ 9049	0.71183	0.00019	0.027 %	136	9	15 %
D_ST_T_ 9049	0.71055	0.00019	0.027 %	316	21	15 %
E_ST_T_ 9051	0.70960	0.00019	0.027 %	71	5	15 %
D_ST_T_ 9051	0.71045	0.00019	0.027 %	481	32	15 %
E_ST_T_ 9052	0.71024	0.00019	0.027 %	127	8	15 %
D_ST_T_ 9052	0.71049	0.00019	0.027 %	470	31	15 %
E_ST_T_ 9054	0.70995	0.00019	0.027 %	120	8	15 %
D_ST_T_ 9054	0.71040	0.00019	0.027 %	411	27	15 %
E_ST_T_ 9023	0.71204	0.00019	0.027 %	185	12	15 %
D_ST_T_ 9023	0.71144	0.00019	0.027 %	260	17	15 %
E_ST_T_ 9026	0.71027	0.00019	0.027 %	143	10	15 %
D_ST_T_ 9026	0.71057	0.00019	0.027 %	621	41	15 %
E_ST_T_1377	0.71007	0.00019	0.027 %	113	8	15 %
D_ST_T_1377	0.71067	0.00019	0.027 %	283	19	15 %

9.2 Animal Teeth

Table 20 Amount of sampled enamel and dentine in mg in animal teeth

Sample ID	Amount enamel (mg)	Amount dentine (mg)
ST_21307	9.4	10.3
ST_CF_8855	7.9	7.0
ST_SS_13238	12.0	12.9
ST_CE_7473	10.8	11.5
ST_CA_13286	8.6	9.5
ST_CF_13285	10.9	9.9
ST_SD_13332	13.1	10.3

Table 21 MEA results of animal enamel (part 1)

Animal enamel	^{7}Li	^{9}Be	^{10}B	^{11}B	^{23}Na	^{24}Mg	^{25}Mg	^{26}Mg	^{27}Al
Unit [µg g^{-1}]									
U re (k=2)	15%	15%	15%	15%	15%	15%	15%	15%	15%
LOD	0.05	0.04	8.77	8.03	194.93	215.53	204.79	195.75	-9.53
21307	14.0921833	LOD	LOD	LOD	6954.14469	LOD	LOD	LOD	33.3377186
8855	12.8933996	LOD	LOD	LOD	5633.07844	6610.30531	6742.76605	6555.76762	25.2936703
13238	25.2865789	LOD	LOD	LOD	6671.62497	LOD	LOD	LOD	18.1950425
7473	12.9312005	LOD	LOD	LOD	6746.72973	LOD	LOD	LOD	30.5556348
13286	9.33773184	LOD	LOD	LOD	9605.65307	LOD	LOD	LOD	36.6599338
13285	4.85535834	LOD	LOD	LOD	8045.0743	LOD	3952.85649	3913.48273	34.1323316
13332	24.1053507	LOD	LOD	LOD	7230.92964	LOD	LOD	LOD	13.4972686

Table 22 MEA results of animal enamel (part 2)

Animal enamel	^{39}K	^{42}Ca	^{43}Ca	^{44}Ca	^{51}V	^{52}Cr	^{53}Cr	^{55}Mn	^{56}Fe
Unit [µg g^{-1}]									
U re (k=2)	15%	15%	15%	15%	15%	15%	15%	15%	15%
LOD	71.54	345.78	428.65	473.30	0.11	6.35	0.55	-0.70	64.07
21307	LOD	446465.783	439672.518	436649.1831	LOD	LOD	LOD	5.6350982	LOD
8855	LOD	372077.521	363030.203	361346.8668	LOD	LOD	LOD	39.982049	LOD
13238	LOD	453007.515	418840.762	438494.3065	1.9634507	LOD	LOD	8.0222907	LOD
7473	LOD	477692.698	445873.587	464527.0042	LOD	LOD	LOD	5.91086626	LOD
13286	LOD	677386.995	628004.325	658938.0426	LOD	LOD	LOD	9.80454944	LOD
13285	LOD	493404.169	454277.449	470543.1872	LOD	LOD	LOD	10.4742641	LOD
13332	LOD	525127.735	485490.116	509688.9797	LOD	LOD	LOD	12.6967574	LOD

Table 23 MEA results of animal enamel (part 3)

Animal enamel	**^{57}Fe**	**^{58}Ni**	**^{59}Co**	**^{60}Ni**	**^{63}Cu**	**^{65}Cu**	**^{66}Zn**	**^{68}Zn**	**^{71}Ga**
Unit [µg g^{-1}]									
U re (k=2)	15%	15%	15%	15%	15%	15%	15%	15%	15%
LOD	103.03	17.08	0.02	16.47	-6.50	-6.49	114.02	112.62	0.01
21307	LOD	LOD	0.4925589	LOD	4.08837685	4.29050776	LOD	LOD	1.09354092
8855	LOD	LOD	0.61778969	LOD	7.24355942	7.25003815	LOD	LOD	0.9068327
13238	LOD	LOD	0.50059058	LOD	1.5222501	1.61399578	LOD	LOD	1.06874162
7473	LOD	LOD	0.55517432	LOD	1.90412287	2.20438237	LOD	LOD	1.15019548
13286	1924.59238	LOD	0.79754131	LOD	10.8436323	11.213026	LOD	LOD	1.52326919
13285	LOD	LOD	0.54312774	LOD	2.4131151	2.59373218	LOD	LOD	1.15303596
13332	LOD	LOD	0.61426999	LOD	7.36659494	7.7604081	LOD	LOD	1.19994141

Table 24 MEA results of animal enamel (part 4)

Animal enamel	**^{75}As**	**^{77}Se**	**^{82}Se**	**^{85}Rb**	**^{88}Sr**	**^{98}Mo**	**^{107}Ag**	**^{109}Ag**	**^{111}Cd**	**^{114}Cd**	**^{115}In** (IS)
Unit [µg g^{-1}]											
U re (k=2)	15%	15%	15%	15%	15%	15%	15%	15%	15%	15%	15%
LOD	0.70	1.22	2.71	0.05	2.46	-0.51	0.02	0.01	0.00	-0.03	3.63
21307	LOD	LOD	LOD	LOD	233.398928	0.3612875	LOD	LOD	0.00745137	0.01164919	LOD
8855	LOD	LOD	LOD	LOD	528.5737	1.48781491	LOD	LOD	0.9041197	0.86848643	LOD
13238	LOD	LOD	LOD	LOD	271.792325	0.87575675	LOD	LOD	-0.0027674	0.01061501	LOD
7473	LOD	LOD	LOD	LOD	254.095785	2.05643835	LOD	LOD	0.02069417	0.01691462	LOD
13286	LOD	LOD	LOD	LOD	1511.47595	6.69884601	LOD	LOD	0.02059503	0.03623253	LOD
13285	LOD	LOD	LOD	LOD	299.971775	11.037448	LOD	LOD	0.02710288	0.04479076	LOD
13332	LOD	LOD	LOD	LOD	250.376447	0.14842194	LOD	LOD	0.00880778	0.00971542	LOD

Table 25 MEA results of animal enamel (part 5)

Animal enamel	^{128}Te	^{137}Ba	^{138}Ba	^{205}Tl	^{206}Pb	^{207}Pb	^{208}Pb	^{209}Bi	^{238}U
Unit [µg g^{-1}]									
U re (k=2)	15%	15%	15%	15%	15%	15%	15%	15%	15%
LOD	0.22	0.72	0.61	0.02	-1.04	-0.88	-0.91	0.01	0.01
21307	LOD	101.66983	102.37275	LOD	0.59508013	0.49373595	0.52334443	LOD	0.30768342
8855	LOD	133.813497	137.609721	LOD	0.82648261	0.73321748	0.77215718	LOD	2.09728037
13238	LOD	27.9737701	28.5001207	LOD	0.14538658	0.15111461	0.15309862	LOD	LOD
7473	LOD	176.964538	178.80071	LOD	0.36326424	0.37480377	0.35594235	LOD	0.23807469
13286	LOD	80.8992973	82.2687499	LOD	0.67790452	0.57742301	0.64354669	LOD	LOD
13285	LOD	34.6278039	35.1685262	LOD	1.42727714	1.2195544	1.38514097	LOD	LOD
13332	LOD	28.7844238	29.1943004	LOD	0.51423893	0.49528522	0.49540371	LOD	LOD

Table 26 MEA results of animal dentine (part 1)

Animal dentine	^{7}Li	^{9}Be	^{10}B	^{11}B	^{23}Na	^{24}Mg	^{25}Mg	^{26}Mg	^{27}Al
Unit [µg g^{-1}]									
U re (k=2)	15%	15%	15%	15%	15%	15%	15%	15%	15%
LOD	0.05	0.04	8.77	8.03	194.93	215.53	204.79	195.75	-9.53
21307	9.58645545	LOD	LOD	LOD	LOD	8574.70423	8755.41587	8507.9257	269.723845
8855	14.6415655	LOD	LOD	LOD	LOD	13235.8148	13635.1069	13306.2751	18.9644286
13238	13.9221587	LOD	LOD	LOD	3430.15349	7534.47423	7726.31709	7563.05446	85.2321477
7473	10.6055011	LOD	LOD	LOD	LOD	4630.55672	4735.47164	4633.89684	89.3437123
13286	14.7473578	LOD	LOD	LOD	LOD	4537.65144	4664.84953	4503.06213	0.98386948
13285	7.17379163	LOD	LOD	LOD	4420.7431	5963.06857	6123.73878	5972.91779	-13.731626
13332	15.8516907	LOD	LOD	LOD	3973.52109	5019.02546	5158.14961	5038.15544	5.59971297

Table 27 MEA results of animal dentine (part 2)

Animal dentine	^{39}K	^{42}Ca	^{43}Ca	^{44}Ca	^{51}V	^{52}Cr	^{53}Cr	^{55}Mn	^{56}Fe
Unit [µg g^{-1}]									
U re (k=2)	15%	15%	15%	15%	15%	15%	15%	15%	15%
LOD	71.54	345.78	428.65	473.30	0.11	6.35	0.55	-0.70	64.07
21307	LOD	413351.561	402331.936	399849.451	7.14230798	LOD	20.5333618	109.790588	LOD
8855	LOD	335230.094	327965.38	322097.126	4.07251636	LOD	19.2572576	7.59305432	LOD
13238	LOD	335480.593	324754.539	320571.94	21.1650685	LOD	LOD	204.111087	LOD
7473	LOD	396430.244	383818.482	387813.724	4.87783786	LOD	19.8459759	4.78216845	LOD
13286	LOD	425546.192	407514.895	410866.5	2.58743835	LOD	LOD	7.07720652	LOD
13285	LOD	350078.235	338366.195	341687.835	11.0559996	LOD	LOD	2.17152643	LOD
13332	LOD	352303.271	338167.678	340732.428	10.9003159	LOD	LOD	27.4938349	LOD

Table 28 MEA results of animal dentine (part 3)

Animal dentine	^{57}Fe	^{58}Ni	^{59}Co	^{60}Ni	^{63}Cu	^{65}Cu	^{66}Zn	^{68}Zn	^{71}Ga
Unit [µg g^{-1}]									
U re (k=2)	15%	15%	15%	15%	15%	15%	15%	15%	15%
LOD	103.03	17.08	0.02	16.47	-6.50	-6.49	114.02	112.62	0.01
21307	LOD	LOD	0.78727145	LOD	4.66035055	4.93751598	LOD	LOD	1.04178969
8855	LOD	LOD	0.5221041	LOD	-9.819782	-9.5143616	LOD	LOD	0.76624425
13238	LOD	LOD	0.52754732	LOD	-7.5617331	-7.4183108	LOD	LOD	0.77231269
7473	LOD	LOD	0.93379115	LOD	-0.025485	-0.0280162	LOD	LOD	0.89123767
13286	LOD	LOD	0.5065226	LOD	-10.455758	-10.272228	LOD	LOD	0.95916311
13285	LOD	LOD	0.34849323	LOD	-14.413902	-14.394676	LOD	LOD	0.78501093
13332	LOD	LOD	0.4346566	LOD	-7.9640526	-7.8958157	LOD	LOD	0.77344967

Table 29 MEA results of animal dentine (part 4)

Animal dentine	^{75}As	^{77}Se	^{82}Se	^{85}Rb	^{88}Sr	^{98}Mo	^{107}Ag	^{109}Ag	^{111}Cd
Unit [µg g^{-1}]									
U re (k=2)	15%	15%	15%	15%	15%	15%	15%	15%	15%
LOD	0.70	1.22	2.71	0.05	2.46	-0.51	0.02	0.01	0.00
21307	LOD	LOD	LOD	LOD	1067.47595	-0.1998358	LOD	LOD	0.15270045
8855	LOD	LOD	LOD	LOD	910.945009	-0.5527892	LOD	0.41381434	0.15922945
13238	13.6446056	LOD	LOD	LOD	711.475164	8.33001611	LOD	LOD	0.25090735
7473	LOD	LOD	LOD	LOD	764.752204	0.566567	LOD	LOD	0.03953635
13286	LOD	LOD	LOD	LOD	862.254845	6.58748263	LOD	LOD	0.01987367
13285	LOD	LOD	LOD	LOD	625.88089	2.93216618	LOD	LOD	0.07628121
13332	LOD	LOD	LOD	LOD	577.892668	3.51245871	LOD	LOD	0.22651184

Table 30 MEA results of animal dentine (part 5)

Animal dentine	^{114}Cd	^{115}In (IS)	^{128}Te	^{137}Ba	^{138}Ba	^{205}Tl
Unit [µg g^{-1}]						
U re (k=2)	15%	15%	15%	15%	15%	15%
LOD	-0.03	3.63	0.22	0.72	0.61	0.02
21307	0.08133969	LOD	LOD	963.038989	974.649014	LOD
8855	0.13315855	LOD	LOD	789.694437	812.329283	LOD
13238	0.17542944	LOD	LOD	208.355847	212.939658	LOD
7473	0.00161889	LOD	LOD	763.150888	770.80398	LOD
13286	-0.0517817	LOD	LOD	145.025332	148.315452	LOD
13285	0.02423736	LOD	LOD	87.6671244	89.3529905	LOD
13332	0.19064397	LOD	LOD	98.9153243	101.914685	LOD

Table 31 MEA results of animal dentine (part 6)

Animal dentine	^{206}Pb	^{207}Pb	^{208}Pb	^{209}Bi	^{238}U
Unit [µg g^{-1}]					
U re (k=2)	15%	15%	15%	15%	15%
LOD	-1.04	-0.88	-0.91	0.01	0.01
21307	-3.3106304	-2.985544	-3.1005303	LOD	11.7687885
8855	-5.3710126	-4.7080404	-4.9560374	LOD	5.79020074
13238	0.35834506	0.18126402	0.23047534	LOD	0.2971406
7473	-3.3045023	-2.9576097	-3.1038421	LOD	11.8498674
13286	-3.5940477	-3.1660823	-3.3282927	LOD	LOD
13285	-3.579176	-3.1192215	-3.3647795	LOD	LOD
13332	-3.6382917	-3.221474	-3.4125764	LOD	LOD

Table 32 n(^{87}Sr)/n(^{86}Sr) ratios of the animal teeth. D=dentine, E= enamel

Sample ID	$n(^{87}Sr)/n(^{86}Sr)$ isotope-amount ratio	*U(k=2)*	U_{rel} *(k=2)*	Sr mass fraction [µg g^{-1}]	*U (k=2)*	U_{rel} *(k=2)*
E_ST_21307	0.71041	0.00027	0.038 %	233	16	15 %
D_ST_21307	0.71074	0.00027	0.038 %	1067	71	15 %
E_ST_CF_8855	0.71068	0.00027	0.038 %	529	35	15 %
D_ST_CF_8855	0.71061	0.00027	0.038 %	911	61	15 %
E_ST_SS_13238	0.71028	0.00027	0.038 %	272	18	15 %
D_ST_SS_13238	0.71064	0.00027	0.038 %	711	47	15 %
E_ST_CE_7473	0.71054	0.00027	0.038 %	254	17	15 %
D_ST_CE_7473	0.71062	0.00027	0.038 %	765	51	15 %
E_ST_CA_13286	0.70998	0.00036	0.051%	1511	101	15 %
D_ST_CA_13286	0.71008	0.00038	0.054%	862	57	15 %
E_ST_CF_13285	0.71072	0.00027	0.038 %	300	20	15 %
D_ST_CF_13285	0.71023	0.00027	0.038 %	626	42	15 %
E_ST_SD_13332	0.71082	0.00027	0.038 %	250	17	15 %
D_ST_SD_13332	0.71031	0.00027	0.038 %	578	39	15 %

9.3 Mussel samples

Table 33 Amount of mg sampled in mussel samples

Sample ID	Amount (mg)
ST_M_13272	7.9
ST_M_13289	10.0
ST_M_13238a	9.5
ST_M_13238b	11.2
ST_M_13311	11.5

Table 34 MEA results of the mussel sample (part 1)

	^{7}Li	**^{9}Be**	**^{10}B**	**^{11}B**	**^{23}Na**	**^{24}Mg**	**^{25}Mg**	**^{26}Mg**
Unit [µg g^{-1}]								
U re (k=2)	15%	15%	15%	15%	15%	15%	15%	15%
13289	0.372372812	-0.0072335	3.09484101	3.36812343	2029.51915	-213.17687	-208.58011	-191.19863
13238a	0.174511464	-0.0312939	0.93560232	1.3182325	314.435135	-12.440549	-12.64102	-11.312971
13238b	0.220821751	-0.0208869	1.82611047	1.49065628	2401.71983	-216.38453	-219.81772	-207.06472
13272	0.202012793	-0.0312386	2.37113463	1.96918955	1645.04844	-253.43967	-254.47871	-240.86917
13311	0.252681861	6.9588E-06	1.28484959	1.23335566	2340.99603	-40.080827	-41.825508	-37.452387

Table 35 MEA results of the mussel sample (part 2)

	^{27}Al	^{39}K	^{42}Ca	^{43}Ca	^{44}Ca	^{51}V	^{52}Cr	^{53}Cr
Unit [µg g^{-1}]								
U re (k=2)	15%	15%	15%	15%	15%	15%	15%	15%
13289	7.59998711	25.3557884	449085.806	464255.272	457797.217	0.21211502	0.24243384	0.06530712
13238a	0.07310752	-3.169007	488484.783	498194.382	502291.82	0.05777452	0.57558436	0.04023929
13238b	-0.0103743	45.345479	496085.617	516337.021	509870.165	0.24096685	1.70621261	1.07424393
13272	1.48928198	-17.247846	499190.847	514519.397	523076.242	0.28982286	3.29271948	2.27562199
13311	6.53391171	65.5938975	507688.384	542168.591	520894.394	0.14500068	1.18665362	0.00292834

Table 36 MEA results of the mussel sample (part 3)

	^{55}Mn	^{56}Fe	^{57}Fe	^{58}Ni	^{59}Co	^{60}Ni	^{63}Cu	^{65}Cu
Unit [µg g^{-1}]								
U re (k=2)	15%	15%	15%	15%	15%	15%	15%	15%
13289	664.583295	277.83493	1154.30302	0.37926646	0.46629057	9.39787891	-0.2620988	-0.0272795
13238a	471.895542	350.387311	1314.77679	-0.4639226	0.52846418	9.18931162	0.04622128	0.35410863
13238b	131.014375	547.270006	1507.2727	-0.6361665	0.54281171	9.25274721	0.13752829	0.4802892
13272	446.581649	506.59796	1388.06884	-0.7990674	0.55877646	9.30628937	1.44073803	1.98417462
13311	108.677175	492.572177	1385.80822	-0.7020727	0.52638314	9.48965923	0.27756611	0.57842622

Table 37 MEA results of the mussel sample (part 4)

	^{66}Zn	^{68}Zn	^{71}Ga	^{75}As	^{77}Se	^{82}Se	^{85}Rb	^{88}Sr
Unit [µg g^{-1}]								
U re (k=2)	15%	15%	15%	15%	15%	15%	15%	15%
13289	-17.290723	-16.2648	0.006583718	0.13700863	2.45280756	1.05383502	0.01073563	305.9947902
13238a	-16.143424	-13.773032	0.057743848	-0.0030773	0.55914651	-0.4808026	0.00786517	661.7342674
13238b	-24.567787	-23.447309	0.020586433	0.30880123	0.68908199	-0.2195529	0.01529516	378.5795017
13272	-13.007902	-10.650807	-0.00866767	-0.0356601	0.96407862	1.01806026	-0.0100959	520.9147727
13311	-19.474132	-18.450372	-0.00769001	0.09852629	0.49251892	-0.0811298	0.00093452	376.2917588

Table 38 MEA results of the mussel sample (part 5)

	^{98}Mo	**^{107}Ag**	**^{109}Ag**	**^{111}Cd**	**^{114}Cd**	**^{115}In** (IS)	**^{128}Te**	**^{137}Ba**
Unit [µg g^{-1}]								
U re (k=2)	15%	15%	15%	15%	15%	15%	15%	15%
13289	0.202559133	0.00255415	0.00513889	0.00857169	-0.0051649	1.42377336	-0.644383	37.4888729
13238a	0.101766065	0.02021163	0.02520156	0.00631778	0.00020381	1.266590912	-1.3398946	86.4049972
13238b	0.063819037	0.04132308	0.04476591	0.00473591	0.00349801	0.562348715	-0.5458662	38.799396
13272	0.073877758	0.03334451	0.04661019	0.00830792	-0.0034129	0.957910893	-1.2099389	75.2449303
13311	0.070762427	-0.004252	0.00661425	-0.0052449	0.00419171	0.094449663	-0.4833992	32.4969187

Table 39 MEA results of the mussel sample (part 6)

	^{138}Ba	**^{205}Tl**	**^{206}Pb**	**^{207}Pb**	**^{208}Pb**	**^{209}Bi**	**^{238}U**
Unit [µg g^{-1}]							
U re (k=2)	15%	15%	15%	15%	15%	15%	15%
13289	36.6217465	0.00227743	0.05130563	0.04469075	0.060364	0.0035164	-2.131E-06
13238a	85.1700765	0.00441519	-0.0696331	-0.0426652	-0.0457957	-0.0001002	0.02271894
13238b	37.5817319	0.00434892	0.81059325	0.76050809	0.7222182	0.00174892	0.00300424
13272	73.1292586	-0.002294	0.12449487	0.08693837	0.11286649	0.00419886	0.00998435
13311	32.2673856	-0.0004475	0.09692313	0.10047289	0.08772081	0.00105326	0.02566601

Table 40 n*(^{87}Sr)/*n*(^{86}Sr) ratios of the mussel samples*

Sample ID	$n(^{87}Sr)/n(^{86}Sr)$ isotope-amount ratio	*U(k=2)*	U_{rel} *(k=2)*	Sr mass fraction [µg g^{-1}]	*U (k=2)*	U_{rel} *(k=2)*
ST_M_13272	0.71123	0.00024	0.034 %	521	35	15 %
ST_M_13289	0.71044	0.00024	0.034 %	306	20	15 %
ST_M_13238a	0.71007	0.00024	0.034 %	662	44	15 %
ST_M_13238b	0.71025	0.00024	0.034 %	379	25	15 %
ST_M_13311	0.71053	0.00024	0.034 %	376	25	15 %

9.4 Archaeological environmental samples

Table 41 MEA results of the archaeological soil samples (part 1)

	^{7}Li	^{9}Be	^{10}B	^{11}B	^{23}Na	^{24}Mg	^{25}Mg	^{26}Mg	^{27}Al
Unit [µg g^{-1}]									
U re (k=2)	15%	15%	15%	15%	15%	15%	15%	15%	15%
LOD	0.00	0.00	0.06	0.05	5.55	0.28	0.29	0.27	0.07
13307	0.08796827	0.00	1.40179334	1.3769518	167.201666	823.854683	841.508102	820.762203	LOD
13289	0.04198183	0.00	0.6087366	0.60772499	116.794728	208.543751	213.523025	214.918668	LOD

Table 42 MEA results of the archaeological soil samples (part 2)

	^{31}P	^{39}K	^{42}Ca	^{43}Ca	^{44}Ca	^{51}V	^{52}Cr	^{53}Cr	^{55}Mn
Unit [µg g^{-1}]									
U re (k=2)	15%	15%	15%	15%	15%	15%	15%	15%	15%
LOD	0.00	0.48	4.00	2.94	2.88	0.00	0.00	0.00	0.01
13307	0.00	1450.04306	1891.66817	1837.73763	1894.08408	0.00774471	LOD	LOD	0.48996279
13289	0.00	1449.71861	883.506443	849.097777	854.441483	0.00897804	LOD	LOD	0.1155765

Table 43 MEA results of the archaeological soil samples (part 3)

	^{56}Fe	^{57}Fe	^{58}Ni	^{59}Co	^{60}Ni	^{63}Cu	^{65}Cu	^{66}Zn	^{68}Zn
Unit [µg g^{-1}]									
U re (k=2)	15%	15%	15%	15%	15%	15%	15%	15%	15%
LOD	0.98	0.37	0.06	0.00	0.06	0.01	0.01	0.10	0.11
13307	LOD	2.7379758	LOD	0.00263028	LOD	0.0366778	0.03784681	LOD	LOD
13289	1.56824913	1.21646159	LOD	0.00113806	LOD	0.00897804	0.00998965	LOD	0.24341877

Table 44 MEA results of the archaeological soil samples (part 4)

	^{69}Ga	^{71}Ga	^{75}As	^{77}Se	^{82}Se	^{85}Rb	^{88}Sr	^{98}Mo	^{107}Ag
Unit [µg g^{-1}]									
U re (k=2)	15%	15%	15%	15%	15%	15%	15%	15%	15%
LOD	0.00	0.00	0.00	0.02	0.02	0.00	0.01	0.00	0.00
13307	0.08373059	0.00	0.03068661	LOD	LOD	0.7522602	10.90894196	0.244031573	0
13289	0.23064719	0.00	0.03452121	0.02174963	LOD	1.28714787	4.359788224	0.081434643	0

Table 45 MEA results of the archaeological soil samples (part 5)

	^{109}Ag	^{111}Cd	^{114}Cd	^{115}In (IS)	^{128}Te	^{137}Ba	^{138}Ba	^{205}Tl
Unit [µg g^{-1}]								
U re (k=2)	15%	15%	15%	15%	15%	15%	15%	15%
LOD	0.00	0.00	0.00	0.00	0.00	0.03	0.03	0.00
13307	0	0	0	0	LOD	2.61552163	2.51221006	0.00131514
13289	0	0	0	0	LOD	6.92030077	6.98453804	0.00227612

Table 46 MEA results of the archaeological soil samples (part 6)

	^{206}Pb	^{207}Pb	^{208}Pb	^{209}Bi	^{238}U
Unit [µg g^{-1}]					
U re (k=2)	15%	15%	15%	15%	15%
LOD	0.00	0.00	0.00	0.00	0.00
13307	LOD	0	0	0	0
13289	LOD	0	0	0	0.00113806

Table 47 MEA results of archaeological straw and wood samples (part 1)

	^{7}Li	^{9}Be	^{10}B	^{11}B	^{23}Na	^{24}Mg	^{25}Mg	^{26}Mg
Unit [µg g^{-1}]								
U re (k=2)	15%	15%	15%	15%	15%	15%	15%	15%
9864_1	4.093721827	0.206535039	175.396453	172.01532	430.775217	4553.1744	4527.43348	4395.24155
9864_2	4.775783094	0.252245133	144.382878	139.793288	389.460096	4192.15161	3985.65	3849.27632
9864_3	2.593922813	0.159805575	184.828886	179.593165	440.937398	4483.41923	4318.04299	4290.94896
7649_1	3.283399785	0.388000202	19.8028603	20.0147569	673.590629	3995.18582	3913.88288	3856.64745
7649_2	3.687222847	0.235736955	21.3379675	21.3312961	679.911369	4214.54539	4135.93596	4133.49945
7649_3	4.364080848	0.249502034	21.0241904	20.6377872	654.25998	4413.94402	4348.35062	4212.56037

Table 48 MEA results of archaeological straw and wood samples (part 2)

	^{27}Al	^{39}K	^{42}Ca	^{43}Ca	^{44}Ca	^{51}V	^{52}Cr	^{55}Mn
Unit [µg g^{-1}]								
U re (k=2)	15%	15%	15%	15%	15%	15%	15%	15%
9864_1	4898.20948	2874.29673	67738.0475	67333.2727	22.9052569	17.2001816	117.160057	4898.20948
9864_2	5610.11902	2852.55719	53463.6108	53328.4382	19.7464435	16.3042871	122.091234	5610.11902
9864_3	3337.28271	2361.87878	70162.9923	70829.1404	15.8400943	12.2898104	77.6459816	3337.28271
7649_1	5809.30116	3786.2648	37291.9067	37503.5766	14.896626	11.682087	721.219243	5809.30116
7649_2	5478.89975	4097.84281	38483.5092	38666.935	14.2691362	11.5915058	189.765209	5478.89975
7649_3	6674.77893	4170.11097	34262.8757	35123.9088	16.5172664	14.0697904	237.869602	6674.77893

Table 49 MEA results of archaeological straw and wood samples (part 3)

	^{56}Fe	**^{57}Fe**	**^{58}Ni**	**Co^{59}**	**Ni^{60}**	**Cu^{63}**	**Cu^{65}**	**Zn^{66}**
Unit [µg g^{-1}]								
U re (k=2)	15%	15%	15%	15%	15%	15%	15%	15%
9864_1	5395.77877	5430.52083	33.0946346	3.31902231	30.8323314	37.5120411	37.9039447	29.5033988
9864_2	5946.0471	5897.60172	32.0079389	3.26625614	27.6235012	34.1120893	34.3218387	24.2413565
9864_3	3909.21498	3938.20008	26.3566977	2.48614683	25.8061201	35.1503264	35.3404559	21.7901058
7649_1	4496.09468	4545.98187	23.056527	11.3396331	19.8359218	13.1701231	13.2554227	46.802575
7649_2	4541.70513	4606.42161	12.2308992	2.62363991	9.35052908	12.5045719	12.7517462	50.9502688
7649_3	5809.18059	5725.65595	12.9916542	2.92056271	8.92049592	14.1676634	14.2021904	51.4034912

Table 50 MEA results of archaeological straw and wood samples (part 4)

	^{68}Zn	**^{69}Ga**	**^{75}As**	**^{77}Se**	**^{82}Se**	**^{85}Rb**	**^{88}Sr**	**^{98}Mo**
Unit [µg g^{-1}]								
U re (k=2)	15%	15%	15%	15%	15%	15%	15%	15%
9864_1	34.0981947	1.897674073	2.08233319	7.29572385	7.3004753	13.0697387	158.71637	2.93999833
9864_2	29.0991942	2.159912931	2.4232294	6.8663381	6.6309258	14.3248032	130.655643	1.50146741
9864_3	26.349697	1.339633131	1.6190884	8.4712934	8.24060001	8.45674253	157.781202	2.21198679
7649_1	51.5494216	1.987116747	2.0116618	3.3659171	3.17858659	13.0691528	112.36887	9.00605378
7649_2	57.0206482	1.906763438	1.92702919	3.50578842	3.42295716	13.9778156	118.447023	3.52709165
7649_3	55.9160098	2.395064696	2.30094524	3.03635561	3.1475268	17.0270068	112.637141	3.44928727

Table 51 MEA results of archaeological straw and wood samples (part 5)

	^{107}Ag	**^{109}Ag**	**^{111}Cd**	**^{114}Cd**	**^{115}In** (IS)	**^{128}Te**	**^{137}Ba**	**^{138}Ba**
Unit [µg g^{-1}]								
U re (k=2)	15%	15%	15%	15%	15%	15%	15%	15%
9864_1	0.1676767	0.165049788	0.18272656	0.18663147	0	-1.4677299	90.7378928	91.4753076
9864_2	0.16175188	0.159012589	0.14973609	0.15694125	0	-1.4159858	86.8338853	87.8234778
9864_3	0.13157393	0.128458338	0.15079708	0.14657179	0	-1.3910251	85.9488308	86.5996371
7649_1	0.06215995	0.047418663	0.15480979	0.15793399	0	-1.4708801	90.7873245	91.3518999
7649_2	0.03869857	0.038813889	0.09121166	0.09426978	0	-1.4910124	91.9867866	91.5954696
7649_3	0.03920173	0.037442739	0.07816834	0.08941171	0	-1.6741522	103.398994	104.000503

Table 52 MEA results of archaeological straw and wood samples (part 6)

	^{205}Tl	^{206}Pb	^{207}Pb	^{208}Pb	^{209}Bi	^{238}U
Unit [µg g^{-1}]						
U re (k=2)	15%	15%	15%	15%	15%	15%
9864_1	0.066637472	2.47904842	2.1100473	2.38152867	0.038232491	0.460638187
9864_2	0.073416229	2.70016009	2.30931055	2.59037284	0.040517012	0.470028594
9864_3	0.043959404	1.7587313	1.47691828	1.68765035	0.023419132	0.365816601
7649_1	0.137542156	5.49109396	4.73269947	5.22755083	0.036943116	0.294111247
7649_2	0.114664352	2.8715678	2.49888178	2.75837173	0.031360148	0.277903002
7649_3	0.125846284	3.14563747	2.70201737	2.99790051	0.037398464	0.394711133

Table 53 n*(*^{87}*Sr)/*n*(*^{86}*Sr) ratios of the archaeological environmental samples*

Sample ID	Sample type	$n(^{87}Sr)/n(^{86}Sr)$ isotope-amount ratio	*U(k=2)*	U_{rel} *(k=2)*	Sr mass fraction [µg g^{-1}]	*U (k=2)*	U_{rel} *(k=2)*
13307	Charcoal and soil	0.71044	0.00017	0.024 %	10.91	1	15 %
13289	mudbrick	0.71048	0.00017	0.024 %	4.36	0.3	15 %
7649	Charred straw	0.71116	0.00031	0.043%	114	8	15 %
9864	Wooden balk	0.71110	0.00035	0.049%	149	10	15 %

9.5 Recent soil samples

Table 54 MEA results of the recent soil samples (part 1)

	^{7}Li	^{9}Be	^{10}B	^{11}B	^{23}Na	^{24}Mg	^{25}Mg	^{26}Mg
Unit [µg g^{-1}]								
U re (k=2)	15%	15%	15%	15%	15%	15%	15%	15%
LOD	0.00	0.00	0.06	0.05	5.55	0.28	0.29	0.27
P18	0.04455735	0	LOD	LOD	LOD	46.4103943	46.4879181	44.7772771
P2	0.03491086	0	LOD	LOD	LOD	69.4251201	68.7012816	67.2413183
P1	0.07315877	0	LOD	LOD	LOD	214.507945	220.136179	214.709559
P3	0.03760231	0	0.04109119	0.04186649	4.19502236	60.2609984	59.9645992	58.4408915
P4	0.10535554	0	0.08348391	0.08491342	LOD	173.792906	169.977234	170.255561
P20	0.11436964	0	LOD	LOD	LOD	104.838638	104.797171	102.989562
P5	0.04815327	0	0.08119686	0.0864217	11.8982342	101.991159	100.353242	98.6341277
P6	0.09208421	0	LOD	LOD	LOD	342.145847	350.425108	335.960729
P6b	0.04798276	0	LOD	LOD	LOD	107.851778	107.94538	107.277115
P7	0.02398805	0	LOD	LOD	LOD	116.772193	118.052874	116.638472
P8	0.04279325	0	0.0882523	0.09218086	10.3634019	118.319398	120.894429	119.581589
P9	0.05220933	0	LOD	LOD	6.81573988	155.784142	158.541656	157.533424
P10	0.07002962	0	LOD	LOD	LOD	189.75938	192.977821	192.947809
P11	0.07614677	0	0.06613646	0.07161219	4.2120286	166.160807	164.872728	160.972046
P12	0.04752834	0	0.11850952	0.12888689	LOD	160.988751	160.943194	160.720288
P13	0.03702139	0	LOD	LOD	LOD	93.0564401	94.8363351	94.3799771
P14	0.05811018	0	0.12230719	0.12753806	LOD	127.922096	128.35369	127.728268
P15	0.09196194	0	LOD	LOD	8.75684411	141.634471	142.786948	139.049518

Table 55 MEA results of the recent soil samples (part 2)

	^{27}Al	^{31}P	^{39}K	^{42}Ca	^{43}Ca	^{44}Ca	^{51}V	^{52}Cr
Unit [µg g^{-1}]								
U re (k=2)	15%	15%	15%	15%	15%	15%	15%	15%
LOD	0.07	0.00	0.48	4.00	2.94	2.88	0.00	0.00
P18	LOD	0	131.803954	1606.53649	1593.1994	1552.11887	0.00255904	LOD
P2	LOD	0	142.31106	1223.38706	1190.37277	1184.79872	0.00659261	LOD
P1	LOD	0	187.316263	1835.77968	1801.68979	1834.42854	0.00223285	LOD
P3	LOD	0	149.555323	833.569193	825.57029	830.512939	0.00410912	LOD
P4	LOD	0	418.985707	1857.22584	1846.25986	1831.39286	0.00500332	0.00400265
P20	LOD	0	352.470017	2076.7389	2031.29433	2090.62403	0.00254487	0.00688613
P5	LOD	0	219.704006	1611.32816	1576.7424	1576.90437	0.00494242	0.00522484
P6	LOD	0	164.624708	3116.83578	3070.36363	3076.99621	0.00328872	0.00715781
P6b	LOD	0	109.574636	1790.02778	1752.03982	1761.74518	0.0017467	0.00565107
P7	LOD	0	67.1848002	1272.13338	1241.20972	1249.58181	LOD	LOD
P8	LOD	0	515.055869	1510.16946	1457.52732	1514.8568	0.0049107	0.00771681
P9	LOD	0	206.070555	1491.65549	1444.02335	1468.88694	0.00279885	0.00301415
P10	LOD	0	282.109859	1849.1596	1819.27616	1824.17045	0.00150506	0.00407252
P11	LOD	0	67.1089179	1465.31513	1468.50499	1496.57269	LOD	0.00316565
P12	LOD	0	231.537614	1914.2267	1853.6784	1855.97824	0.00456604	0.00477359
P13	LOD	0	331.759501	1457.96526	1391.51357	1425.4318	0.00394417	0.00573697
P14	LOD	0	239.689181	1878.553	1835.04588	1841.6868	0.00332873	0.00694279
P15	LOD	0	182.158472	1851.17801	1810.31105	1826.67289	0.00179284	0.00390205

Table 56 MEA results of the recent soil samples (part 3)

	^{53}Cr	**^{55}Mn**	**^{56}Fe**	**^{57}Fe**	**^{58}Ni**	**^{59}Co**	**^{60}Ni**	**^{63}Cu**
Unit [µg g^{-1}]								
U re (k=2)	15%	15%	15%	15%	15%	15%	15%	15%
LOD	0.00	0.01	0.98	0.37	0.06	0.00	0.06	0.01
P18	LOD	0.01701007	LOD	2.30975671	LOD	0.00135478	LOD	0.02694515
P2	LOD	0.03311288	LOD	1.62073306	LOD	0.00134849	LOD	0.39091176
P1	LOD	0.05148696	LOD	2.78962134	LOD	0.0023642	LOD	0.02823902
P3	LOD	0.04434747	LOD	1.19869965	LOD	0.00069777	LOD	0.12970859
P4	LOD	0.05346401	LOD	2.70036125	LOD	0.00257313	LOD	0.17997643
P20	LOD	0.04790351	1.45911111	3.14037476	LOD	0.00538915	LOD	0.06317276
P5	LOD	0.04137509	LOD	2.34849549	LOD	0.00254181	LOD	0.06594597
P6	LOD	0.24471959	LOD	4.87659406	LOD	0.00348218	LOD	0.0642268
P6b	LOD	0.02363176	1.26964224	2.85173752	LOD	0.00184944	LOD	0.08682105
P7	LOD	0.01097326	LOD	1.84759062	LOD	0.00114836	LOD	0.04925207
P8	LOD	0.23304781	1.59359244	2.33089904	LOD	0.0025255	LOD	0.14381337
P9	LOD	0.07029421	1.3079245	2.32218496	LOD	0.00096883	LOD	0.07643016
P10	LOD	0.06418644	0.93304953	3.03331845	LOD	0.00159359	LOD	0.20867234
P11	LOD	0.21295428	0.95867927	2.50865104	LOD	0.00154005	LOD	0.00992475
P12	LOD	0.01639624	1.26925565	3.13147401	LOD	0.00186793	LOD	0.030717
P13	LOD	0.17874249	1.24402619	2.30805494	LOD	0.00484057	LOD	0.04428224
P14	LOD	0.01160301	1.75129437	3.10447218	LOD	0.00171192	LOD	0.02472774
P15	LOD	0.02900176	1.3031809	2.97072936	LOD	0.0018983	LOD	0.01508092

Table 57 MEA results of the recent soil samples (part 4)

	^{65}Cu	**^{66}Zn**	**^{68}Zn**	**^{69}Ga**	**^{71}Ga**	**^{75}As**	**^{77}Se**	**^{82}Se**
Unit [µg g^{-1}]								
U re (k=2)	15%	15%	15%	15%	15%	15%	15%	15%
LOD	0.01	0.10	0.11	0.00	0.00	0.00	0.02	0.02
P18	0.03085898	LOD	0.26809676	0.30031052	0	0.00587073	LOD	LOD
P2	0.40289833	LOD	0.3410177	0.26655118	0	0.00719194	LOD	LOD
P1	0.03520027	LOD	0.57436857	0.50554417	0	LOD	LOD	LOD
P3	0.13730658	LOD	0.23018817	0.21049541	0	0.00441924	LOD	LOD
P4	0.18755288	LOD	0.45658835	0.43185767	0	0.00943482	LOD	LOD
P20	0.07110678	LOD	0.71121749	0.64355378	0	LOD	LOD	LOD
P5	0.07088839	LOD	0.43832181	0.39101582	0	0.00296545	LOD	LOD
P6	0.07622096	LOD	1.11236178	1.05451897	0	LOD	LOD	LOD
P6b	0.09134191	LOD	0.55195583	0.5240087	0	LOD	LOD	LOD
P7	0.05371793	LOD	0.45462468	0.44518257	0	LOD	LOD	LOD
P8	0.15377508	LOD	0.47339152	0.42260085	0	0.01178568	LOD	LOD
P9	0.08019784	LOD	0.52499982	0.49959486	0	0.00419828	LOD	LOD
P10	0.21734857	LOD	0.58476062	0.53358853	0	0.00185919	LOD	LOD
P11	0.01368931	LOD	0.5882124	0.52643941	0	LOD	LOD	LOD
P12	0.03621701	LOD	0.40990596	0.40035879	0	0.0059151	LOD	LOD
P13	0.04903317	LOD	0.25807403	0.25386094	0	0.00430273	LOD	LOD
P14	0.02720051	LOD	0.44842799	0.38575269	0	0.00199724	LOD	LOD
P15	0.0197212	LOD	0.66809509	0.60808781	0	LOD	LOD	LOD

Table 58 MEA results of the recent soil samples (part 5)

	^{85}Rb	**^{88}Sr**	**^{98}Mo**	**^{107}Ag**	**^{109}Ag**	**^{111}Cd**	**^{114}Cd**	**^{115}In** (IS)
Unit [µg g^{-1}]								
U re (k=2)	15%	15%	15%	15%	15%	15%	15%	15%
LOD	0	0.01	0	0	0	0	0	0
P18	0.10838274	2.098410355	LOD	0	0	0	0	0
P2	0.12540941	2.566023327	LOD	0	0	0	0	0
P1	0.17495059	5.426883298	LOD	0	0	0	0	0
P3	0.05023979	1.913918865	LOD	0	0	0	0	0
P4	0.19941789	5.915492269	LOD	0	0	0	0	0
P20	0.20613481	5.225974017	LOD	0	0	0	0	0
P5	0.13471617	3.787162567	LOD	0	0	0	0	0
P6	0.67554215	7.806845174	LOD	0	0	0	0	0
P6b	0.1174396	3.364033077	LOD	0	0	0	0	0
P7	0.05626985	3.36343154	LOD	0	0	0	0	0
P8	0.19825199	3.689619695	0.004489783	0	0	0	0	0
P9	0.0968833	5.167647364	LOD	0	0	0	0	0
P10	0.08286691	6.023698375	LOD	0	0	0	0	0
P11	0.37808154	5.572574589	LOD	0	0	0.00077002	0.00077002	0
P12	0.19613222	7.427703585	LOD	0	0	0	0	0
P13	0.14199002	3.273748421	LOD	0	0	0	0	0
P14	0.19002314	5.460930339	LOD	0	0	0	0	0
P15	0.17369418	4.966788667	LOD	0	0	0	0	0

Table 59 MEA results of the recent soil samples (part 6)

	^{128}Te	**^{137}Ba**	**^{138}Ba**	**^{205}Tl**
Unit [µg g^{-1}]				
U re (k=2)	15%	15%	15%	15%
LOD	0.00	0.03	0.03	0.00
P18	LOD	9.2379731	9.18844821	0.00135478
P2	LOD	8.17963012	8.13707783	0.00134849
P1	LOD	15.3327382	15.6973499	0.0011821
P3	LOD	6.24981421	6.32827511	0.00069777
P4	LOD	12.8563785	12.7334398	0.00128657
P20	LOD	18.8549729	19.0280244	0.00134729
P5	LOD	11.3730671	11.3990501	0.00127091
P6	LOD	30.7106645	31.259881	0.00348218
P6b	LOD	14.9506873	15.0953548	0.00092472
P7	LOD	12.4882069	12.6644171	0
P8	LOD	11.7445715	12.0140988	0.00126275
P9	LOD	14.2164396	14.2004	0.00096883
P10	LOD	15.3580892	15.2763732	0.0007968
P11	LOD	14.8528124	14.8616249	0.00154005
P12	LOD	11.1709233	11.1928196	0.00093396
P13	LOD	7.09044731	7.28765567	0.00080676
P14	LOD	10.6898955	10.9111136	0.00085596
P15	LOD	16.9601237	17.244341	0.00094915

Table 60 MEA results of the recent soil samples (part 7)

	^{206}Pb	^{207}Pb	^{208}Pb	^{209}Bi	^{238}U
Unit [µg g^{-1}]					
U re (k=2)	15%	15%	15%	15%	15%
LOD	0.00	0.00	0.00	0.00	0.00
P18	LOD	0	LOD	0	0.00135478
P2	LOD	0	0	0	0.00134849
P1	LOD	0	0	0	0
P3	0.00155061	0.00139555	0.00139555	0	0.00069777
P4	LOD	0	0	0	0.00128657
P20	LOD	0	0	0	0.00269457
P5	LOD	0	0	0	0.00127091
P6	LOD	0	0	0	0
P6b	LOD	0	0	0	0.00092472
P7	LOD	0	0	0	0.00114836
P8	LOD	0	0	0	0
P9	LOD	0	0	0	0.00484416
P10	LOD	0	0	0	0.00239039
P11	0.01018142	0.00924028	0.00924028	0	0
P12	LOD	0	0	0	0.00093396
P13	LOD	0	0	0	0.00080676
P14	LOD	0.00085596	0.00085596	0	0
P15	LOD	0	0	0	0

Table 61 n(^{87}Sr)/n(^{86}Sr) ratios of the recent soil samples

Sample ID	$n(^{87}Sr)/n(^{86}Sr)$ isotope-amount ratio	*U(k=2)*	U_{rel} *(k=2)*	Sr mass fraction [µg g^{-1}]	*U (k=2)*	U_{rel} *(k=2)*
ST_S_P1	0.70929	0.00034	0.048%	5.43	0.36	15 %
ST_S_P2	0.70949	0.00029	0.041%	2.57	0.17	15 %
ST_S_P3	0.70955	0.00029	0.041%	1.91	0.13	15 %
ST_S_P4	0.70955	0.00029	0.041%	5.92	0.39	15 %
ST_S_P5	0.70948	0.00029	0.041%	3.79	0.25	15 %
ST_S_P6	0.71100	0.00036	0.051%	7.81	0.52	15 %
ST_S_P6b	0.70980	0.00029	0.041%	3.36	0.23	15 %
ST_S_P7	0.71004	0.00029	0.041%	3.36	0.23	15 %
ST_S_P8	0.70890	0.00029	0.041%	3.69	0.25	15 %
ST_S_P9	0.70994	0.00017	0.024%	5.17	0.35	15 %
ST_S_P10	0.71024	0.00017	0.024%	6.02	0.40	15 %
ST_S_P11	0.70965	0.00017	0.024%	5.57	0.37	15 %
ST_S_P12	0.70864	0.00017	0.024%	7.43	0.49	15 %
ST_S_P13	0.70915	0.00017	0.024%	3.27	0.22	15 %
ST_S_P14	0.70940	0.00017	0.024%	5.46	0.37	15 %
ST_S_P15	0.71002	0.00017	0.024%	4.97	0.33	15 %
ST_S_P18	0.70905	0.00017	0.024%	2.09	0.14	15 %
ST_S_P20	0.70866	0.00017	0.024%	5.23	0.35	15 %

9.6 Recent water samples

Table 62 MEA results of the recent water samples (part 1)

	^{7}Li	**^{9}Be**	**^{10}B**	**^{11}B**	**^{23}Na**	**^{24}Mg**	**^{25}Mg**	**^{26}Mg**
Unit [µg g^{-1}]								
U re (k=2)	15%	15%	15%	15%	15%	15%	15%	15%
P16_1	0.01076552	0.00	0.07113535	0.0701619	39.1169747	32.4368954	33.7486342	34.0120877
P16_2	0.01217782	0.00	0.07433147	0.07434542	40.9978519	35.237842	37.2170505	37.7796673
P17_1	0.0163048	0.00	0.08623758	0.08281725	41.6819161	21.5361723	21.6512004	22.0945533
P17_2	0.01666917	0.00	0.08454173	0.08153118	41.4097037	21.1535479	21.2903899	22.5435953
P19	0.03679557	0.00	0.37533286	0.37117431	40.4728766	162.114298	169.087458	170.35041
P21_1	0.01015274	0.00	0.16276895	0.15873235	26.422642	26.2963002	27.1337929	28.4325712
P21_2	0.00950739	0.00	0.15028068	0.14945909	25.4185375	25.3260708	25.7506157	26.6311371
P22_1	0.00486962	0.00	0.01587924	0.01645011	14.2510868	18.5784701	18.7305981	18.9443613
P22_2	0.00511777	0.00	0.01678248	0.01621235	14.6291035	19.4036035	19.8671974	19.5488972

Table 63 MEA results of the recent water samples (part 2)

	^{27}Al	**^{39}K**	**^{42}Ca**	**^{43}Ca**	**^{44}Ca**	**^{51}V**	**^{52}Cr**
Unit [µg g^{-1}]							
U re (k=2)	15%	15%	15%	15%	15%	15%	15%
P16_1	0.01032423	8.95119257	63.9215639	65.8017074	66.9243719	0.00094308	-0.0003774
P16_2	0.00849016	9.2957161	68.4513772	69.7740763	69.7412203	0.00084908	-2.378E-05
P17_1	0.03527188	10.9190778	73.8892219	76.2047913	77.221539	0.00237862	-0.0004657
P17_2	0.03792232	10.6764218	71.9380426	75.3401259	77.3634097	0.00247765	-0.0013929
P19	-0.0022067	8.39524133	171.191705	170.059537	171.383198	0.00252868	-0.0021671
P21_1	0.01850289	8.88698901	118.575146	121.645936	121.140005	0.00436171	-7.677E-05
P21_2	0.01879703	7.27942528	111.777154	114.181044	114.313619	0.00444376	-0.0007422
P22_1	0.02613878	14.8319662	93.9374706	96.9138341	97.8249618	0.00219955	-0.0009
P22_2	0.01324981	15.3406781	98.6994163	100.546984	99.6839045	0.00225553	-0.0006911

Table 64 MEA results of the recent water samples (part 3)

	^{53}Cr	**^{55}Mn**	**^{56}Fe**	**^{57}Fe**	**^{58}Ni**	**^{59}Co**	**^{60}Ni**	**^{63}Cu**
Unit [µg g^{-1}]								
U re (k=2)	15%	15%	15%	15%	15%	15%	15%	15%
P16_1	0.00082888	0.31430976	-0.0075722	0.14728946	0.00321781	0.00034371	0.00407845	0.00133198
P16_2	0.00094203	0.23286194	0.09498271	0.18440392	0.00311722	0.00036973	0.00424851	0.00122211
P17_1	0.00116963	0.01017643	0.01463137	0.14266044	0.00344372	0.00030319	0.00494305	0.00293855
P17_2	0.00196447	0.0103654	-0.3199775	0.10702553	0.00345153	0.00031027	0.00396318	0.00283394
P19	0.0041163	0.21588703	-0.3855505	0.20057958	0.00430737	0.00139608	0.00626352	0.00256441
P21_1	0.00278179	0.04251147	0.05364884	0.17422868	0.00240106	0.00022003	0.00411104	0.00934425
P21_2	0.00324378	0.04523972	-0.2542572	0.13925381	0.00145688	0.00022809	0.00240281	0.00878073
P22_1	0.00114984	0.05847822	-0.1368164	0.17414781	0.00282573	0.00041799	0.00405639	0.011581
P22_2	0.00082611	0.05789862	-0.1642666	0.20922495	0.00410845	0.00045522	0.00469773	0.01210869

Table 65 MEA results of the recent water samples (part 4)

	^{65}Cu	^{66}Zn	^{68}Zn	^{69}Ga	^{71}Ga	^{75}As	^{77}Se	^{82}Se
Unit [µg g^{-1}]								
U re (k=2)	15%	15%	15%	15%	15%	15%	15%	15%
P16_1	0.00086737	0.0112719	0.01313663	0.000026497	0.00229127	0.00169311	-0.00008553	0.00086737
P16_2	0.00078044	0.010973	0.01377145	0.000033306	0.00231513	0.00194872	0.00035647	0.00078044
P17_1	0.00245772	0.01167805	0.0139126	0.000040549	0.00267099	0.00074666	0.00052476	0.00245772
P17_2	0.00255397	0.01099901	0.01250601	0.000025034	0.00276398	0.00154681	0.00047042	0.00255397
P19	0.00283726	0.03152517	0.0340307	0.000004906	0.001985	0.02416755	0.01978106	0.00283726
P21_1	0.00918142	0.05457207	0.05708626	0.000025272	0.00199801	0.00199873	-0.00023928	0.00918142
P21_2	0.00897924	0.02625265	0.02878223	0.000022324	0.00212474	0.0027394	0.00131913	0.00897924
P22_1	0.01196263	0.00971348	0.01114124	0.000024038	0.0047483	0.00175971	-0.00005001	0.01196263
P22_2	0.01275157	0.02688591	0.02794209	0.000016973	0.00494179	0.00053918	0.00058777	0.01275157

Table 66 MEA results of the recent water samples (part 5)

	^{85}Rb	^{88}Sr	^{98}Mo	^{107}Ag	^{109}Ag	^{111}Cd	^{114}Cd
Unit [µg g^{-1}]							
U re (k=2)	15%	15%	15%	15%	15%	15%	15%
P16_1	0.00202842	0.352938344	0.002673019	-0.000040067	-0.00003510	0.00000124	0.00000742
P16_2	0.00209173	0.371849785	0.002788582	-0.000040442	-0.00003370	0.00001390	0.00001459
P17_1	0.0046106	0.340017393	0.000887648	-0.000044071	-0.00004703	-0.00001249	0.00001021
P17_2	0.00459914	0.337603332	0.000719028	-0.000050983	-0.00004709	0.00000911	0.00000678
P19	0.00140328	1.096788947	0.002504175	-0.000043490	-0.00004653	0.00000795	0.00002536
P21_1	0.00349438	0.259281506	0.000597863	-0.000050979	-0.00003862	0.00001921	0.00002568
P21_2	0.00310696	0.251581718	0.000520389	-0.000000974	0.00000765	0.00001707	0.00002162
P22_1	0.00222178	0.264054307	0.0016307	-0.000050596	-0.00004438	-0.00000084	0.00000428
P22_2	0.00228205	0.27542891	0.001645558	-0.000050204	-0.00004389	0.00000136	0.00002388

Table 67 MEA results of the recent water samples (part 6)

	^{115}In (IS)	**^{128}Te**	**^{137}Ba**	**^{138}Ba**	**^{205}Tl**
Unit [µg g^{-1}]					
U re (k=2)	15%	15%	15%	15%	15%
P16_1	0.002144290	-0.001302	0.0864398	0.0819866	0.0000015
P16_2	0.001662595	-0.0013325	0.08441203	0.08062308	-0.0000098
P17_1	0.001534560	-0.0008231	0.05972112	0.05678219	-0.0000060
P17_2	0.002538889	-0.0007299	0.05911295	0.05637451	-0.0000077
P19	0.003382479	-0.0013723	0.08615323	0.08217912	0.0000032
P21_1	-0.000102283	-0.0013177	0.07478178	0.07009125	0.0000050
P21_2	0.000996403	-0.001233	0.07167229	0.06807973	0.0000000
P22_1	0.000147013	-0.0009359	0.05370976	0.0512416	-0.0000137
P22_2	0.000004104	-0.0010265	0.05580077	0.05418579	-0.0000069

Table 68 MEA results of the recent water samples (part 7)

	^{206}Pb	**^{207}Pb**	**^{208}Pb**	**^{209}Bi**	**^{238}U**
Unit [µg g^{-1}]					
U re (k=2)	15%	15%	15%	15%	15%
P16_1	0.00037095	0.00032619	0.00032122	0.0000004	0.00255882
P16_2	0.00027633	0.00023724	0.00023801	0.0000015	0.00269398
P17_1	0.00017041	0.00013123	0.00012582	-0.0000001	0.00164889
P17_2	0.00021079	0.00016928	0.00017993	-0.0000089	0.0016374
P19	0.00028585	0.00020476	0.00025863	-0.0000089	0.02924891
P21_1	0.00022947	0.00019584	0.00022025	-0.0000054	0.00207009
P21_2	0.000026251	0.000042433	0.00003984	-0.0000006	0.00201489
P22_1	0.00022933	0.00021402	0.00019435	-0.0000063	0.00178843
P22_2	0.00021117	0.00021688	0.00022749	-0.0000085	0.00188247

Table 69 n(*^{87}Sr)/*n(*^{86}Sr) ratios of the recent water samples*

Sample ID	$n(^{87}Sr)/n(^{86}Sr)$ isotope-amount ratio	*U(k=2)*	U_{rel} *(k=2)*	Sr mass fraction [µg g^{-1}]	*U (k=2)*	U_{rel} *(k=2)*
ST_W_P16	0.71050	0.00017	0.023%	0.362	0.024	15 %
ST_W_P17	0.71077	0.00017	0.023%	0.339	0.023	15 %
ST_W_P19	0.71008	0.00017	0.023%	1.097	0.073	15 %
ST_W_P21	0.70954	0.00017	0.023%	0.255	0.017	15 %
ST_W_P22	0.70990	0.00017	0.023%	0.270	0.018	15 %

9.7 Certificates

National Institute of Standards & Technology

Certificate of Analysis

Standard Reference Material® 987

Strontium Carbonate
(Isotopic Standard)

This Standard Reference Material (SRM) is certified for use as an isotopic reference material for the calibration of mass spectrometers. The material consists of highly purified strontium carbonate of high homogeneity. A unit of SRM 987 consists of 1 g of powder.

Certified Values: The certified values for the absolute strontium isotopic abundance ratios and the atom fractions of ^{88}Sr, ^{87}Sr, ^{86}Sr and ^{84}Sr are listed in Table 1. A NIST-certified value is a value for which NIST has the highest confidence in its accuracy, in that all known or suspected sources of bias have been investigated or accounted for by NIST. A certified value is the present best estimate of the true value based on the results of analyses performed at NIST and cooperating laboratories. Value assignment categories are based on the definition of terms and modes used at NIST for chemical reference materials [1]. The uncertainties listed with the values are expanded uncertainties (95 % confidence interval) and are calculated according to the methods in the ISO and NIST Guides [2].

Table 1. Certified Values for SRM 987 Strontium Carbonate

Absolute Abundance Ratios	$^{88}Sr/^{86}Sr = 8.378\ 61 \pm 0.003\ 25$
	$^{87}Sr/^{86}Sr = 0.710\ 34 \pm 0.000\ 26$
	$^{84}Sr/^{86}Sr = 0.056\ 55 \pm 0.000\ 14$
that yield atom percents of:	$^{88}Sr = 82.584\ 5 \pm 0.006\ 6$
	$^{87}Sr = 7.001\ 5 \pm 0.002\ 6$
	$^{86}Sr = 9.856\ 6 \pm 0.003\ 4$
	$^{84}Sr = 0.557\ 4 \pm 0.001\ 5$

This material was used as the reference sample in a determination of the absolute abundance ratios and atomic weight of strontium [3]. The atomic weight of strontium calculated from the absolute abundance ratios is 87.616 81 ± 0.000 12.

Expiration of Certification: The certification of this SRM is deemed to be indefinite within the stated uncertainties. However, certification is nullified if the SRM is contaminated or otherwise altered.

Maintenance of Certified Values: NIST will monitor this SRM and, if substantive changes occur in the certified values, NIST will notify the purchaser. Registration (see attached sheet) will facilitate notification.

Stephen A. Wise, Chief
Analytical Chemistry Division

Gaithersburg, MD 20899
Certificate Issue Date: 19 June 2007
See Certificate Revision History on Last Page

Robert L. Watters, Jr., Chief
Measurement Services Division

The overall direction and coordination of the technical measurements leading to the certification of this SRM were performed under the chairmanship of I.L. Barnes and W.R. Shields of the NIST Analytical Chemistry Division.

The characterization of this SRM was performed by G. Marinenko, E.E. Etz, D.G. Friend, I.L. Barnes, L.J. Moore, T.C. Rains, T.A. Rush, L.A. Machlan, T.J. Murphy, and P.J. Paulsen, all of the NIST Analytical Chemistry Division.

The support aspects involved in the preparation of this SRM were coordinated through the NIST Measurement Services Division. The current revised certificate was coordinated by Robert D. Vocke, Jr. of the Analytical Chemistry Division.

Storage and Handling: There are no special storage or handling instructions. While strontium carbonate is slightly hygroscopic (absorbing approximately 0.02 % moisture at 90 % humidity), this has no effect on the isotopic abundances.

The strontium carbonate used for this SRM was obtained from Spex Industries, Inc[1]. of Metuchen, NJ. The material, when received, was of high purity in relation to cationic impurities but assayed only 99.0 % due to moisture and other volatile impurities. The impurities reported in the strontium carbonate material are lithium, 4 mg/kg; sodium, 6 mg/kg; potassium, < 1 mg/kg; magnesium, < 2 mg/kg; calcium, 5 mg/kg; barium, < 15 mg/kg; copper, < 3 mg/kg; iron, < 3 mg/kg; aluminum, < 1 mg/kg; and silicon, < 1 mg/kg.

REFERENCES

[1] May, W.E.; Parris, R.M.; Beck II, C.M.; Fassett, J.D.; Greenberg, R.R.; Guenther, F.R.; Kramer; G.W.; Wise; S.A.; Gills, T.E.; Colbert, J.C.; Gettings, R.J.; MacDonald, B.S.; *Definitions of Terms and Modes Used at NIST for Value-Assignment of Reference Materials for Chemical Measurements*; NIST Spec. Pub. 260-136, U.S. Government Printing Office: Washington, DC (2000).

[2] ISO; *Guide to the Expression of Uncertainty in Measurement*; ISBN 92-67-10188-9, 1st ed., International Organization for Standardization: Geneva, Switzerland (1993); see also Taylor, B.N.; Kuyatt, C.E.; *Guidelines for Evaluating and Expressing the Uncertainty of NIST Measurement Results*; NIST Technical Note 1297, U.S. Government Printing Office: Washington, DC (1994); available at http://physics.nist.gov/Pubs/.

[3] Moore, L.J.; Murphy, T.J.; Barnes, I.L.; Paulsen, P.J.; *Absolute Isotopic Abundance Ratios and Atomic Weight of a Reference Sample of Strontium*, J. of Res. (NBS) Vol. 87, No. 1, pp. 1□8 (1982).

Certificate Revision History: 19 June 2007 (Editorial change); 14 June 2007 (Editorial changes and revised as isotopic standard only); 01 May 2000 (Editorial changes); 01 October 1982 (Revision of certified values); 06 March 1972 (Editorial changes); 08 November 1971 (Original certificate date).

Users of this SRM should ensure that the certificate in their possession is current. This can be accomplished by contacting the SRM Program at: telephone (301) 975-6776; fax (301) 926-4751; e-mail srminfo@nist.gov; or via the Internet at http://www.nist.gov/srm.

[1]Certain commercial equipment, instrumentation, or materials are identified in this certificate to specify adequately the experimental procedure. Such identification does not imply recommendation or endorsement by the NIST, nor does it imply that the materials or equipment identified are necessarily the best available for the purpose.

National Institute of Standards & Technology

Certificate of Analysis

Standard Reference Material® 1486

Bone Meal

This Standard Reference Material (SRM) is intended primarily for use in evaluating analytical methods used for the determination of selected major, minor, and trace elements in bone and in material of a similar matrix. It consists of steamed bone meal that was sieved and blended to a high degree of homogeneity. A unit of SRM 1486 consists of approximately 50 g of bone meal.

Certified Mass Fraction Values: Certified mass fraction values for constituent elements on a dry-mass basis, are provided in Table 1. A NIST certified value is a value for which NIST has the highest confidence in its accuracy in that all known or suspected sources of bias have been investigated or taken into account [1]. The measurands are the total concentrations of the elements reported in Table 1. Metrological traceability is to the SI unit of mass expressed as derived unit of mass fraction.

Reference Mass Fraction Value: A reference mass fraction value for mercury is provided in Table 2. Reference values are non-certified values that are the best estimate of the true value; however, the values do not meet NIST criteria for certification and are provided with associated uncertainties that may reflect only measurement precision, may not include all sources of uncertainty, or may reflect a lack of sufficient statistical agreement among multiple analytical methods [1]. The measurand is the concentration of mercury, as determined by the methods indicated in the text. Metrological traceability is to the SI unit of mass expressed as derived unit of mass fraction.

Information Values: Information values for additional constituents are provided in Table 3. An information value is considered to be a value that will be of interest and use to the SRM user, but for which insufficient information is available to assess adequately the uncertainty associated with the value, or only a limited number of analyses were performed [1]. Information values cannot be used to establish metrological traceability.

Expiration of Certification: The certification of **SRM 1486** is valid, within the measurement uncertainty specified, until **01 October 2025**, provided the SRM is handled and stored in accordance with the instructions given in this certificate (see "Instructions for Storage and Use"). The certification is nullified if the SRM is damaged, contaminated or otherwise modified.

Maintenance of SRM Certification: NIST will monitor this SRM over the period of its certification. If substantive technical changes occur that affect the certification before the expiration of this certificate, NIST will notify the purchaser. Registration (see attached sheet or register online) will facilitate notification.

Coordination of the technical measurements leading to the certification of SRM 1486 were provided by S.E. Long of the NIST Chemical Sciences Division and W.F. Koch formerly of the NIST Inorganic Analytical Research Division.

Analytical measurements at NIST were made by C.E. Bryan, B.L. Catron, S.E. Long, T.W. Vetter, R.D. Vocke, and L.J. Wood of the NIST Chemical Sciences Division, and by D.S. Braverman, R. Demilrap, J.D. Fassett, K.M. Garrity, R.R. Greenberg, J.R. Moody, P.J. Paulsen, P.A. Pella, T.A. Rush, J.M. Smeller, and S.F. Stone formerly of NIST.

Carlos A. Gonzalez, Chief
Chemical Sciences Division

Gaithersburg, MD 20899
Certificate Issue Date: 17 February 2017
Certificate Revision History on Last Page

Steven J. Choquette, Director
Office of Reference Materials

Statistical consultation was provided by S.B. Schiller, L.M. Oakley, and J.H. Yen of the NIST Statistical Engineering Division.

Additional collaborating laboratory measurements were made by A.R. Byrne (Josef Stefan Institute, Ljubljana, Slovenia); N. Miller-Ihli (Nutrient Composition Laboratory, U.S. Department of Agriculture, Beltsville, MD); J.B. Bodkin (College of Earth and Mineral Sciences, Mineral Characterization Laboratory, The Pennsylvania State University, University Park, PA); and B. Dainowski (University of Alaska Fairbanks, Fairbanks, AK).

Support aspects involved in the issuance of this SRM were coordinated through the NIST Office of Reference Materials.

INSTRUCTIONS FOR STORAGE AND USE

Storage: SRM 1486 must be stored in its original bottle, tightly capped and away from sunlight or ultraviolet radiation.

Use: Prior to use, the contents of the bottle should be thoroughly mixed by gently rotating the bottle by hand and inverting several times. The mass fractions of constituents in SRM 1486 are reported on a dry-mass basis. A separate sub-sample should be removed from the bottle at the time of analysis and dried (see "Instructions for Drying") to determine a moisture correction factor. Correction for moisture is to be made to the data before comparison with the certified values.

Instructions for Drying: Samples should be dried under vacuum for 24 h, or for 2 h at 105 °C in a conventional drying oven to obtain a correction factor for moisture. The mass loss determined at NIST using this method was approximately 2.4 %. The mass loss determined by the user may be different, depending on ambient conditions when the bottle is sampled.

SOURCE, PREPARATION AND ANALYSIS[1]

Source and Preparation of Material: The material for SRM 1486 was obtained from the Espoma Company (Millville, NJ). The entire material lot was sieved through a nominal 355 µm sieve (45 mesh), blended in a cone blender, and radiation sterilized.

Homogeneity: Samples from randomly selected bottles of SRM 1486 were tested for homogeneity using X-ray fluorescence spectrometry. No evidence of material heterogeneity was observed in any of the elements measured, which included strontium, zinc, copper, iron, phosphorus, calcium and potassium.

Certification Analyses: The certified mass fraction values are the weighted means of method results from a primary analytical method, or the weighted means of results from at least two independent analytical methods or laboratories. The uncertainty of the certified values is a two-sided 95 % confidence interval for the mean (coverage factor $k = 2$).

The reference mass fraction value for mercury is the mean of results from a single primary method [2,3]. The uncertainty provided is an expanded uncertainty about the mean to cover the measurand with approximately 95 % confidence, consistent with the ISO/JCGM Guide [4]. The expanded uncertainty is calculated as $U = ku_c$, where u_c is the combined uncertainty and k is the coverage factor ($k = 2.36$) corresponding to approximately 95 % confidence.

Elements other than those certified are present in this material. Those that were determined, but not certified, are provided as additional information values on the composition.

[1] Certain commercial equipment, instruments, or materials are identified in this certificate to adequately specify the experimental procedure. Such identification does not imply recommendation or endorsement by the National Institute of Standards and Technology, nor does it imply that the materials or equipment identified are necessarily the best available for the purpose.

Table 1. Certified Mass Fraction Values (Dry-Mass Basis) for SRM 1486

Constituent Element	Mass Fraction (%)			Constituent Element	Mass Fraction (mg/kg)		
Calcium (Ca)[a,b,c]	26.58	±	0.24	Iron (Fe)[d,e]	99	±	8
Magnesium (Mg)[b,f]	0.466	±	0.017	Lead (Pb)[e]	1.335	±	0.014
Phosphorus (P)[a,d]	12.30	±	0.19	Potassium (K)[e,g]	412	±	4
				Strontium (Sr)[e,g]	264	±	7
				Zinc (Zn)[d,e]	147	±	16

[a] Gravimetry
[b] Instrumental neutron activation analysis (INAA)
[c] Titrimetry
[d] Inductively coupled plasma optical emission spectrometry (ICP-OES)
[e] Isotope dilution thermal ionization mass spectrometry (ID TIMS)
[f] Isotope dilution inductively coupled plasma mass spectrometry (ID ICPMS)
[g] Flame atomic emission spectrometry (FAES)

Table 2. Reference Mass Fraction Value (Dry-Mass Basis) for SRM 1486

Constituent Element	Mass Fraction (mg/kg)		
Mercury (Hg)[a]	0.0023	±	0.0014

[a] Isotope dilution cold vapor inductively coupled plasma mass spectrometry (ID CVICPMS) [2,3]

Table 3. Information Values (Dry-Mass Basis) for SRM 1486

Constituent Element	Mass Fraction (%)	Constituent Element	Mass Fraction (mg/kg)
Carbon, Total (C)	18.6	Aluminum (Al)	<1
Silicon (Si)	<0.02	Arsenic (As)	0.006
Sodium (Na)	0.5	Cadmium (Cd)	0.003
		Copper (Cu)	0.8
Loss on Ignition at	31.5	Fluorine (F)	800
1000 °C		Manganese (Mn)	1
		Selenium (Se)	0.13

REFERENCES

[1] May, W.; Parris, R.; Beck, C.; Fassett, J.; Greenberg, R.; Guenther, F.; Kramer, G.; Wise, S.; Gills, T.; Colbert, J.; Gettings, R.; MacDonald, B.; *Definitions of Terms and Modes Used at NIST for Value-Assignment of Reference Materials for Chemical Measurements*; NIST Special Publication 260-136 (2000); available at http://www.nist.gov/srm/upload/SP260-136.pdf (accessed Feb 2017).

[2] Christopher, S.J.; Long, S.E.; Rearick, M.S.; Fassett, J.D.; *Development of Isotope Dilution Cold Vapor Inductively Coupled Plasma Mass Spectrometry and Its Application to the Certification of Mercury in NIST Standard Reference Materials*; Anal. Chem., Vol. 73, pp. 2190–2199 (2001).

[3] Long, S.E.; Kelly, W.R.; *Determination of Mercury in Coal by Isotope Dilution Cold-Vapor Generation Inductively Coupled Plasma Mass Spectrometry*; Anal. Chem., Vol. 74, pp. 1477–1483 (2002).

[4] JCGM 100:2008; *Evaluation of Measurement Data - Guide to the Expression of Uncertainty in Measurement*; (GUM 1995 with Minor Corrections), Joint Committee for Guides in Metrology (JCGM) (2008); available at http://www.bipm.org/utils/common/documents/jcgm/JCGM_100_2008_E.pdf (accessed Feb 2017); see also Taylor, B.N.; Kuyatt, C.E.; *Guidelines for Evaluating and Expressing the Uncertainty of NIST Measurement Results*; NIST Technical Note 1297, U.S. Government Printing Office: Washington, DC (1994); available at http://www.nist.gov/pml/pubs/index.cfm (accessed Feb 2017).

Certificate Revision History: 17 February 2017 (Change of expiration date, addition of a reference value for mercury, editorial changes); 18 December 1992 (Original certificate issue date).

Users of this SRM should ensure that the Certificate of Analysis in their possession is current. This can be accomplished by contacting the SRM Program: telephone (301) 975-2200; fax (301) 948-3730; e-mail srminfo@nist.gov; or via the Internet at http://www.nist.gov/srm.

National Institute of Standards & Technology

Certificate of Analysis

Standard Reference Material 1400

Bone Ash

This Standard Reference Material (SRM) is intended primarily for use in evaluating analytical methods for the determination of selected major, minor, and trace elements in bone and in material of a similar matrix. It consists of bone ash that was blended to a high degree of homogeneity and bottled in 50 g units.

Certified and Non-certified Concentrations of Constituent Elements: The certified concentrations of the constituent elements are shown in Table 1. These concentrations are based on the results of a definitive analytical method or the agreement of results by at least two independent analytical methods. Non-certified concentrations, for information only, are provided in Table 2.

NOTICE AND WARNINGS TO USERS:

Expiration of Certification: This certification is valid for five years from the date of shipment from NIST. Should any of the certified values significantly change before then, purchasers will be notified by NIST. Please return the attached registration card to facilitate notification.

Storage: The material should be kept tightly closed in its original bottle away from sunlight or ultraviolet radiation.

Use: The bottle should be mixed well by rotating the bottle before each use. The sample should be dried for 4 hours at 105 °C in a conventional drying oven. A minimum sample of 150 mg of the dried material should be used to relate analytical determinations to the certified values on this certificate.

Dissolution Procedure: Samples may be dissolved by heating with hydrofluoric and nitric acids, followed by heating to dryness with perchloric acid, cooling, and adding dilute nitric acid.

Coordination of the analyses was performed by W.F. Koch of the NIST Inorganic Analytical Research Division.

Statistical analysis of the experimental data was performed by S.B. Schiller and L.M. Oakley of the NIST Statistical Engineering Division.

The technical and support aspects involved in the certification and issuance of this SRM were coordinated through the Standard Reference Materials Program by R. Alvarez and T.E. Gills.

Gaithersburg, MD 20899
December 18, 1992

William P. Reed, Chief
Standard Reference Materials Program

(over)

Material Source: The material for this SRM was produced by the Monsanto Co., St Louis, MO.

Homogeneity Assessment: Samples from randomly selected bottles of SRM 1400 were tested for homogeneity using x-ray fluorescence spectrometry. No evidence of material heterogeneity was observed in any of the elements measured which included strontium, zinc, copper, iron, phosphorus, calcium, and potassium.

Certified Concentrations and Uncertainties: The certified value is the mean of method results from a definitive analytical method or the weighted mean of results from at least two independent analytical methods or laboratories. The uncertainty is the half-width of a 95% confidence interval for the mean with an allowance for systematic differences between methods.

Table 1. Certified Concentrations of Constituent Elements

Element	Concentration, wt. percent			Element	Concentration µg/g		
Calcium	38.18	±	0.13	Iron	660	±	27
Magnesium	0.684	±	0.013	Lead	9.07	±	0.12
Phosphorus	17.91	±	0.19	Potassium	186	±	8
				Strontium	249	±	7
				Zinc	181	±	3

Non-certified Concentrations: Elements other than those certified are present in this material. Those that were determined but are not certified are provided as additional information on the composition.

Table 2. Non-certified Concentrations of Constituent Elements

Element	Concentration, wt. percent	Element	Concentration µg/g
Silicon	(0.13)		
Sodium	(0.6)	Aluminum	(530)
Moisture		Arsenic	(0.4)
2 h @ 105 °C	(0.2)	Cadmium	(0.03)
		Copper	(2.3)
----------		Fluorine	(1250)
Loss on Ignition		Manganese	(17)
@ 1000 °C	(0.87)	Selenium	(0.08)

Table 3. Methods and Analysts for Certified Elemental Determinations

Element	Method Code	Element	Method Code
Calcium	TITR	Potassium	FAES ID TIMS TITR
Iron	ICP ID TIMS	Strontium	FAES ID TIMS
Magnesium	INAA ID ICPMS	Zinc	ICP ID TIMS
		Phosphorus	GRAV ICP
		Lead	IDTIMS

Methods Used for Analysis of SRM 1400:

FAAS = Flame Atomic Absorption Spectrometry
FAES = Flame Atomic Emission Spectrometry
ICP = Inductively-Coupled Plasma Emission Spectrometry
ID ICPMS = Isotope Dilution, Inductively Coupled Plasma Mass Spectrometry
ID TIMS = Isotope Dilution, Thermal Ionization Mass Spectrometry
INAA = Instrumental Neutron Activation Analysis
RNAA = Radiochemical Neutron Activation Analysis
TITR = Titrimetry
XRF = X-ray Fluorescence Spectrometry
GRAV =Gravimetry

Analysts, National Institute of Standards and Technology

D.S. Braverman
R. Demiralp (Guest Researcher)
J.D. Fassett
K.M. Garrity
R.R. Greenberg
J.R. Moody
P.J. Paulsen
P.A. Pella
T.W. Vetter
T.A. Rush
J.M. Smeller
S.F. Stone
R.D. Vocke

Cooperating Analysts

A.R. Byrne, Jozef Stefan Institute, Ljubljana, Slovenia, Yugoslavia

N. Miller-Ihli, Nutrient Composition Laboratory, U.S. Department of Agriculture, Beltsville, MD

J.B. Bodkin, College of Earth and Mineral Sciences, Mineral Characterization Laboratory, The Pennsylvania State University, University Park, PA.

10 List of Figures

11 List of Tables